

---

Electronic Thesis and Dissertation Repository

---

7-12-2022 4:00 PM

# The Role of Urinary Modulators in the Development of Infectious Kidney Stones

Brendan Wallace, *The University of Western Ontario*

Supervisor: Razvi, Hassan, *The University of Western Ontario*

Co-Supervisor: Burton, Jeremy, *The University of Western Ontario*

Co-Supervisor: Bjazevic, Jennifer, *The University of Western Ontario*

A thesis submitted in partial fulfillment of the requirements for the Master of Science degree in Surgery

© Brendan Wallace 2022

Follow this and additional works at: <https://ir.lib.uwo.ca/etd>



Part of the [Medical Microbiology Commons](#), and the [Urology Commons](#)

---

## Recommended Citation

Wallace, Brendan, "The Role of Urinary Modulators in the Development of Infectious Kidney Stones" (2022). *Electronic Thesis and Dissertation Repository*. 8687.  
<https://ir.lib.uwo.ca/etd/8687>

This Dissertation/Thesis is brought to you for free and open access by Scholarship@Western. It has been accepted for inclusion in Electronic Thesis and Dissertation Repository by an authorized administrator of Scholarship@Western. For more information, please contact [wlsadmin@uwo.ca](mailto:wlsadmin@uwo.ca).

## **Abstract**

The pathogenesis of infectious kidney stones is poorly understood, while equally unclear is the role of urinary modulators and bacteria. An experimental model was created and utilized to test a variety of urinary modulators and bacterial strains commonly associated with struvite and calcium phosphate stones to evaluate their potential roles in influencing crystal formation. Modulators such as acids, citrate, and osteopontin had strong inhibitory effects on infectious crystal formation while the remaining modulators had neutral, mixed, inhibitory, or enhancing effects. Lastly, it was determined that the presence of urease may not directly lead to calcium phosphate and struvite stones in all cases, and in the absence of urease, bacteria may promote calcium phosphate stone formation. Ultimately, this model will help to provide researchers with the ability to rapidly test a wider range of urinary modulators with infectious kidney stone formation and how they relate to individual bacterial species.

## **Keywords**

Infectious stones, kidney stones, struvite, calcium phosphate, urinary modulators, inhibitors, promoters, bacteria, urinary tract infections, urease, artificial urine, pH

## Summary for Lay Audience

Kidney stones will affect about 10-11% of the population at some point during their lifetime and that rate appears to be increasing. As this is a common condition, it has a significant financial impact on the healthcare system. There are different types of kidney stones, but only two associated with urinary tract infections, struvite and calcium phosphate stones. Struvite and calcium phosphate stones represent about 10-15% of stones in patients, however, their clinical importance cannot be understated. The occurrence of these stones can lead to recurrent infections, sepsis, and even death. They also tend to have a higher recurrence rate than the more common calcium oxalate stones and typically require surgical management.

Researchers' understanding of kidney stone development has improved over recent history, but a lot is still yet to be uncovered. One question that eludes researchers is how certain stones commonly associated with urinary tract infections, such as calcium phosphate, can form even in the absence of an infection. Furthermore, researchers believe there must be more to the equation in understanding how struvite or calcium phosphate stones can form even in the presence of an infection. Several proteins and substances in the urine are thought to play a role in the development of these stones and discovering their mechanism will have major clinical implications. Using a novel high-throughput laboratory model with artificial urine, the following document outlines our approach in testing a high number of these modulators and select bacterial strains to see their effect on infectious stone formation.

## Acknowledgements

To my supervisors, Dr. Hassan Razvi, Dr. Jeremy Burton, and Dr. Jennifer Bjazevic, I cannot thank you enough for your mentorship and guidance throughout this project. My limited experience in the lab made this project seem like an extremely daunting undertaking. However, you were there every step of the way to help me celebrate the successes, no matter how small, and encouraged me to keep going when things did not go as planned. Dr. Razvi, you have been a mentor from both a clinical and research perspective and I am eternally grateful for the career path you have set me on. Dr. Burton, you always made a point to check in with me when I was in the lab to be sure that I was finding my way around and making steady progress. Dr. Bjazevic, since I arrived as a visiting resident to London to consider the fellowship, you have been remarkably supportive and have always made time to discuss clinical or research challenges.

To my advisors, Johnny Chmiel, Dr. Harvey Goldberg, and Dr. Kait Al. Johnny, where do I begin. Johnny, the lab was a completely new place for me, and you spent a great deal of time with me to get me orientated. You always were willing to share your ideas and answer my questions at night, on the weekend or during the holidays. Your patience and kindness were unwavering, and you were critical to the success of this project. Dr. Goldberg, thank you for your generosity and help procuring inhibitors for the project. You brought a wealth of knowledge and a unique perspective to the project that raised it to another level. Dr. Al, I have greatly appreciated your generosity with your time in the lab and development of the project.

I also need to thank my dear friend, Dr. Jeff Lupker who generously offered to read my thesis and provide his expert writing skills to improve my own. Looking forward to sharing more good books and wine with you in the future.

To my parents and siblings, thank you for all your unwavering support through all my academic and life endeavors. Mom and Dad, you have been there to help me throughout my entire life and have provided me the opportunity to pursue my dreams. Colin and Monica, we have not always been in close proximity, but I have always felt your love and support. Specifically, I must recognize Colin's input for the project by providing his expertise in statistics and teaching me how to code.

Most of all, I need to thank my wife, Megan. Without your love and support this project would not have been possible. The time in the lab required lots of time away from home and usually took more time than anticipated. You encouraged me to keep writing when I didn't have the energy or motivation. At this point your knowledge on kidney stones has far exceeded what you would ever want by being my sounding board. I hope I have been and continue to be as supportive for you in your endeavors, forever and always.

## Table of Contents

Abstract.....	ii
Keywords.....	ii
Summary for Lay Audience.....	iii
Acknowledgements.....	iv
Table of Contents.....	vi
List of Tables.....	xi
List of Figures.....	xiii
List of Abbreviations.....	xv
Chapter 1.....	1
1 Introduction.....	1
1.1 Epidemiology of urolithiasis.....	3
1.2 Clinical presentation of urolithiasis.....	6
1.3 Pathogenesis of urolithiasis.....	7
1.4 Composition of urolithiasis.....	9
1.4.1 Calcium oxalate stone formation.....	10
1.4.2 Uric acid stone formation.....	12
1.4.3 Infectious stone formation.....	13
1.4.4 Cystine stone formation.....	15
1.5 Medical management of urolithiasis.....	17
1.6 Surgical management of urolithiasis.....	24
1.7 Urinary modulators.....	26
1.7.1 pH.....	26

1.7.2 Urinary tract infections.....	27
1.7.3 Pyrophosphate.....	27
1.7.4 Citrate.....	28
1.7.5 Glycosaminoglycans.....	29
1.7.6 Tamm-Horsfall protein.....	30
1.7.7 Nephrocalcin.....	31
1.7.8 Osteopontin.....	31
1.7.9 Inter- $\alpha$ -Inhibitor.....	32
1.7.10 Urinary prothrombin fragment-1.....	32
1.7.11 Calgranulin/Calprotectin.....	33
1.7.12 Albumin.....	33
1.7.13 Polyaspartic acid.....	34
1.7.14 Lipids/Cellular membranes.....	34
1.7.15 CD44.....	34
1.7.16 Magnesium.....	35
1.7.17 Methionine.....	35
1.7.18 Miscellaneous.....	36
1.8 Experimental models.....	37
1.9 References.....	40
Chapter 2.....	50
2 Creating and validating a high-throughput experimental model for infectious stone formation.....	50
2.1 Introduction.....	51
2.1.1 Experimental models.....	51

2.1.2 Urine media.....	53
2.2 Materials and Methods.....	54
2.2.1 Infectious stone experimental model.....	54
2.2.1.1 Optimization of crystal forming assay.....	54
2.2.1.2 Microscopic analysis of crystal formation.....	57
2.2.1.3 Scanning electron microscopy and X-ray diffraction.....	58
2.2.1.4 Adjusting Tris buffering capacity.....	58
2.2.2 Statistical analysis.....	59
2.3 Results.....	59
2.3.1 Experimental model.....	59
2.3.1.1 Comparing Brooks and Griffith’s artificial urine to pooled human urine.....	59
2.3.1.2 Comparing Brooks and Griffith’s artificial urine to human urine from a non-stone former.....	62
2.3.2 Determining the effect of urease and calcium concentration on crystal formation and pH.....	67
2.3.2.1 Identifying the optimal urease concentration.....	67
2.3.2.2 A trial of normal Griffith’s artificial urine compared to low calcium Griffith’s artificial urine.....	68
2.4 Discussion.....	73
2.5 References.....	79
Chapter 3.....	82
3 Testing urinary modulators in infectious stone formation using a high throughput experimental model.....	82
3.1 Introduction.....	83
3.1.1 Infectious stone pathogenesis.....	83

3.1.2 Urinary modulators.....	84
3.2 Materials and Methods.....	85
3.2.1 Experimental conditions for model.....	86
3.2.2 Making stock solutions for each urinary inhibitor.....	86
3.2.3 Running experimental model with urinary modulators.....	87
3.2.4 Microscopic analysis of crystal formation.....	88
3.2.5 Statistical analysis.....	88
3.3 Results.....	89
3.3.1 Urinary modulators that prevented crystal formation.....	89
3.3.2 Urinary modulators that inhibited crystal formation.....	90
3.3.3 Urinary modulators that promoted crystal formation.....	92
3.3.4 Urinary modulators with no effect on crystal formation.....	95
3.3.5 Urinary modulators with mixed effects on crystal formation.....	96
3.4 Discussion.....	99
3.5 References.....	106
Chapter 4.....	110
4 Testing bacterial species for infections stone formation in an experimental model using artificial urine.....	110
4.1 Introduction.....	110
4.1.1 Urease producing bacteria and stone formation.....	110
4.1.2 Alternative bacterial pathways leading to stone formation.....	111
4.2 Materials and Methods.....	114
4.2.1 Preparation of intracellular bacterial proteins.....	114

4.2.2 Running experimental model with bacteria.....	115
4.2.3 Microscopic crystal evaluation and identification.....	115
4.2.4 Qualitative urease test with Christensen’s agar.....	116
4.2.5 Statistical analysis.....	117
4.3 Results.....	117
4.3.1 Urease results from Christensen’s agar.....	117
4.3.2 Bacterial species that did not produce crystals.....	120
4.3.3 Bacterial species that produced crystals.....	120
4.4 Discussion.....	127
4.5 References.....	133
Appendices.....	136
Appendix A: R code for “growth curver package” .....	136
Appendix B: Crystal growth curves of Griffith’s artificial urine with varying urease concentrations measured by absorbance at a wavelength of 660 nm.....	137
Curriculum Vitae.....	138

## List of Tables

Table 1: Stone type and occurrence rate <sup>12,29</sup> .....	10
Table 2: Urease producing organisms <sup>29</sup> .....	15
Table 3: Tests for metabolic stone workup with normal reference ranges <sup>44,46,47</sup> .....	19
Table 4: Composition of Griffith's artificial urine .....	55
Table 5: Composition of Brooks artificial urine .....	55
Table 6: Growth curve output for Griffith's, Brooks, and human pooled urine at varying urease concentrations .....	60
Table 7: Growth curve output for Griffith's, Brooks, and human urine from a non-stone former at varying urease concentrations .....	66
Table 8: pH levels in Griffith's artificial urine and urease without a buffer after 4 hours .....	67
Table 9: Urine media and urease with Tris buffer (pH =8.0 at 37°C) .....	71
Table 10: Griffith's artificial urine with Tris buffer (pH = 7.5 at 37°C) .....	72
Table 11: Concentrations of urinary modulators. <sup>5,18-23</sup> .....	87
Table 12: pH values of urinary modulators with no crystal growth before and after experiment .....	89
Table 13: Growth curve output for urinary modulators with no crystal formation .....	90
Table 14: pH values of osteopontin before and after experiment .....	91
Table 15: Growth curve output for osteopontin .....	91
Table 16: pH values of urinary modulators that promote crystal growth before and after experiment .....	93
Table 17: Growth curve output for urinary modulators promoting crystal formation .....	94
Table 18: pH values of urinary modulators with no effect on crystal growth before and after experiment .....	95
Table 19: Growth curve output for urinary modulators with no effect on crystal formation .....	96

Table 20: pH values of urinary modulators with mixed effect on crystal growth before and after experiment.....	97
Table 21: Growth curve output for urinary modulators with mixed effect on crystal formation.....	98
Table 22: List of bacterial strains tested for infections stone formation with experimental model.....	114
Table 23: Initial ingredients for Christensen’s agar <sup>22</sup> .....	116
Table 24: Final ingredients for Christensen’s agar after autoclaving <sup>22</sup> .....	116
Table 25: Bacterial strains incubated on Christensen’s agar after 48 hours.....	117
Table 26: pH values after 24 hours for bacterial species that did not produce crystals...120	
Table 27: pH values for bacterial species that produced crystals.....	121
Table 28: Growth curve analysis for crystal producing bacterial strains.....	122

## List of Figures

Figure 1: Crystal growth curves with Griffith's, Brooks, and human pooled urine with varying urease concentrations measured by absorbance at a wavelength of 660 nm.....	61
Figure 2: A) Crystal growth curves of Brooks artificial urine measured by absorbance at a wavelength of 660 nm. B) Brightfield microscopy of crystals in Brooks artificial urine at 400x. C) Polarized microscopy of crystals in Brooks artificial urine at 400x.....	63
Figure 3: A) Crystal growth curves of Griffith's artificial urine measured by absorbance at a wavelength of 660 nm. B) Brightfield microscopy of crystals in Griffith's artificial urine at 400x. C) Polarized microscopy of crystals in Griffith's artificial urine at 400x.....	64
Figure 4: A) Crystal growth curves of human urine measured by absorbance at a wavelength of 660 nm. B) Brightfield microscopy of crystals in human urine at 400x. C) Polarized microscopy of crystals in human urine at 400x.....	65
Figure 5: Crystal growth curves of Griffith's artificial urine measured by absorbance at a wavelength of 660 nm.....	68
Figure 6: A) Crystal growth curves of Griffith's artificial urine with 0.15U/ml urease with or without Tris buffer measured by absorbance at a wavelength of 660 nm. B) Brightfield microscopy of calcium phosphate crystals at 400x. C) Polarized microscopy of calcium phosphate crystals at 400x. D) Scanning electron micrograph of calcium phosphate crystals with corresponding x-ray diffraction in E.....	70
Figure 7: A) Crystal growth curves of low calcium Griffith's artificial urine with 0.15U/ml urease with or without Tris buffer measured by absorbance at a wavelength of 660 nm. B) Brightfield microscopy of struvite crystals at 400x. C) Polarized microscopy of struvite crystals at 400x. D) Scanning electron micrograph of struvite crystals with corresponding x-ray diffraction in E.....	71
Figure 8: Crystal growth curves of Griffith's artificial urine with a Tris buffer (pH = 7.5 at 37°C) measured by absorbance at a wavelength of 660 nm.....	72
Figure 9: A) Crystal growth curve of osteopontin measured by absorbance at a wavelength of 660 nm. Bright field microscopy (B) and polarized light microscopy (C) of struvite crystal from OPN reaction at 200x.....	92
Figure 10: Crystal growth curves for modulators that promote crystal formation measured by absorbance at a wavelength of 660 nm.....	93

Figure 11: Brightfield (A) and polarized (B) microscopy of crystals from chondroitin sulfate reaction at 100x.....	94
Figure 12: Brightfield (A) and polarized (B) microscopy of crystals from Na bicarbonate reaction at 100x.....	95
Figure 13: Crystal growth curves for modulators with a no effect on crystal formation measured by absorbance at a wavelength of 660 nm.....	96
Figure 14: Crystal growth curves for modulators with mixed effect on crystal formation measured by absorbance at a wavelength of 660 nm.....	97
Figure 15: Brightfield (A) and polarized (B) microscopy of crystals from Na pyrophosphate reaction at 200x.....	98
Figure 16: Brightfield (A) and polarized (B) microscopy of crystals from P-Cresol reaction at 200x.....	99
Figure 17: Brightfield (E) and polarized (F) microscopy of crystals from polyaspartic acid reaction at 200x. ....	99
Figure 18: Christensen’s agar after 48 hours for <i>K. oxytoca</i> RCA+2 (A), <i>S. aureus</i> USA300 (B), <i>K. pneumoniae</i> RCA+18 (C), <i>P. mirabilis</i> 175A (D), <i>S. epidermidis</i> A2-FV-12 (E), and <i>P. mirabilis</i> 177A (F).....	119
Figure 19: Crystal growth curves from crystal producing bacterial strains measured by absorbance at a wavelength of 660 nm.....	121
Figure 20: <i>P. mirabilis</i> 175A crystals under brightfield light (A) and polarized light (B) at 200x magnification. <i>P. mirabilis</i> 177A crystals under brightfield light (C) and polarized light (D) at 200x magnification.....	123
Figure 21: <i>K. oxytoca</i> RCA+2 crystals under brightfield light (A) and polarized light (B) at 200x magnification. <i>K. pneumoniae</i> RCA+18 crystals under brightfield light (C) and polarized light (D) at 200x magnification. <i>P. aeruginosa</i> PAO1 under brightfield light (E) and polarized light (F) at 200x magnification.....	124
Figure 22: A) Christensen’s agar with colony of <i>P. mirabilis</i> 175A. <i>P. mirabilis</i> 175A crystals under SEM at 500x (B) and SEM (C) with EDX analysis (D).....	125
Figure 23: A) Christensen’s agar with colony of <i>P. aeruginosa</i> PAO1. <i>P. aeruginosa</i> PAO1 crystals under SEM at 5000x (B) and SEM (C) with EDX analysis (D).....	126
Figure 24: A) Christensen’s agar with colony of <i>K. oxytoca</i> RCA+2. <i>K. oxytoca</i> RCA+2 crystals under SEM at 2000x (B) and SEM (C) with EDX analysis (D).....	127

### List of Abbreviations

Abbreviation	Description
NHANES	National Health and Nutrition Examination Survey
UTI, UTIs	Urinary tract infection, urinary tract infections
THP	Tamm-Horsfall protein, uromodulin
UPTF-1	Urinary prothrombin fragment-1
GAG	Glycosaminoglycans
OPN	Osteopontin, uropontin
I $\alpha$ I	Inter- $\alpha$ -inhibitors
dRTA, RTA	Distal renal tubular acidosis, renal tubular acidosis
sp	Species
PHPT	Primary hyperparathyroidism
PTH	Parathyroid hormone
AHA	Acetohydroxamic acid
SWL	Extracorporeal shockwave lithotripsy
URS	Ureteroscopy
PCNL	Percutaneous nephrolithotomy
EHDP	Ethane-1-hydroxy-1,1-diphosphonate
CS	Chondroitin sulfate
Hyaluronic acid	HA
SEM	Scanning electron microscopy
EDX	X-ray diffraction
MDCK	Madine Darby Canine Kidney
HPU	Human pooled urine

## Chapter 1

### 1 Introduction

The first identified urinary stone was found in the bladder of a 4500-year-old Egyptian mummy by the English archeologist Smith.<sup>1</sup> Detailed documentation describing the treatment of urinary stones goes back over 1500 years.<sup>1</sup> The late 18<sup>th</sup> century saw a rise in interest within the scientific community regarding the composition of urinary stones and their etiologies.<sup>2</sup> It is no surprise that the origins of urinary stone study can be traced back this far given that urinary stones kidney stones (nephrolithiasis) are a common condition that affects around 10-11% of people during their lifetime.<sup>3-5</sup> While not typically a fatal condition, significant morbidity including sepsis and chronic kidney disease can occur. Furthermore, kidney stone patients have been shown to have a lower quality of life compared to those without stones<sup>6</sup> owing to frequent emergency room visits for acute renal colic and the possible need for surgery. Due to the prevalence of kidney stones and extensive medical resource use, the United States alone saw the cost of kidney stones to health care rise 50% from 1994 to almost \$2.1 billion dollars in 2000.<sup>7</sup>

Not only are kidney stones prevalent, but they can be a recurrent condition. Without any intervention there is a 50% chance of developing another stone within 10 years for all stone formers.<sup>8</sup> However, the likelihood of recurrence can rise to 60-75% (or greater) in some patients depending on their stone type, urinary/metabolic abnormalities, or other environmental factors.<sup>9,10</sup> Therefore, there is a major clinical focus on evaluating these patients and initiating lifestyle modifications or pharmacotherapies to minimize the risk of recurrence. Dietary modifications and appropriate medical management are examples of methods to reduce stone recurrence rate<sup>11</sup> yet despite the moderate success

with these clinical approaches, there is still a significant amount that we do not understand regarding the pathogenesis of urinary stone disease.<sup>12,13</sup> Even more evident, is the lack of pathophysiologic understanding in infectious urinary stones and a paucity of preventative strategies with a proven track record of clinical benefit. Patients with infectious-based stones are a serious burden to the health care system because of the stone recurrence rate, recurrent infections, sepsis, and the higher rate of surgical intervention. A better understanding of the mechanisms behind infectious stone formation and more reliable prevention of their occurrence, may lead to improvement in patient care and quality of life.

## 1.1 Epidemiology of urolithiasis

The lifetime prevalence of kidney stones has been approximately 10%<sup>3,5</sup> but a more recent update to the National Health and Nutrition Examination Survey (NHANES) shows that the prevalence has increased to 11% in the US.<sup>4</sup> The incidence of kidney stones has also been increasing over time with the most contemporary data at 2.1%<sup>4</sup> which has increased since a review of US patients from 2005-2015 showing a 1% incidence rate.<sup>3</sup> Historically, it was thought that the ratio between males and females was 3:1, however the gender gap has been closing. The NHANES in the United States from 2007-2010 showed that the prevalence of stones in males was 10.6% compared to 7.1% in females, with the overall prevalence being markedly higher compared to the NHANES III study from 1988-1994.<sup>14</sup> However, in 2015, Tundo et al. found that stone formers in the US were approximately 52% male and 48% female<sup>3</sup> and the most updated NHANES data shows relative risk of stones between sexes is not significantly different.<sup>4</sup> The increase in stone incidence is being demonstrated in both males and females.<sup>15</sup>

The average age of stone formers is 47 years for males and 45 years for females.<sup>16</sup> The prevalence of kidney stones, for both males and females, increases as people get older.<sup>5,14</sup> For example, the prevalence in males and females over the age of 70 is 18.8% and 9.4%, respectively.<sup>14</sup> Non-Hispanic Whites (10.3%) have the highest prevalence of stones compared to Hispanics (6.4%) and non-Hispanic Blacks (4.3%).<sup>14</sup> While the difference for this is not clear, diet and environmental factors could be associated. In regards to environmental factors, higher rates of stone formation have been shown in warmer climates<sup>9</sup> such as in the Middle East, where stone prevalence has been reported to be between 20-25%.<sup>17</sup> The most likely cause for this finding is dehydration from excess

sweating with a further possibility of limited access to water. Areas with seasonal variation have also supported this claim with an increase of stones in the warmer months of the year,<sup>17</sup> however, this has not been consistently demonstrated in the literature.<sup>18</sup> Furthermore, there tends to be a higher risk of developing stones in the Western hemisphere (5-15%) compared to the Eastern hemisphere (1-5%).<sup>19</sup>

A family history of stones can also be a significant predictor for developing kidney stones and can be identified in 34% of stone patients.<sup>16</sup> A study by Curhan et al. observing family history in a group of all male participants demonstrated someone with a first-degree relative with a stone was 2.6 times more likely to develop urolithiasis. The familial relationship was also stronger when the stone patient was younger than 60.<sup>20</sup> Genetic or familial inheritance has also been investigated with a twin registry, which showed a 56% inheritability of stones based on a genetic model.<sup>21</sup>

As stated earlier, the cost of kidney stones to health care in the US was almost \$2.1 billion dollars in 2001, an increase of 50% from 1994.<sup>7</sup> There are estimates that this number could balloon to \$4.1 billion dollars by 2030.<sup>22</sup> The costs associated with kidney stone disease relies on a number of factors including emergency room visits, outpatient visits, admissions to hospital, surgery, medications/prescriptions, and other indirect costs. Acute renal colic leads to more than 1.3 million visits to the emergency department per year in the United States.<sup>22</sup> However, these numbers are likely inflated by patients returning to the emergency department multiple times. Over 10% of patients with kidney stones will likely return to the emergency department within 30 days and about one third of those patients will undergo urgent intervention. The number of emergency room and outpatient visits for patients with kidney stones has been increased by 50% and 40%,

respectively. In a 25-year-long study by Johnson et al., it was found that 44% of patients with an obstructing stone will eventually be admitted to hospital.<sup>18</sup> When admission is required, the typical length of stay is 2.2 days for all patients, but increases to 4.4 days for patients over 80 years old.<sup>7</sup> Overall, the funding required to take care of kidney stone patients is staggering and it appears that kidney stone disease will increasingly burden the healthcare system without the implementation of robust preventative strategies.

## 1.2 Clinical presentation of urolithiasis

Patients presenting with a kidney stone will typically have pain that will usually originate from the flank, but can also radiate to the ipsilateral abdomen, groin, testicle, or labia. The pain often will have an abrupt onset and can last anywhere from 15 minutes to several hours with fluctuating severity. Acute renal colic is caused by obstruction of the urinary tract and distension of the renal capsule. There can also be associated nausea and vomiting due to the shared innervation with the celiac plexus between the kidney and bowels.<sup>23</sup> It is important to take a careful history to delineate the origin of the symptoms because there can be overlap between renal colic and other painful conditions within the abdomen and pelvis. Additional symptoms include hematuria, dysuria, urinary urgency, and urinary frequency. If the working diagnosis is renal colic, then imaging (plain film X-ray, ultrasound, or computerized tomography) is performed to confirm the diagnosis. It is possible for patients to be asymptomatic with an obstructing stone, but this is uncommon. Urolithiasis can be picked up incidentally on imaging and this is usually associated with non-obstructing caliceal stones.

In a patient with an obstructing stone and a normal contralateral kidney, there is typically no renal dysfunction present. However, an obstructing stone in a patient with a solitary kidney or bilateral obstructing stones can lead to acute kidney injury and even renal failure. Another important clinical presentation is an obstructing stone in the presence of infection which can lead to sepsis and even death. Evaluating the patient's vital signs, serum leukocytes, urinalysis and urine culture can help determine if the patient has an active urinary tract infection (UTI). Both clinical scenarios require urgent renal drainage and broad-spectrum antibiotics are required in the presence of infection.

### 1.3 Pathogenesis of urolithiasis

Kidney stones are made up of urinary salts and other macromolecules. A salt placed in solution can be dissolved up to a certain concentration which is referred to as the saturation point.<sup>24</sup> These phase changes are determined by the supersaturation in solution, which is the ratio of the concentration of these salts to their solubilities.<sup>25</sup> This has been considered the most important factor in stone formation for over 50 years because without being above supersaturation, no stone could ever be formed.<sup>26</sup> Urine is typically metastable so that it can handle an increased concentration of salts, however there is an upper threshold that when surpassed will lead to crystallization of the salts out of solution.<sup>27</sup>

If the supersaturation exceeds the solubility, then the dissolved free ions form solids in a process called nucleation, which typically occurs on an existing surface. *In vivo*, the possible surfaces on which this can occur include cell debris, urinary casts, epithelium, collecting ducts, and other crystals.<sup>17,28</sup> Once nucleation has occurred and is fixed in the urinary collecting system, crystals can materialize more easily compared to forming the initial nucleus.<sup>24</sup> Aggregation is a term to describe amalgamation of crystals in solution that lead to multiple individual components coming together to make a larger solid. Crystal growth occurs when ions move directly out of solution and solidify to increase the size of one crystal.<sup>27</sup> Crystal retention is another mechanistic theory for stone growth, which occurs when a crystal is physically stuck or the movement of the particle is slower than the flow of urine.<sup>26</sup>

While it plays a prominent role, supersaturation of salt ions is not the whole equation in stone formation. There is a complex interplay between other factors including

urinary pH, urinary modulators, genetics, and urinary milieu that can lead to stone formation, growth, or inhibition. A longstanding theory for the pathogenesis of calcium oxalate stones was the initial formation of Randall's plaques. These plaques begin in the thin loop of Henle and are composed of apatite (calcium phosphate) crystals. Calcium oxalate stones then form on the outer surface of these plaques because they are stable and decrease the threshold to crystallize out of solution.<sup>25</sup> Altering urinary pH can lead to changes in the supersaturation of urinary salts and can also promote certain types of stones to form (low pH = uric acid stones, high pH = struvite or calcium phosphate stones). Urinary modulators can be broken down into promoters and inhibitors of crystal formation. Some promoters include low urine volume, bacterial products and urate<sup>27,28</sup> while some inhibitors include magnesium, pyrophosphate, Tamm-Horsfall protein (THP), urinary prothrombin fragment-1 (UPTF-1), glycosaminoglycans (GAG), citrate, osteopontin (OPN), nephrocalcin, lipids, inter- $\alpha$ -inhibitors (I $\alpha$ I) and hyaluronic acid (HA).<sup>24,27,28</sup>

## 1.4 Composition of urolithiasis

Calcium oxalate stones account for approximately 60-75% of all urinary stones and can be further subclassified into monohydrate (whewellite) and dihydrate (weddellite) forms.<sup>17,29</sup> Under the microscope, the crystal's shape for calcium oxalate monohydrate is similar to “dumbbell” while calcium oxalate dihydrate has a more tetragonal “envelope” appearance. Calcium phosphate can also be subdivided into apatite ( $\text{Ca}_{10}[\text{PO}_4]_6[\text{OH}]_2$ ) and brushite ( $\text{CaHPO}_4 \cdot 2\text{H}_2\text{O}$ ). Amorphous shards are the typical appearance of calcium phosphate crystals. Calcium phosphate stones can either be pure or, more commonly, they are mixed with calcium oxalate. The standard nomenclature assigns the stone type based on the most predominant crystal (i.e., >50% calcium oxalate or calcium phosphate) found within the makeup of the stone.

The remaining non-calcium-based stone types include uric acid, struvite and cystine stones. Uric acid stones are the second most common non-calcium stone and have an appearance similar to “barrels, rhomboids, or needles.” Struvite ( $\text{MgNH}_4\text{PO}_4 \cdot 2\text{H}_2\text{O}$ ) stones, which are classically associated with infections and not necessarily a metabolic abnormality, have the appearance of a “coffin-lid.” Cystine stones are caused by a rare genetic abnormality and the crystal appearance is a “hexagonal” shape. There are also other rare types of stones that can be related to medications including: magnesium trisilicate, ciprofloxacin, sulphonamides, triamterene, indinavir and ceftriaxone.<sup>17</sup>

**Table 1: Stone type and occurrence rate.**<sup>12,29</sup>

Crystal Type	Occurrence (%)
Calcium oxalate	60%
Calcium phosphate	20-25%
Uric acid	5-10%
Struvite	5-10%
Cystine	1-3%
Other	< 1%

#### 1.4.1 Calcium oxalate stone formation

As indicated above, there can be two formulations of calcium oxalate stones: monohydrate (whewellite) and dihydrate (weddelite). These stones are thought to originate on Randall's plaques.<sup>17</sup> Low urinary volume, hypercalciuria, hyperoxaluria, hypocitraturia, or lack of stone inhibitors can lead to calcium oxalate stone formation.

Low urine volume is a very common metabolic issue ranging from 38-70% in stone formers<sup>11,27,30</sup> which leads to higher urinary supersaturation of calcium oxalate and subsequent stone development. However, this can be further exacerbated if the urinary concentration of calcium and/or oxalate are elevated. Dehydration is not solely a calcium oxalate stone issue but is pervasive in many stone formers.

While not consistent across all studies,<sup>11</sup> hypercalciuria is generally thought of as the most common metabolic abnormality identified in a stone metabolic workup. For calcium-based stone disease, some see it as the most significant pathophysiologic variable<sup>12</sup> with an overall prevalence varying from 25-60% of stone formers.<sup>27</sup> Hypercalciuria is typically idiopathic and can originate from defects in the kidney (renal leak), gut (absorptive), and bone (resorptive).<sup>12</sup> Further causes can also be from primary hyperparathyroidism, sarcoidosis, malignancy, immobilisation, granulomatous disease,

use of carbonic anhydrase inhibitors, and milk-alkali syndrome.<sup>27,28</sup> Acid load from a high animal protein diet can increase urinary calcium by stimulating bone loss and reducing renal tubular absorption of calcium.<sup>31</sup> Not only does protein increase excretion of urinary calcium, but also decreases excretion of urinary citrate.<sup>32</sup> Thus, it is not surprising that increased purine load from animal protein leads to more kidney stones.<sup>33</sup> There is a significant association between increased dietary sodium intake and elevated urinary calcium in stone formers and non-stone formers which should also be considered when evaluating idiopathic hypercalciuria.<sup>34</sup>

Consumption of dietary oxalate comprises anywhere from 10-50% of oxalate filtered in the urine.<sup>35</sup> Foods that are typically higher in oxalates are teas, nuts, beans, green leafy vegetables, rhubarb, coffee and chocolates. The majority of oxalate within the body comes from endogenous sources like the liver or metabolism of vitamin C. Hyperoxaluria can occur from excessive dietary intake, intestinal disorders, gastric bypass surgery, prior bowel resection or genetic disorders.<sup>27</sup> Primary hyperoxaluria is a genetic condition that has three types with variable clinical presentations due to different errors in the oxalate metabolic pathway. Primary hyperoxaluria type 1 is the most significant because it presents at a young age and can lead to kidney failure. In addition, certain bacteria within the gut degrade oxalate and prevent it from building up in the urine. *Oxalobacter formigenes* is one of the more common species found in the gut that can degrade oxalate. Persistent antibiotic use can disrupt the bowel microbiome leading to increase uptake of oxalate and development of calcium oxalate stone disease.<sup>36</sup>

Citrate can form a highly soluble complex with calcium and acts as inhibitor of stone formation by interfering with crystallization.<sup>28</sup> Acidosis is a major cause of

hypocitraturia and can occur in 20-60% of stone patients. Other causes of hypocitraturia include distal renal tubular acidosis (dRTA), chronic diarrhea, hypokalemia, physical exercise and a diet rich in animal protein.<sup>37</sup> Hyperuricosuria can also promote calcium oxalate formation because sodium urate can initiate calcium oxalate crystallization in the background of calcium oxalate supersaturation leading to heterogenous nucleation.<sup>12</sup> Causes of hyperuricosuria are excess dietary purine intake, gout, myeloproliferative disorders, tumour lysis syndrome, and Lesch-Nyhan syndrome.<sup>28</sup>

#### **1.4.2 Uric acid stone formation**

There are three factors involved in uric acid stone formation including low urine volume, acidic urine, and hyperuricosuria. The most important factor for uric stone formation is urinary pH. At a urinary pH of 5.5, uric acid is in equilibrium with urate, but when the pH drops below 5.5, it leads to undissociated uric acid and crystal precipitation.<sup>12</sup> Uric acid stones can form in the absence of hyperuricosuria if the pH is low enough because uric acid has very low solubility when compared to urate. Hyperuricosuria can be caused by increased purine catabolism, increased endogenous uric acid production (i.e., gout), consumption of a purine rich diet or chronic diarrhea.

Individuals with metabolic syndrome (hypertension, diabetes, obesity and/or hyperlipidemia) have consistently shown to be at a higher risk of stone development, but they tend to have higher rates of uric acid stones compared to other stone formers as the urinary pH declines with increasing bodyweight.<sup>17,25</sup> The presumed mechanism of uric acid stone formation in metabolic syndrome is insulin resistance and impaired ammonium

excretion leading to lower urinary pH.<sup>12</sup> Uric acid calculi make up 34% of stones in patients with diabetes but only 6% of those patients without.<sup>38</sup>

### **1.4.3 Infectious stone formation**

In contrast to other stones, infectious stones are not necessarily associated with any metabolic abnormalities and can be a result of the urinary environment leading to bacterial proliferation and alkaline urine. The two types of infectious stones are struvite and calcium phosphate. Struvite is associated with UTIs with urease producing bacteria (*Klebsiella* species (sp), some *Proteus* sp, some *Pseudomonas* sp, etc.). Urease reacts with urea to create ammonia and carbon dioxide, which raises the urine pH. UTIs can be seen in 33.3% of patients with only calcium phosphate stones, but the percentage increases to 73.1% if you include apatite and struvite stone composition. Calcium phosphate stones can also occur in the absence of infection and can be associated with specific conditions, namely dRTA and primary hyperparathyroidism (PHPT). Distal RTA patients develop hypokalemia and acidosis due to the kidneys inability to excrete protons, which leads to persistently alkaline urine and hypocitraturia. Primary hyperparathyroidism occurs due to excessive excretion of parathyroid hormone (PTH) from the parathyroid gland leading to hypercalcemia.

Two hypotheses have been proposed to explain why calcium phosphate stones form in the absence of clinical infection and without any struvite component. The first theory is that a clinically asymptomatic UTI was responsible for the stone formation.<sup>10</sup> The second theory is that an infectious process was involved in the initial steps of the stone formation and disappeared secondarily.<sup>10</sup> However, neither of these theories have

been scientifically validated and the scientific community remains largely unfamiliar with the pathogenesis of calcium phosphate stones.

In their review of 39 patients with calcium phosphate stones, Carpentier et al. showed that three of the stones analyzed had bacterial imprints without any history of UTI and 24 out of 39 patients with calcium phosphate stones had hypercalciuria.<sup>39</sup>

Although we have typically focused on pH levels with struvite stone formation, calcium phosphate crystallization has been shown to be more sensitive to pH changes compared to struvite.<sup>39</sup> This could explain why calcium phosphate stones form instead as struvite crystallization requires a high magnesium ammonium phosphate molar product, which is not always found in infected urine.<sup>39,40</sup>

**Table 2: Urease producing organisms.**<sup>29</sup>

<b>Organisms</b>	<b>Usually (&gt;90% of isolate)</b>	<b>Occasionally (5-30% of isolates)</b>
<b>Gram-negative</b>	<i>Proteus rettgeri</i> <i>Proteus vulgaris</i> <i>Proteus mirabilis</i> <i>Proteus morgani</i> <i>Providencia stuartii</i> <i>Haemophilus influenzae</i> <i>Bordetella pertussis</i> <i>Bacteroides corrodens</i> <i>Yersinia enterocolitica</i> <i>Brucella</i> species	<i>Klebsiella pneumoniae</i> <i>Klebsiella oxytoca</i> <i>Serratia marcescens</i> <i>Haemophilus parainfluenzae</i> <i>Bordetella bronchiseptica</i> <i>Aeromonas hydrophila</i> <i>Pseudomonas aeruginosa</i> <i>Pasteurella</i> species
<b>Gram positive</b>	<i>Flavobacterium</i> species <i>Staphylococcus aureus</i> <i>Micrococcus</i> <i>Corynebacterium ulcerans</i> <i>Corynebacterium renale</i> <i>Corynebacterium ovis</i> <i>Corynebacterium hofmannii</i>	<i>Staphylococcus epidermidis</i> <i>Bacillus</i> species <i>Corynebacterium murium</i> <i>Corynebacterium equi</i> <i>Peptococcus asaccharolyticus</i> <i>Clostridium tetani</i> <i>Mycobacterium rhodochrous</i> group
<b>Mycoplasma</b>	T-strain <i>Mycoplasma</i> <i>Ureaplasma urealyticum</i>	
<b>Yeast</b>	<i>Cryptococcus</i> <i>Rhodotorula</i> <i>Sporobolomyces</i> <i>Candida humicola</i> <i>Trichosporon cutaneum</i>	

#### 1.4.4 Cystine stone formation

Cystine stones typically present in individuals with a strong family history or a personal history of stones during childhood. While patients can have 100% cystine stones, generally more than half of cystine stones have mixed composition due to other physiological abnormalities putting them at risk for other stone types.<sup>28</sup> The basis of cystine stone formation is genetically inherited defects in renal transport. Originally, the inheritance pattern was thought to be autosomal recessive, but there are heterozygotes and even autosomal dominance patterns with incomplete penetrance leading to variable

clinical presentations.<sup>17</sup> A heavy chain subunit rBAT (SLC3A1 gene mutation) and the light subunit b<sup>0+</sup>AT (SLC7A9 gene mutation) of the amino acid transporter interact with each other at the brush border of the proximal renal tubule. Defects in either component can clinically present with cystinuria and can be categorized as type A or B, respectively (also known as cystinuria type I or cystinuria type II). These subtypes are clinically indistinguishable and have the same standards for diagnosis.<sup>25</sup> These genetic mutations prevent the kidney from being able to reabsorb the amino acids ornithine, arginine, lysine and cystine (oxidized dimer form of cysteine). The excessive excretion of cysteine from the kidney and its lower solubility in water leads to stone formation, while the other amino acids can remain in solution and not cause any clinical sequelae.

## 1.5 Medical management of urolithiasis

During an acute renal colic episode, the most critical step is symptom management. If the patient can manage the initial phase of pain, it will usually settle to a tolerable level where the patient can manage at home to either pass the stone themselves or wait for surgical management. Non-steroidal anti-inflammatories have been shown to be most effective for renal colic and are thus recommended to be used in conjunction with acetaminophen to minimize narcotic use.<sup>41</sup> Depending on the patient's symptoms and clinical presentation, antiemetics and intravenous fluids may be required. Calcium channel blockers and alpha blockers have also been used to help facilitate passage of stones ("medical expulsive therapy") from the ureter, however, the clinical utility has been debated as there may only be a mild benefit for stones over 5 mm in the distal ureter.<sup>42,43</sup>

There is a varied approach to medically managing kidney stones based on the stone type and metabolic abnormalities. All stone formers should have basic bloodwork including electrolytes, calcium, creatinine, and a urinalysis as part of their initial workup to help screen for kidney dysfunction and help rule out PHPT. General recommendations to reduce stone recurrence include optimal fluid intake (>2 L of urine output/day), minimizing salt intake (<2300mg/day), minimizing animal protein (<0.8-1g/kg/day), avoiding oxalate rich foods (<100 mg/day), adding dietary citrate, and consuming a normal amount of daily calcium (800-1000 mg/day).<sup>44</sup> This advice can be given to all patients that are identified to have a kidney stone and have been shown to be effective even with metabolically active stone disease.<sup>45</sup>

In addition to the above-mentioned general approaches, more individualized recommendations can be made based on the results of a metabolic stone workup and stone analysis. A metabolic stone workup includes serum tests, spot urine and 24-hour urine collection. See table 3 below for complete investigations included in metabolic workup. Stone analysis should be completed whenever possible because identifying stone type can help direct management for kidney stones. This can be especially helpful when a full metabolic workup is not practical, or the patient is uninterested.

Indications for a metabolic stone work up include recurrent stone formers (> 1 stone event), bilateral stones, stone in a solitary functioning kidney, pediatric patient (< 18 years of age), complicated presentation (AKI, sepsis, hospitalization, etc.), patient request/interest, family history, renal insufficiency, pure non-calcium stone former (cystine, uric acid, struvite, etc.), pure calcium phosphate stones, patient requiring percutaneous stone removal, systemic diseases increasing risk of stone formation (IBD, bowel surgery, sarcoidosis, chronic diarrhea, etc.) and high risk occupation (military personnel, pilot, police officer, etc.).<sup>29</sup>

**Table 3: Tests for metabolic stone workup with normal reference ranges.**<sup>44,46,47</sup>

<b>Serum Investigations</b>	<b>Normal Range for Adults</b>
Calcium	2.2-2.57 mmol/L
Phosphate	0.81-1.62 mmol/L
Creatinine	53-106 µmol/L
Bicarbonate	20-28 mmol/L
Chloride	95-105 mmol/L
Potassium	3.5-4.8 mmol/L
Uric Acid	Female: 140-360 µmol/L Male: 200-430 µmol/L
Vitamin D	50-250 nmol/L
<b>24-hour Urine Collection</b>	
pH	5.8-6.2
Volume	>1.5 L/day
Creatinine	Female: 15-19 mg/kg/day Male: 20-24 mg/kg/day
Calcium	2.5-7.5 mmol/day
Oxalate	80-420 µmol/day
Citrate	1.68-6.45 mmol/day
Uric Acid	2.5-4.5 mmol/day
Sodium	50-250 mmol/day
Potassium	20-100 mmol/day
Magnesium	2.3-4.9 mmol/day
Cystine*	< 1500 mmol/day

\* Cystine only needs to be measured if there is clinical suspicion for cystinuria.

Increasing fluid intake to address low urinary volume should be recommended in every stone former because small daily improvements can have dramatic results. For example, every 500 mL increase of fluid intake has been shown to significantly decrease stone recurrence.<sup>48</sup> A randomized trial looking at only adjusting fluid intake had an absolute reduction in stone recurrence by 15% and that the time to recurrence was over 1 year longer compared to the control group.<sup>49</sup> A meta-analysis and systematic review by Fink et al. looked at secondary prevention for kidney stones and found that high fluid intake can lead to a 60% reduction in the long term risk of kidney stone recurrence. Exceeding 2.5 L of urinary volume per day can make the urine undersaturated for calcium phosphate, uric acid and barely supersaturated for calcium oxalate.<sup>50</sup>

Hypercalciuria management differs from the aforementioned management methods as its management can vary depending on the primary cause. Patients with PHPT would also present with elevated serum calcium and PTH. This is usually associated with a parathyroid adenoma that requires surgical removal to correct the problem. Secondary hyperparathyroidism can be induced due to inadequate dietary calcium absorption or low vitamin D intake. With adequate vitamin D supplementation, serum values for vitamin D and PTH will normalize. Idiopathic hypercalciuria treatment starts with conservative management by consuming a normal amount of calcium, minimizing dietary salt intake and animal protein.<sup>51</sup> High sodium intake not only increases urinary calcium, but decreases urinary citrate and mildly elevates urinary pH.<sup>31</sup> While consuming a low calcium diet may seem intuitive, it has been shown to increase the risk of developing kidney stones.<sup>33,52</sup> If hypercalciuria persists then treatment with a

diuretic can be considered (i.e., hydrochlorothiazide, indapamide, and chlorthalidone), which have been shown to decrease stone recurrence by 21.3%.<sup>53</sup>

Some argue that hyperoxaluria is more important in the formation of calcium oxalate crystal formation because there is naturally a high calcium to oxalate molar ratio in urine so relative increases in oxalate concentration lead to greater calcium oxalate crystallization.<sup>54</sup> The cornerstone of treatment for hyperoxaluria is avoiding oxalate rich foods to minimize dietary sources. Timely calcium intake through diet or supplements can be done with meals to chelate the oxalate in the gut and avoid absorption into the urinary tract. Pyridoxine (Vitamin B<sub>6</sub>) is a cofactor in the alanine-glyoxylate-transaminase pathway and can decrease oxalate production. While studies have been done which demonstrate the effectiveness of pyridoxine in decreasing stone recurrence, there are currently no long term randomized trials supporting its use.<sup>47</sup>

As hyperuricosuria can lead to calcium oxalate stones or uric acid stones, management will vary depending on stone type and other patient metabolic abnormalities. Conservative strategies would be to decrease animal protein, increase fluid intake and add dietary citrate. Treating hyperuricemia in the setting of calcium oxalate stone disease has been successful with xanthine oxidase inhibition typically with allopurinol. This medication works within 3 months and significantly decreases stone recurrence by over 80%.<sup>55</sup>

Addressing hypocitraturia can be done successfully via increased dietary citrate, minimizing animal protein or pharmacologic supplementation. Hypocitraturia is found in up to 20% of stone formers and can be related to intestinal, renal, dietary, pharmacologic or idiopathic causes.<sup>47</sup> Distal RTA is a classic condition associated with hypocitraturia

and subsequent stone formation that will typically require pharmacologic therapy.

Potassium citrate has shown not only a significant benefit for decreasing stone recurrence in hypocitraturic patients, but also normocitraturic calcium stone formers.<sup>56,57</sup>

Uric acid stone prevention similarly focuses on a few of the lifestyle modifications previously mentioned. Dietary modifications should focus on minimizing animal protein, increasing fluid intake, and adding citrate. As the association between uric acid urolithiasis and metabolic syndrome becomes stronger, there is a greater push to focus on weight loss as part of the conservative management plan.<sup>58</sup> If the patient is still forming stones and pH is not reaching 6-6.5, then alkali therapy should be first line treatment and dose adjusted accordingly.<sup>59</sup> In pure uric acid stone formation there is not necessarily a higher level of urinary urate so a xanthine oxidase inhibitor is reserved for patients with concurrent gout, hyperuricosuria or failure of alkali therapy.<sup>58,60</sup>

Treating cystinuria is challenging because it requires dedication from the patient to follow all recommendations because any small deviation from the appropriate diet can lead to rapid stone formation. Dietary measures include aggressive hydration (3-4L of urine volume/day while also determinedly minimizing salt intake and animal protein. If this is not successful in avoiding stone recurrence, then the first step would be to add an alkalinizing agent (potassium citrate) and secondly a chelating agent (tiopronin or D-penicillamine).

Unfortunately, infection-based stones do not have an effective, durable, and safe medical treatment to avoid stone recurrence. Acetohydroxamic acid (AHA) is a urease inhibitor that has shown success in small studies but has a significant side effect profile that has prevented its widespread use. Antimicrobial agents cannot fully penetrate the

crystal lattices of the stone to treat all bacteria, so its benefit is limited once a stone has formed.<sup>61</sup> There are also long term-risks with prolonged antibiotic use including bacterial resistance and secondary infections.<sup>61</sup> Colonization of bacteria from ileal conduits, indwelling bladder catheters, stents or patients with neurogenic bladders can lead to impaired host defenses and infectious stone formation.<sup>62</sup> Patients with a neurogenic bladder can develop backflow of urine to the kidneys from elevated bladder pressures and residual urine. Urinary stasis and refluxing urine can lead to urinary tract infections that can lead to pyelonephritis and stone development.<sup>63</sup> Foreign bodies, like stents and catheters, within the urinary tract also provide an additional surface for stones to form on. Patients requiring chronic urinary drainage with a stent or catheter tend to have more medical comorbidities. Considering these factors, surgical management is more complex and clinical outcomes can be suboptimal.

## 1.6 Surgical management of urolithiasis

Ureteral stones less than 5 mm in size have a very high chance of spontaneous passage (>95%), those that are 5-7 mm have about a 50% chance of passage, while stones > 7 mm almost always require surgical intervention.<sup>25</sup> This equates to about 20% of patients with stones requiring surgical management.<sup>8</sup> The three main surgical modalities for treating stones are extracorporeal shockwave lithotripsy (SWL), ureteroscopy (URS) and percutaneous nephrolithotomy (PCNL) where the choice of procedure depends on a variety of clinical factors and patient preference.

SWL is an outpatient procedure that is the least invasive surgical modality. It is usually performed under intravenous sedation but can be done with the patient fully awake. The technique is based on using real-time imaging (fluoroscopy or ultrasound) and an external energy source to fragment the stone *in situ* where after the procedure, the patient will pass fragments spontaneously. Location of the stone, stone size, skin-to-stone distance, renal anatomy, and stone composition all play a part in the overall success of the treatment. Stones less than 20 mm can be offered SWL, but larger stone volumes are associated with lower stone free rates.<sup>64</sup> Thus, stones < 10 mm are ideal for SWL. Brushite and cystine stones are resistant to fragmentation with SWL and should be avoided in patients with these stone types.<sup>64</sup> A lower pole stone location, Hounsfield units > 1000, and a skin-to-stone distance > 10 cm yield lower stone clearance results.<sup>64</sup>

Development of ureteroscopic technology has revolutionized stone management and has led to a migration from ESWL to URS for definitive management of renal and ureteric calculi. Ureteroscopes today are smaller calibre and can traverse the urinary tract all the way into the kidney with excellent visualisation. Stone treatment during URS is

typically carried out with a holmium laser. Recommendations for ureteroscopy include stones < 20 mm, mid or distal ureteric stones, SWL resistant stones or those unable to undergo safe PCNL. This is an outpatient procedure that can have stone free rates up to 95% with low morbidity.<sup>65</sup>

Since the 1970s, PCNL has been used for more complex stone removal cases.<sup>66</sup> The technique and equipment have developed over time, but it remains part of the surgical armamentarium due to its superior stone free rates for stones larger than 20 mm. It can also be the procedure of choice in larger (>15 mm) lower pole stones or when retrograde access for URS may be very challenging or impossible.<sup>67</sup> The downside with a percutaneous approach is the increased rate of complications. Also, it may not be an appropriate management option for some patients (significant co-morbidities, pregnant, requiring continuous anticoagulation, etc.). Historically these patients were admitted to hospital postoperatively, but there has been a transition towards same day discharge especially with the use of smaller diameter tracts (i.e., miniPCNL, ultraminiPCNL and microPCNL). In many cases there is more than one surgical option but using clinical gestalt and having a well-informed discussion with the patient in a shared decision-making model will help guide the clinician to the appropriate treatment.

## 1.7 Urinary modulators

Urinary modulators are compounds within the urinary system that may have a role in the prevention and promotion of urinary stone formation. Urine pH and urinary tract infections alter the urinary environment and can drastically affect stone formation conditions. It is theorized that pH can affect urinary modulator effectiveness.<sup>68</sup> Overall, it appears there are many urinary components that play a part in crystal formation and the search for the most impactful modulators and ideal conditions to decrease stone formation is ongoing. Current knowledge regarding the effect of urinary pH, bacterial pathogens, and urinary modulators will be reviewed as they relate to urolithiasis.

### 1.7.1 pH

Calcium phosphate crystals have been detected *in vitro* at pH levels starting at 6.8 and struvite only when pH exceeds 7.0. Maximal crystallization for both occurred between pH 7.5-8.0 and the density of struvite crystals have been noted to increase at higher pH levels.<sup>69,70</sup> Further, increasing pH by 1.0 increases crystal aggregation 27.5-38%.<sup>71</sup> Conversely with pH values below 6.0 in Griffith's artificial urine, struvite crystals can be completely dissolved within 24 hours and this occurs at a much more rapid rate compared to solutions with a pH of 6.5.<sup>72</sup> Urine at physiologic baselines can be intermittently supersaturated with calcium phosphate, but this supersaturation is in alkaline urine due to the conversion of bicarbonate into carbonate.<sup>73</sup> It is clear that pH is a driving force in the formation of infectious stones and is an important experimental and clinical factor to consider. Prior studies have not always controlled for this variable making it difficult to equate the results solely to the urinary modulator.

### 1.7.2 Urinary tract infections

The relationship between bacteria and stones is centred around urease-splitting bacteria and was first discovered in 1901.<sup>73</sup> However, the majority of urinary infections are from non-urease-splitting bacteria. Hellström in 1938 recognized the association of urease-splitting bacteria and rapid stone formation, but he hypothesized that UTIs likely all played a role in all stone types to varying degrees.<sup>74</sup> When stone composition is greater than 80% struvite/calcium phosphate then the patient's UTI was exclusively from a urease producing bacteria.<sup>63</sup> In contrast, if the stone is made up of less than 20% struvite/calcium phosphate then the urinary pathogen was most likely *E. coli*.<sup>63</sup> Chutipongtanate et al. showed that calcium oxalate crystallization was significantly increased in a dose-dependent manner with all bacteria, not just urease-splitting species, including *E. coli*, *K. pneumoniae*, *S. aureus*, and *S. pneumoniae*.<sup>75</sup> The stone-bacterial relationship has been highlighted even further to show that urinary stones have their own microbiome.<sup>76</sup> Even after a century, we are still uncovering the full connectivity between bacteria and stone formation, however, it has become more evident that urease-splitting is not the only chemical reaction occurring and further research is required to obtain the complete picture.

### 1.7.3 Pyrophosphate

Pyrophosphates are phosphorus oxyanions that are good at complexing metal anions, including calcium. Pyrophosphate is present at concentrations of 15-100  $\mu\text{M}$  in human urine.<sup>68</sup> The *Npt2a*<sup>-/-</sup> mice model has shown increased levels of urinary pyrophosphate and data to suggest that it acts an inhibitor of crystal nucleation.<sup>77</sup> The

inhibitory effect does appear to be dose dependent *in vitro*, but urinary excretion in stone formers is variable. Lower pyrophosphate levels have been noted in stone formers including a group of patients with incomplete RTA compared to normal subjects.<sup>78</sup> However, this finding is not universally demonstrated.<sup>68</sup>

Nevertheless, therapeutic solutions have been trialed with orthophosphate therapy and bisphosphonates (non-biodegradable pyrophosphate analogues), without clinical success.<sup>68</sup> Basavaraj et al. suggested that pyrophosphate has an inhibitory effect on calcium oxalate and calcium phosphate crystallization.<sup>79</sup> However, there is a large body of evidence that pyrophosphate does not affect urease-induced crystallization or have any measurable inhibitory effect on calcium oxalate or calcium phosphate crystallization.<sup>80-82</sup> Sodium pyrophosphate has also been investigated as an inhibitor of crystallization but it has no influence on pH changes, urease activity and bacterial growth.<sup>83</sup> Ethane-1-hydroxy-1,1-diphosphonate (EHDP) displaces previously bound pyrophosphate on apatite crystals and has been shown to be a more effective inhibitor of apatite crystals compared to pyrophosphate.<sup>83</sup>

#### **1.7.4 Citrate**

Most citrate is made through endogenous oxidative metabolism and it is freely filtered through the glomerulus.<sup>79</sup> Clinically, we know that hypocitraturia is a risk for stone formation, and correcting this does decrease the risk of stone formation.

Concentrations of citrate in the distal and collecting ducts have been measured at 0.9 mM.<sup>68</sup> Citrate has shown to inhibit crystal aggregation and growth at concentrations of 0.1 mM by complexing with calcium, but others have demonstrated that the concentration

needs to be 100x greater than physiologic levels to strongly inhibit crystal aggregation.<sup>71</sup> Interestingly, the inhibitory ability of citrate is halted when all other macromolecules are removed from the urine.<sup>68</sup> In addition, citrate inhibited urease-induced crystallization and delayed the onset of nucleation and growth of struvite crystals.<sup>84</sup> An indirect mechanism of improved inhibition may be the increased effectiveness of citrate at higher pH levels.<sup>68</sup> The benefits of citrate in calcium oxalate stone disease is well understood, but its role in infectious stone disease is not as clear. *In vitro* studies suggest there may be untapped potential with this urinary modulator and infectious stones.

### 1.7.5 Glycosaminoglycans (GAGs)

GAGs are broadly characterized as linear polysaccharides with amino sugars. There are several GAGs identified in the urine including heparan sulfate, chondroitin sulfate (chondroitin A and C), dermatan sulfate, and hyaluronic acid. Normal level of GAGs in non-stone formers is 0-50  $\mu$ moles per 24 hours.<sup>68</sup> GAGs are an important part of bladder defence by being present in the urothelial lining and preventing bacterial adhesion. If bacteria cannot adhere to the urothelium and proliferate then this would prevent infection stones from forming.<sup>85</sup> There has not been a consistent demonstration in the literature that stone formers and non-stone formers have significantly different levels of GAGs in the urine.<sup>68</sup>

Chondroitin sulfate (CS) is the most abundant GAG in urine and is present within struvite and calcium phosphate stones, but not calcium oxalate stones.<sup>24</sup> Despite its presence, chondroitin sulfate appears to have no effect on calcium phosphate crystal formation.<sup>86</sup> There may be some inhibitory effect by heparin with calcium oxalate

crystallization, but heparin has no impact on urease-induced stone crystallization.<sup>80,82</sup> *In vitro* studies by Torzewska and Rozalski showed that chondroitin sulfate in Griffith's artificial urine infected with *Proteus mirabilis* actually led to increased struvite and apatite crystallization.<sup>83</sup>

Hyaluronic acid (HA) is an extremely large and high molecular weight GAG. Its size, negative ionic charge, and ability to form hydrated gel-like matrices make it an excellent binding molecule for stone formation. High fluid intake leads to high interstitial HA in the kidney which prevents calcium phosphate precipitation by binding  $\text{Ca}^{2+}$  with the  $\text{COO}^-$  in the HA matrix. This is important because of the role of Randall's plaque formation (calcium phosphate deposits) and kidney stone development.<sup>24</sup> The exact type of GAGs that are clinically impactful is not entirely clear. It is possible that GAGs could be promoters or inhibitors and the difference could depend on stone type, molecular structure, or both.

#### **1.7.6 Tamm-Horsfall Protein (THP)**

THP, also known as uromodulin, is one of the most abundant proteins in normal human urine and is a major component of urinary casts. There is a large variation in daily excretion of THP in urine ranging from 20-100 mg/day.<sup>24</sup> While being one of the more extensively investigated urinary modulators in the literature, the results of these studies have not been consistent. The amount of THP excreted between healthy subjects and stone formers is not significantly different, but there is less carbohydrate (sialic acid) present in THP excreted in from stone formers.<sup>79</sup> Some have posited that THP may have a moderate inhibitory effect on calcium oxalate and calcium phosphate

crystallization.<sup>86-88</sup>

### **1.7.7 Nephrocalcin**

Nephrocalcin was first identified in 1978 by Nakagawa et al.<sup>24</sup> and is composed of 110 amino acid residues where 25% of which are glutamic and aspartic acid. There are also 2 cysteine and 2-3  $\gamma$ -carboxyglutamic acid (Gla) molecules attached.<sup>68</sup> It has been localized in the proximal tubules and thick ascending loops of Henle in the kidney and the daily excretion is 5-16 mg/day.<sup>68</sup> Coe et al. demonstrated how nephrocalcin could inhibit calcium oxalate formation by 50%.<sup>88</sup> Initially, it was thought to be a potent inhibitor of calcium oxalate, but further investigation estimates a more limited role of about 16% of total crystallization inhibition in the urine.<sup>68</sup>

### **1.7.8 Osteopontin (OPN)**

OPN is a negatively-charged aspartic acid rich protein<sup>79</sup> and is found in multiple locations throughout the body including the kidneys, gastrointestinal tract, gallbladder, pancreas, lung, salivary gland, inner ear and bone. It is involved in several biological functions including leukocyte recruitment, cell survival, inflammation, wound healing, and mineral modulation. It has also been called uropontin, but nucleotide sequencing showed that uropontin was not a distinct protein and just a urinary form of OPN.<sup>24</sup> OPN is found in the thick ascending limb of the loop of Henle and distal convoluted tubules within the kidney and its expression is upregulated by phosphate and pyrophosphate.

Normal urinary concentration of OPN is around 100nM and the expression of OPN increases with injury and the inflammatory process associated with healing.<sup>68,79</sup>

OPN is detected in the calcium phosphorus deposits of *Npt2a*<sup>-/-</sup> mice and is thought to affect intraluminal and interstitial renal mineralization.<sup>89</sup> Urine OPN levels is inversely correlated with percent of calcified area in kidney sections obtained from the mice *Npt2a*<sup>-/-</sup>.<sup>89</sup> OPN has also been identified in calcium oxalate monohydrate, calcium oxalate dihydrate and uric acid stones. In addition, there have been studies showing *in vivo* and *in vitro* inhibition of calcium oxalate stone formation and decreased aggregation of calcium phosphate crystal formation with OPN.<sup>68,86</sup>

### **1.7.9 Inter- $\alpha$ -Inhibitor (I $\alpha$ I)**

I $\alpha$ I and other related molecules fall under plasma protease inhibitors, which are typically synthesized in the liver. They are comprised of heavy chains covalently linked to a light chain called bikunin.<sup>68</sup> Urinary excretion ranges from 2-10 mg/day (5.01  $\mu$ g/mL in healthy subjects or 2.54  $\mu$ g/mL in stone patients), but can increase 50-100 times under certain pathologic conditions such as cancer or decrease in other conditions like renal failure.<sup>24</sup> Isolated bikunin concentrations of 20  $\mu$ g/mL inhibited crystal nucleation by 9% and crystal aggregation 21%.<sup>24</sup> Bikunin isolated from stone formers shows less sialic acid compared to bikunin from healthy subjects.<sup>68</sup> Furthermore, it appears that bikunin and I $\alpha$ I may inhibit calcium oxalate crystallization.

### **1.7.10 Urinary prothrombin fragment-1 (UPTF-1)**

The blood clotting factor prothrombin is degraded into three components and Fragment-1 is excreted in the urine.<sup>79</sup> UPTF-1 has also been called “crystal matrix protein” and is a principal constituent of calcium oxalate and calcium phosphate stones.<sup>24</sup>

Staining has localized UPTF-1 in the cytoplasm in epithelial cells of the thick ascending limb of the loop of Henle and the macula densa of the kidney.<sup>68</sup> The normal daily urinary excretion is 13.4 nM/day, but can increase to almost 50 nM/day in pregnant women. UPTF-1 has demonstrated strong inhibition of crystal nucleation, but the effectiveness can vary depending on an individual's race.<sup>68</sup>

### **1.7.11 Calgranulin/Calprotectin**

Calgranulin is a S100 calcium binding protein, and the normal urinary concentration is 3.5-10 nM. In artificial urine, calprotectin has shown a dramatic effect on struvite crystal formation by delaying nucleation and decreasing the size of the crystals.<sup>90</sup> Calgranulin has been identified in calcium oxalate, calcium phosphate, uric acid, and struvite stones.<sup>24</sup> It has been shown to inhibit calcium oxalate crystal growth and aggregation at the extremely low concentrations that are observed in human urine.<sup>68</sup>

### **1.7.12 Albumin**

Albumin is a very abundant urinary protein and has been identified in the matrix of stones and crystals in human urine. Albumin will bind other urinary proteins and incorporate them into the stone matrix.<sup>24</sup> It appears that albumin can be a promotor or inhibitor depending on the urinary environment. *In vitro* urease-induced crystallization was promoted via albumin by increasing pH and ammonium production, but this effect did not translate to human urine.<sup>91</sup> Albumin has been demonstrated to inhibit calcium oxalate crystal aggregation, but also to mediate strong crystal nucleation at a pH of 7.0.<sup>68</sup> Interestingly, albumin does not appear to have an effect on calcium phosphate

crystallization.<sup>86</sup> While albumin may be an inhibitor in calcium oxalate stone disease, it could also be neutral or a promoter in infectious stone formation.

### **1.7.13 Polyaspartic acid (PASP)**

PASP is a carboxylated protein that has shown some promise as a urinary inhibitor. PASP decreases growth kinetics of calcium phosphate at levels of 1 nM and there does appear to be a dose-dependent response with increasing concentrations leading to more inhibition.<sup>92,93</sup> The inhibitory effect with calcium phosphate crystal formation is on reducing aggregation.<sup>86,94</sup> Structural changes to calcium phosphate crystals in the presence of PASP has been documented with scanning electron microscopy (SEM).<sup>95</sup>

### **1.7.14 Lipids/Cellular membranes**

Under normal conditions, there are a small amount of lipids in the urine. Stone formers tend to have more and different phospholipids in the urine compared to healthy subjects. Lipids have been demonstrated to be sites of initiation for calcium phosphate crystals and are found in the matrix of struvite, uric acid, calcium oxalate and calcium phosphate stones.<sup>24,68</sup> Phospholipids appear to promote calcium phosphate and calcium oxalate crystals while also helping to expand the crystal matrix.<sup>24</sup>

### **1.7.15 CD44**

CD44 is a extracellular matrix glycoprotein involved in cell-cell interactions that is a receptor for hyaluronan, HA and OPN.<sup>24</sup> CD44 is upregulated during injury and inflammation and is found on the distal collecting duct cells within the kidney.

Proliferating cells are open to adhesion by calcium oxalate crystals and it is believed that an intact epithelium will prevent crystal adhesion so an upregulation of CD44 would be associated with a higher risk of stone formation.<sup>68</sup>

#### **1.7.16 Magnesium**

Magnesium complexes with oxalate and is more stable than calcium oxalate, this leads to decreased particle formation by 50%.<sup>79</sup> In whole human urine, magnesium reduces the incidence of calcium oxalate crystal formation that has been subjected to removal of water in a manner analogous to the collecting tubules of the kidney.<sup>96</sup> Oral magnesium has been shown to decrease oxalate urinary excretion and increase urinary citrate in hypomagnesemic patients.<sup>79</sup> Further evidence suggests that magnesium inhibits calcium phosphate crystallization, but findings have not been consistent.<sup>71,82</sup>

#### **1.7.17 Methionine**

Methionine has been shown to acidify urine in normal men.<sup>97</sup> Oral supplementation with methionine leads to significant decreases in supersaturation of brushite and struvite crystals with no effect on calcium oxalate crystallization. Not surprisingly, the supersaturation increased significantly for uric acid.<sup>98</sup> Methionine has shown success in decreasing infectious stone recurrence in a small cohort of patients and has also been used to treat an infected and encrusted ureteric stent after a urinary tract infection.<sup>98,99</sup>

### 1.7.18 Miscellaneous

Vanillic acid added at a concentration of 0.5mg/mL to *P. mirabilis* infected urine shows a delay in the pH rise. However, at 2.5-5 mg/mL there was no increase in pH after 24 hours. Vanillic acid at higher concentrations can be bactericidal for *P. mirabilis* and can also inhibit urease at very low concentrations.<sup>83</sup>

Sulfate is predominantly produced by sulfur amino acid oxidation and excreted by the kidney as a titratable acid. Normal urinary concentration of sulfate is 10  $\mu\text{M}$  – 1000 $\mu\text{M}$ . Sulfate has shown a modest effect in decreasing urinary calcium supersaturation and raised the upper limit of metastability for calcium oxalate and calcium phosphate crystal formation.<sup>100</sup>

Edwards et al. showed that oral phosphate supplementation significantly decreased urinary calcium and magnesium and increased excretion of citrate. They demonstrated persistent results with 2 years of follow up with only 2 out of the 20 participants developing stones.<sup>101</sup>

Zinc has been shown to stimulate calcium aggregation and aid stone formation.<sup>71</sup> Curcumin (diferuloylmethane) is a pigment extracted from the roots of turmeric (*Curcuma longa*) with effectiveness at reducing urease activity at 1 mM. Curcumin does not affect struvite crystal morphology, but the crystals are smaller in number and size compared to a control.<sup>102</sup>

Urinary modulators in stone formation have been an area of interest in the scientific community for decades. Despite the extensive exploration, there is limited clarity of urinary modulators in calcium oxalate stone disease and even less so for infectious stone disease. Due to the significant urinary biochemical changes with urinary

tract infections, the effects cannot be assumed to be equivalent. Therefore, testing a wide variety of these modulators under consistent experimental conditions would be the first step to further our understanding of infectious stone modulation.

## 1.8 Experimental models

Recent growth has occurred in the development of animal models for kidney stone disease, especially with the *Drosophila melanogaster* model.<sup>103–107</sup> Unfortunately, this model has only been validated for calcium oxalate stone disease and it is unknown whether or not they can form calcium phosphate or struvite stones. Rat, porcine and canine are examples of animal models have been used to study stone formation.<sup>77,89,108–111</sup> Despite their important use in the pre-clinical study of kidney stone disease, animal models still have some limitations. For example, only rat and canine models have been shown to form infectious stones.

Rat models take at least 4 weeks before they are old enough to introduce the intervention and obtain results.<sup>77,89</sup> Nickel et al. were able to circumnavigate this issue by cultivating bacteria and inoculating the bladder of rats. This was technically challenging as it required the rat to first be anesthetized and then surgery was performed on it to introduce the bacteria on a zinc disc through a cystotomy and subsequent closure. Delays from intervention and results is longer in canines so it has been used less frequently in the literature. Naito et al. developed a renal cell culture model from canine renal distal tubular epithelium, which makes the repeatability a bit easier, but it is still a technically challenging model to use.<sup>112</sup>

Other artificial mediums for studying stone development include: gel-based plate assays, diffusion gels, and polystyrene films that have been used to study biologic crystal formation.<sup>69,113–115</sup> Only the diffusion gel techniques have been used for infectious stone formation,<sup>69</sup> however, a concern with that model is the variability of the experimental conditions. For example, the pH ranged from 4.5-10 in one test tube, thus making the data impossible to interpret. Currently, only a basic understanding of infectious stone pathogenesis exists, and a comprehensive study of a wide variety of urinary modulators and conditions is needed. This could be accomplished best with a reliable, high yield, rapid and affordable experimental model that can produce results that could be later used in animal models or even a clinical study.

High-throughput experimental models have used pooled human urine, non-stone formers and stone formers urine. While ideal for clinical applicability, it is more difficult to account for all substances and the various concentrations within human urine that can affect outcomes. Artificial urine has been used extensively in a plethora of study designs to stimulate stone formation. Perhaps best known is the work by Griffith et al. who described a recipe for artificial urine that has been used extensively throughout the literature.<sup>62,70,83,116–118</sup> When required, investigators will alter the chemical composition of artificial urine to achieve a desired outcome.<sup>119</sup> For example, Brooks and Keevil made an artificial urine that was more directed for the growth of urinary pathogens and not necessarily the study of stones.<sup>120</sup>

An area where Griffith's artificial urine has been used is to investigate struvite and calcium phosphate stone formation. In an effort to instigate the formation of infectious crystals, Jack bean urease or inoculation with urease producing bacteria is

used.<sup>62,70,83,84,117-119</sup> The concern with using bacterial inoculation is that the level of urease could be variable and difficult to control. This is important as the difference in crystal formation is clearly increased with higher concentrations of urease.<sup>70</sup> An increase in crystal formation is also seen with rising pH so this effect can be limited with a pH buffer and Tris buffer has been used with good effect.<sup>62,70</sup> Ebisuno et al. showed that Griffith's artificial urine with Jack bean urease can yield calcium phosphate and struvite crystals concurrently in varying amounts.<sup>117</sup> They were able to confirm the composition of the crystals on light microscopy and infrared spectrum analysis. One benefit of this experimental model is that it can yield results within 24 hours and allows investigators to trial a multitude of urinary modulators under identical experimental conditions.

Given the gap in the research regarding a high-throughput experimental model that can yield reliable results, this project will attempt to develop and validate a high-throughput experimental model to test urinary modulators in infectious kidney stone formation. After validation, the model will be used to test a variety of urinary modulators and to explore the role of different bacterial strains on stone formation.

We have three main aims for this project. Firstly, we plan to create an experimental model that can successfully produce calcium phosphate and struvite that is easily reproducible. Secondly, using our validated experimental model, we will test a variety of urinary modulators and their effects on infectious stone formation. Thirdly, we will use our experimental model to explore the relationship between bacteria and kidney stone formation.

## 1.9

## References

1. Tefekli A, Cezayirli F. The history of urinary stones: In parallel with civilization. *Sci World J*. 2013;2013:1-5. doi:10.1155/2013/423964
2. Richet G. The chemistry of urinary stones around 1800: A first in clinical chemistry. *Kidney Int*. 1995;48(3):876-886. doi:10.1038/ki.1995.364
3. Tundo G, Vollstedt A, Meeks W, Pais V. Beyond prevalence: Annual cumulative incidence of kidney stones in the United States. *J Urol*. 2021;205(6):1704-1709. doi:10.1097/JU.0000000000001629
4. Hill AJ, Basourakos SP, Lewicki P, et al. Incidence of kidney stones in the United States: The continuous national health and nutrition examination survey. *J Urol*. 2022;207(4):851-856. doi:10.1097/ju.0000000000002331
5. Chewcharat A, Curhan G. Trends in the prevalence of kidney stones in the United States from 2007 to 2016. *Urolithiasis*. 2021;49(1):27-39. doi:10.1007/s00240-020-01210-w
6. Bensalah K, Tuncel A, Gupta A, Raman JD, Pearle MS, Lotan Y. Determinants of quality of life for patients with kidney stones. *J Urol*. 2008;179(6):2238-2243. doi:10.1016/j.juro.2008.01.116
7. Pearle MS, Calhoun EA, Curhan GC. Urologic diseases in America project: Urolithiasis. *J Urol*. 2005;173(3):848-857. doi:10.1097/01.ju.0000152082.14384.d7
8. Uribarri J, Oh MS, Carroll HJ. The first kidney stone natural course of renal stone disease. *Ann Intern Med*. 1989;111:1006-1009.
9. Strohmaier WL. Course of calcium stone disease without treatment. What can we expect? *Eur Urol*. 2000;37(3):339-344. doi:10.1159/000052367
10. Maurice-Estépa L, Levillain P, Lacour B, Daudon M. Crystalline phase differentiation in urinary calcium phosphate and magnesium phosphate calculi. *Scand J Urol Nephrol*. 1999;33(5):299-305. doi:10.1080/003655999750017365
11. Abu-Ghanem Y, Kleinmann N, Erlich T, Winkler HZ, Zilberman DE. The impact of dietary modifications and medical management on 24-hour urinary metabolic profiles and the status of renal stone disease in recurrent stone formers. *Isr Med Assoc J*. 2021;23(1):12-16.
12. Moe OW. Kidney stones: Pathophysiology and medical management. *Lancet*. 2006;367:333-344. doi:10.1016/S0140-6736(06)68071-9
13. Yasui T, Okada A, Hamamoto S, et al. Pathophysiology-based treatment of urolithiasis.

- Int J Urol.* 2017;24(1):32-38. doi:10.1111/iju.13187
14. Scales CD, Smith AC, Hanley JM, Saigal CS. Prevalence of kidney stones in the United States. *Eur Urol.* 2012;62:160-165.
  15. Yasui T, Iguchi M, Suzuki S, Kohri K. Prevalence and epidemiological characteristics of urolithiasis in Japan: National trends between 1965 and 2005. *Urology.* 2008;71(2):209-213. doi:10.1016/j.urology.2007.09.034
  16. Ferraro PM, Robertson WG, Johri N, et al. A London experience 1995-2012: Demographic, dietary and biochemical characteristics of a large adult cohort of patients with renal stone disease. *Q J Med.* 2015;108(7):561-568. doi:10.1093/qjmed/hcu251
  17. Viljoen A, Chaudhry R, Bycroft J. Renal stones. *Ann Clin Biochem.* 2019;56(1):15-27. doi:10.1177/0004563218781672
  18. Johnson CM, Wilson DM, O'Fallon WM, Malek RS, Kurland LT. Renal stone epidemiology: A 25 year study in Rochester, Minnesota. *Kidney Int.* 1979;16(5):624-631. doi:10.1038/ki.1979.173
  19. López M, Hoppe B. History, epidemiology and regional diversities of urolithiasis. *Pediatr Nephrol.* 2010;25(1):49-59. doi:10.1007/s00467-008-0960-5
  20. Curhan GC, Willett WC, Rimm EB, Stampfer MJ. Family history and risk of kidney stones. *J Am Soc Nephrol.* 1997;8(10):1568-1573. doi:10.1681/asn.v8i101568
  21. Goldfarb DS, Fischer ME, Keich Y, Goldberg J. A twin study of genetic and dietary influences on nephrolithiasis: A report from the Vietnam Era Twin (VET) registry. *Kidney Int.* 2005;67(3):1053-1061. doi:10.1111/j.1523-1755.2005.00170.x
  22. Roberson D, Sperling C, Shah A, Ziemba J. Economic considerations in the management of nephrolithiasis. *Curr Urol Rep.* 2020;21(5):1-9. doi:10.1007/s11934-020-00971-6
  23. Knoll T, Pearle MS. *Clinical Management of Urolithiasis.* Heidelberg: Springer; 2013.
  24. Aggarwal KP, Narula S, Kakkar M, Tandon C. Nephrolithiasis: Molecular mechanism of renal stone formation and the critical role played by modulators. *Biomed Res Int.* 2013;2013:1-22. doi:10.1155/2013/292953
  25. Coe FL, Evan A, Worcester E. Science in medicine kidney stone disease. *J Clin Investig.* 2005;115(10):2598-2608. doi:10.1172/JCI26662.2598
  26. Rodgers AL. Physicochemical mechanisms of stone formation. *Urolithiasis.* 2017;45(1):27-32. doi:10.1007/s00240-016-0942-1
  27. Ratkalkar VN, Kleinman JG. Mechanisms of stone formation. *Clin Rev Bone Miner*

- Metab.* 2011;9:187-197. doi:10.1007/s12018-011-9104-8
28. Bihl G, Meyers A. Recurrent renal stone disease - Advances in pathogenesis and clinical management. *Lancet.* 2001;358:651-656. doi:10.1016/S0140-6736(01)05782-8
  29. Wein AJ, Kavoussi LR, Partin AW&, Peters CA. *Campbell-Walsh Urology.* 11th ed. Philadelphia, PA: Elsevier; 2016.
  30. Huynh LM, Dianatnejad S, Tofani S, et al. Metabolic diagnoses of recurrent stone formers: Temporal, geographic and gender differences. *Scand J Urol.* 2020;54(6):456-462. doi:10.1080/21681805.2020.1840430
  31. Cameron MA, Pak CYC. Approach to the patient with the first episode of nephrolithiasis. *Clin Rev Bone Miner Metab.* 2004;2(3):265-278. doi:10.1385/BMM:2:3:265
  32. Breslau NA, Brinkley L, Hill KD, Pak CYC. Relationship of animal protein-rich diet to kidney stone formation and calcium metabolism. *J Clin Endocrinol Metab.* 1988;66(1):140-146. doi:10.1210/jcem-66-1-140
  33. Curhan G, Willett W, Rimm E, Stampfer J. A prospective study of dietary calcium and other nutrients and the risk of symptomatic kidney stones. *N Engl J Med.* 1993;328(12):833-838.
  34. Rodrigues FG, Lima TM, Zambrano L, Heilberg IP. Dietary pattern analysis among stone formers: Resemblance to a DASH-style diet. *J Bras Nefrol.* 2020;42(3):338-348. doi:10.1590/2175-8239-JBN-2019-0183
  35. Holmes RP, Goodman HO, Assimos DG. Contribution of dietary oxalate to urinary oxalate excretion. *Kidney Int.* 2001;59(1):270-276. doi:10.1046/j.1523-1755.2001.00488.x
  36. Sakhaee K. Recent advances in the pathophysiology of nephrolithiasis. *Kidney Int.* 2009;75(6):585-595. doi:10.1038/ki.2008.626
  37. Pak CYC. Kidney stones. *Lancet.* 1998;351:1797-1801. doi:10.1016/S0140-6736(98)01295-1
  38. Shadman A, Bastani B. Kidney calculi: Pathophysiology and as a systemic disorder. *Iran J Kidney Dis.* 2017;11(3):180-191.
  39. Carpentier X, Daudon M, Traxer O, et al. Relationships between carbonation rate of carapatite and morphologic characteristics of calcium phosphate stones and etiology. *Urology.* 2009;73(5):968-975. doi:10.1016/j.urology.2008.12.049
  40. Elliot JS, Sharp RF, Lewis L. The solubility of struvite in urine. *J Urol.* 1959;81(3):366-368. doi:10.1016/S0022-5347(17)66025-7

41. Portis AJ, Sundaram CP. Diagnosis and initial management of kidney stones. *Am Fam Physician*. 2001;63(7):1329-1338.
42. Pickard R, Starr K, MacLennan G, et al. Medical expulsive therapy in adults with ureteric colic: A multicentre, randomised, placebo-controlled trial. *Lancet*. 2015;386:341-349. doi:10.1016/S0140-6736(15)60933-3
43. Campschroer T, Zhu X, Vernooij RWM, Lock MTWT. Alpha-blockers as medical expulsive therapy for ureteral stones. *Cochrane Database Syst Rev*. 2018;(4):1-164. doi:10.1002/14651858.CD008509.pub3
44. Worcester EM, Coe FL. Calcium kidney stones. *N Engl J Med*. 2010;363(10):954-963. doi:10.1056/nejmcp1001011
45. Hosking DH, Erickson SB, van Den Berg CJ, Wilson DM, Smith LH. The stone clinic effect in patients with idiopathic calcium urolithiasis. *J Urol*. 1983;130(6):1115-1118. doi:10.1016/S0022-5347(17)51711-5
46. Wilkinson H. Clinical investigation and management of patients with renal stones. *Ann Clin Biochem*. 2001;38(3):180-187. doi:10.1258/0004563011900623
47. Reynolds TM. Chemical pathology clinical investigation and management of nephrolithiasis. *J Clin Pathol*. 2005;58(2):134-140. doi:10.1136/jcp.2004.019588
48. Goldfarb DS. Empiric therapy for kidney stones. *Urolithiasis*. 2019;47(1):107-113. doi:10.1007/s00240-018-1090-6
49. Borghi L, Meschi T, Amato F, Briganti A, Novarini A, Giannini A. Urinary volume, water and recurrences in idiopathic calcium nephrolithiasis: A 5-year randomized prospective study. *J Urol*. 1996;155(3):839-843. doi:10.1016/S0022-5347(01)66321-3
50. Borghi L, Meschi T, Maggiore U, Prati B. Dietary therapy in idiopathic nephrolithiasis. *Nutr Rev*. 2006;64(7):301-312. doi:10.1301/nr.2006.jul.301-312
51. Borghi L, Schianchi T, Meschi T, et al. Comparison of two diets for the prevention of recurrent stones in idiopathic hypercalciuria. *N Engl J Med*. 2002;346(2):77-84.
52. Taylor EN, Stampfer MJ, Curhan GC. Dietary factors and the risk of incident kidney stones in men: New insights after 14 years of follow-up. *J Am Soc Nephrol*. 2004;15(12):3225-3232. doi:10.1097/01.ASN.0000146012.44570.20
53. Pearle MS, Roehrborn CG, Pak CYC. Meta-analysis of randomized trials for medical prevention of calcium oxalate nephrolithiasis. *J Endourol*. 1999;13(9):679-685. doi:10.1089/end.1999.13.679
54. Hess B, Jost C, Zipperle L, Takkinen R, Jaeger P. High-calcium intake abolishes

- hyperoxaluria and reduces urinary crystallization during a 20-fold normal oxalate load in humans. *Nephrol Dial Transplant*. 1998;13(9):2241-2247. doi:10.1093/ndt/13.9.2241
55. Ettinger B, Tang A, Citron JT, Livermore B, Williams T. Randomized trial of allopurinol in the prevention of calcium oxalate calculi. *N Engl J Med*. 1986;315(22):1386-1389.
  56. Barcelo P, Wuhl O, Servitge E, Rousaud A, Pak CYC. Randomized double-blind study of potassium citrate in idiopathic hypocitraturic calcium nephrolithiasis. *J Urol*. 1993;150(6):1761-1764. doi:10.1016/S0022-5347(17)35888-3
  57. Ettinger B, Pak CYC, Citron JT, Thomas C, Adams-Huet B, Vangessel A. Potassium-magnesium citrate is an effective prophylaxis against recurrent calcium oxalate nephrolithiasis. *J Urol*. 1997;158(6):2069-2073. doi:10.1016/S0022-5347(01)68155-2
  58. Heilberg IP. Treatment of patients with uric acid stones. *Urolithiasis*. 2016;44(1):57-63. doi:10.1007/s00240-015-0843-8
  59. Abou Chakra M, Dellis AE, Papatsoris AG, Moussa M. Established and recent developments in the pharmacological management of urolithiasis: An overview of the current treatment armamentarium. *Expert Opin Pharmacother*. 2020;21(1):85-96. doi:10.1080/14656566.2019.1685979
  60. Trinchieri A, Montanari E. Biochemical and dietary factors of uric acid stone formation. *Urolithiasis*. 2018;46(2):167-172. doi:10.1007/s00240-017-0965-2
  61. Schwartz BF, Stoller ML. Nonsurgical management of infection-related renal calculi. *Urol Clin North Am*. 1999;26(4):765-778. doi:10.1016/S0094-0143(05)70217-2
  62. Hedelin H, Grenabo L, Pettersson S. The effects of urease in undiluted human urine. *J Urol*. 1986;136(3):743-745. doi:10.1016/S0022-5347(17)45040-3
  63. Bichler K, Eipper E, Naber K, Braun V, Zimmerman R, Lahme S. Urinary infection. *Int J Antimicrob Agents*. 2002;19:488-498. doi:10.1159/000281177
  64. Elmansy HE, Lingeman JE. Recent advances in lithotripsy technology and treatment strategies: A systematic review update. *Int J Surg*. 2016;36:676-680. doi:10.1016/j.ijsu.2016.11.097
  65. Wright AE, Rukin NJ, Somani BK. Ureterscopy and stones: Current status and future expectations. *World J Nephrol*. 2014;3(4):243-248. doi:10.5527/wjn.v3.i4.243
  66. Fernström I, Johansson B. Percutaneous pyelolithotomy - A new extraction technique. *Scand J Urol Nephrol*. 1976;10:257-259.
  67. Sabler IM, Katafigiotis I, Gofrit ON, Duvdevani M. Present indications and techniques of percutaneous nephrolithotomy: What the future holds? *Asian J Urol*. 2018;5(4):287-294.

doi:10.1016/j.ajur.2018.08.004

68. Khan SR, Kok DJ. Modulators of urinary stone formation. *Front Biosci.* 2004;9:1450-1482. doi:10.2741/1347
69. Chauhan CK, Joshi MJ. *In vitro* crystallization, characterization and growth-inhibition study of urinary type struvite crystals. *J Cryst Growth.* 2013;362(1):330-337. doi:10.1016/j.jcrysgro.2011.11.008
70. Hedelin H, Grenabo L, Pettersson S. Urease-induced crystallization in synthetic urine. *J Urol.* 1985;133(3):529-532. doi:10.1016/S0022-5347(17)49047-1
71. Hansen NM, Felix R, Bisaz S, Fleisch H. Aggregation of hydroxyapatite crystals. *Biochim Biophys Acta.* 1976;451:549-559. doi:10.1016/0304-4165(76)90150-1
72. Jacobs D, Heimbach D, Hesse A. Chemolysis of struvite stones by acidification of artificial urine. *Scandinavian J Urol Nephrol.* 2001;35:345-349.
73. Griffith DP. Struvite stones. *Kidney Int.* 1978;13(5):372-382. doi:10.1038/ki.1978.55
74. Hellström J. The significance of *Staphylococci* in the development and treatment of renal and ureteral stones. *Br J Urol.* 1938;10(4):348-372. doi:10.1111/j.1464-410X.1938.tb10342.x
75. Chutipongtanate S, Sutthimethakorn S, Chiangjong W, Thongboonkerd V. Bacteria can promote calcium oxalate crystal growth and aggregation. *J Biol Inorg Chem.* 2013;18(3):299-308. doi:10.1007/s00775-012-0974-0
76. Barr-Beare E, Saxena V, Hilt EE, et al. The interaction between *Enterobacteriaceae* and calcium oxalate deposits. *PLoS One.* 2015;10(10):1-17. doi:10.1371/journal.pone.0139575
77. Caballero D, Li Y, Fetene J, et al. Intraperitoneal pyrophosphate treatment reduces renal calcifications in *Npt2a* null mice. *PLoS One.* 2017;12(7):1-14. doi:10.1371/journal.pone.0180098
78. Wikström B, Danielson BG, Ljunghall S, McGuire M, Russell RGG. Urinary pyrophosphate excretion in renal stone formers with normal and impaired renal acidification. *World J Urol.* 1983;1(3):150-154. doi:10.1007/BF00326903
79. Basavaraj DR, Biyani CS, Browning AJ, Cartledge JJ. The role of urinary kidney stone inhibitors and promoters in the pathogenesis of calcium containing renal stones. *EAU-EBU Updat Ser.* 2007;5:126-136. doi:10.1016/j.eeus.2007.03.002
80. Hedelin H, Grenabo L, Pettersson S. The effects of glycosaminoglycans, pyrophosphate and allopurinol treatment on urease-induced crystallization *in vitro*. *Urol Res.*

- 1986;14(6):305-307. doi:10.1007/BF00262380
81. Hallson PC, Rose GA, Sulaiman S. Pyrophosphate does not influence calcium oxalate or calcium phosphate crystal formation in concentrated whole human urine. *Urol Res.* 1983;11(4):151-154. doi:10.1007/BF00256361
  82. Ryall RL. Urinary inhibitors of calcium oxalate crystallization and their potential role in stone formation. *World J Urol.* 1997;15(3):155-164. doi:10.1007/BF02201852
  83. Torzewska A, Rozalski A. Inhibition of crystallization caused by *Proteus mirabilis* during the development of infectious urolithiasis by various phenolic substances. *Microbiol Res.* 2014;169:579-584. doi:10.1016/j.micres.2013.09.020
  84. Wang Y, Grenabo L, Hedelin H, McLean RJC, Nickel JC, Pettersson S. Citrate and urease-induced crystallization in synthetic and human urine. *Urol Res.* 1993;21(2):109-115. doi:10.1007/BF01788828
  85. McLean RJC, Nickel JC. Glycosaminoglycans and struvite calculi. *World J Urol.* 1994;12(1):49-51. doi:10.1007/BF00182051
  86. Beshensky AM, Wesson JA, Worcester EM, Sorokina EJ, Snyder CJ, Kleinman JG. Effects of urinary macromolecules on hydroxyapatite crystal formation. *J Am Soc Nephrol.* 2001;12(10):2108-2116. doi:10.1681/asn.v12i102108
  87. Grover PK, Ryall RL, Marshall VR. Does Tamm-Horsfall mucoprotein inhibit or promote calcium oxalate crystallization in human urine? *Clin Chim Acta.* 1990;190(3):223-238. doi:10.1016/0009-8981(90)90176-S
  88. Coe FL, Nakagawa Y, Parks JH. Inhibitors within the nephron. *Am J Kidney Dis.* 1991;17(4):407-413. doi:10.1016/S0272-6386(12)80633-0
  89. Caballero D, Li Y, Ponsetto J, Zhu C, Bergwitz C. Impaired urinary osteopontin excretion in *Npt2a*<sup>-/-</sup> mice. *Am J Physiol - Ren Physiol.* 2017;312:F77-F83. doi:10.1152/ajprenal.00367.2016
  90. Asakura H, Selengut JD, Orme-Johnson WH, Dretler SP. The effect of calprotectin on the nucleation and growth of struvite crystals as assayed by light microscopy in real-time. *J Urol.* 1998;159(4):1384-1389. doi:10.1016/S0022-5347(01)63621-8
  91. Hugosson J, Grenabo L, Hedelin H, Pettersson S. Effects of serum, albumin and immunoglobulins on urease-induced crystallization in urine. *Urol Res.* 1990;18(6):407-411. doi:10.1007/BF00297374
  92. Sikirić M, Babić-Ivančić V, Milat O, Sarig S, Füredi-Milhofer H. Factors influencing additive interactions with calcium hydrogenphosphate dihydrate crystals. *Langmuir.* 2000;16(24):9261-9266. doi:10.1021/la000704m

93. Burke EM, Guo Y, Colon L, Rahima M, Veis A, Nancollas GH. Influence of polyaspartic acid and phosphophoryn on octacalcium phosphate growth kinetics. *Colloids Surfaces B Biointerfaces*. 2000;17(1):49-57. doi:10.1016/S0927-7765(99)00084-3
94. Schaad P, Gramain P, Gorce F, Voegel JC. Dissolution of synthetic hydroxyapatite in the presence of lanthanum ions. *J Chem Soc Faraday Trans*. 1994;90(22):3405-3408. doi:10.1039/FT9949003405
95. Bigi A, Bracci B, Panzavolta S, et al. Morphological and structural modifications of octacalcium phosphate induced by poly-L-aspartate. *Cryst Growth Des*. 2004;4(1):141-146. doi:10.1021/cg034078d
96. Hallson PC, Rose GA, Sulaiman S. Magnesium reduces calcium oxalate crystal formation in human whole urine. *Clin Sci*. 1982;62(1):17-19. doi:10.1042/cs0620017
97. Lemann J, Relman AS. The relation of sulfur metabolism to acid-base balance and electrolyte excretion: The effects of DL-methionine in normal man. *J Clin Invest*. 1959;38:2215-2223. doi:10.1172/JCI104001
98. Siener R, Struwe F, Hesse A. Effect of L-methionine on the risk of phosphate stone formation. *Urology*. 2016;98:39-43. doi:10.1016/j.urology.2016.08.007
99. Sabiote L, Emiliani E, Kanashiro AK, et al. Oral acidification with L-Methionine as a noninvasive treatment for encrusted uropathy. *J Endourol Case Reports*. 2020;6(3):143-146. doi:10.1089/cren.2019.0164
100. Rodgers A, Gauvin D, Edeh S, Allie-Hamdulay S, Jackson G, Lieske JC. Sulfate but not thiosulfate reduces calculated and measured urinary ionized calcium and supersaturation: Implications for the treatment of calcium renal stones. *PLoS One*. 2014;9(7):1-12. doi:10.1371/journal.pone.0103602
101. Edwards NA, Russell RGG, Hodgkinson A. The effect of oral phosphate in patients with recurrent renal calculus. *Br J Urol*. 1965;37(4):390-398. doi:10.1111/j.1464-410X.1965.tb09615.x
102. Prywer J, Torzewska A. Effect of curcumin against *Proteus mirabilis* during crystallization of struvite from artificial urine. *Evidence-based Complement Altern Med*. 2012;2012:1-7. doi:10.1155/2012/862794
103. Chi T, Kim MS, Lang S, et al. A *Drosophila* model identifies a critical role for zinc in mineralization for kidney stone disease. *PLoS One*. 2015;10(5):1-21. doi:10.1371/journal.pone.0124150
104. Miller J, Chi T, Kapahi P, et al. *Drosophila melanogaster* as an emerging translational model of human nephrolithiasis. *J Urol*. 2013;190(5):1648-1656. doi:10.1016/j.juro.2013.03.010

105. Al KF, Daisley BA, Chanyi RM, et al. Oxalate-degrading *Bacillus subtilis* mitigates urolithiasis in a *Drosophila melanogaster* model. *mSphere*. 2020;5(5). doi:10.1128/msphere.00498-20
106. Chen YH, Liu HP, Chen HY, et al. Ethylene glycol induces calcium oxalate crystal deposition in Malpighian tubules: A *Drosophila* model for nephrolithiasis/urolithiasis. *Kidney Int*. 2011;80(4):369-377. doi:10.1038/ki.2011.80
107. Ali SN, Dayarathna TK, Ali AN, et al. *Drosophila melanogaster* as a function-based high-throughput screening model for anti-nephrolithiasis agents in kidney stone patients. *Dis Model Mech*. 2018;11(11). doi:10.1242/dmm.035873
108. Nickel JC, Olson M, McLean RJC, Grant SK, Costerton JW. An ecological study of infected urinary stone genesis in an animal model. *Br J Urol*. 1987;59(1):21-30. doi:10.1111/j.1464-410X.1987.tb04573.x
109. Olson ME, Nickel JC, Costerton JW. Animal model of human disease. Infection-induced struvite urolithiasis in rats. *Am J Pathol*. 1989;135(3):581-583.
110. Mandel NS, Henderson JD, Hung LY, Wille DF, Wiessner JH. A porcine model of calcium oxalate kidney stone disease. *J Urol*. 2004;171(3):1301-1303. doi:10.1097/01.ju.0000110101.41653.bb
111. Rosenow EC, Meisser JG. The production of urinary calculi by the devitalization and infection of teeth in dogs with *Streptococci* from cases of nephrolithiasis. *Arch Intern Med*. 1923;31(6):807-829. doi:10.1001/archinte.1923.00110180026003
112. Naito Y, Ohtawara Y, Kageyama S, et al. Morphological analysis of renal cell culture models of calcium phosphate stone formation. *Urol Res*. 1997;25(1):59-65. doi:10.1007/BF00941907
113. Chmiel JA, Stuivenberg GA, Alathel A, et al. High-throughput *in vitro* gel-based plate assay to screen for calcium oxalate stone inhibitors. *Urol Int*. 2021:1-7. doi:10.1159/000519842
114. Gilad R, Williams JC, Usman KD, et al. Interpreting the results of chemical stone analysis in the era of modern stone analysis techniques. *J Nephrol*. 2017;30(1):135-140. doi:10.1007/s40620-016-0274-9
115. Addadi L, Moradian J, Shay E, Maroudas NG, Weiner S. A chemical model for the cooperation of sulfates and carboxylates in calcite crystal nucleation: Relevance to biomineralization. *Proc Natl Acad Sci*. 1987;84(9):2732-2736. doi:10.1073/pnas.84.9.2732
116. Griffith DP, Musher DM, Itin C. Urease. The primary cause of infection induced urinary stones. *Invest Urol*. 1976;13(5):346-350.

117. Ebisuno S, Komura T, Yamagiwa K, Ohkawa T. Urease-induced crystallizations of calcium phosphate and magnesium ammonium phosphate in synthetic urine and human urine. *Urol Res.* 1997;25(4):263-267. doi:10.1007/BF00942096
118. Torzewska A, Rózalski A. *In vitro* studies on the role of glycosaminoglycans in crystallization intensity during infectious urinary stones formation. *Apmis.* 2014;122(6):505-511. doi:10.1111/apm.12191
119. McLean RJC, Downey J, Clapham L, Nickel JC. A simple technique for studying struvite crystal growth *in vitro*. *Urol Res.* 1990;18(1):39-43. doi:10.1007/BF00294580
120. Brooks T, Keevil CW. A simple artificial urine for the growth of urinary pathogens. *Lett Appl Microbiol.* 1997;24(3):203-206. doi:10.1046/j.1472-765X.1997.00378.x

## Chapter 2

### **2 Creating and validating a high-throughput experimental model for infectious stone formation**

Urinary stone disease is an extremely common condition that is recurrent and increasing in incidence. Infectious stones are more common in vulnerable patients and can lead to significant morbidity in all those afflicted. It has been well documented that urease producing bacteria and an elevated urinary pH promote struvite and calcium phosphate stone formation. However, these stones can also form in the absence of diagnosed clinical infections which suggests that there are alternative factors mediating the development of these stones not yet fully appreciated. Understanding the pathways leading to the formation of these two different stone types may have preventative and therapeutic implications.

A variety of experimental models have been used to investigate urinary modulators in infectious stone formation, yet no single model has provided clear and reliable results to test the long list of possible modulators. The following chapter details an improved model able to test for these urinary modulators in infectious stone formation. During our testing stage, multiple urine media, urease concentrations and other experimental conditions were utilized to try and find an optimal system to compare different urinary modulators. Model validation occurred by confirming both struvite and calcium phosphate crystals with the experimental components and conditions used.

## 2.1 Introduction

### 2.1.1 Experimental models

Given the plethora of urinary modulators and bacterial species investigated in infectious stone formation, a reliable experimental model which allows for consistent experimental conditions and rapid results is needed. Currently, many models in this regard have been attempted, however, significant heterogeneity in experimental design exists which complicates the best approach to study both calcium phosphate and struvite formation simultaneously.

Diffusion gel growth models have been used to test inhibitors of struvite crystal formation.<sup>1,2</sup> These are made by creating a silica hydrogel with different concentrations of one reactant (i.e., ammonium dihydrogen phosphate) in a test tube with struvite crystals. A supernatant of the second reactant (i.e., magnesium acetate) and the modulator of interest are added to test tubes that are placed under an airtight seal. Downsides to this technique include the time delay to observe the effects and only one crystal type can be tested at a time. Diffusion gels take two days to create and potentially weeks to see the results depending on the experimental end points.<sup>1,2</sup> Combining the two reactants in a test tube has less clinical relevance because it omits other compounds in urine that may alter the reaction. The use of seed crystals has been used previously to study crystal formation and growth, however this artificially promotes nucleation to a crystal already formed and does not naturally allow for neogenesis of struvite and calcium phosphate crystals.<sup>3-5</sup>

In contrast to the length of time diffusion gel growth models take, microfluidic devices can monitor calcium phosphate and struvite crystal formation in real-time.<sup>6,7</sup> The purpose of this model is to stimulate renal tubular flow by using a single cell layer within

a 3D tubular structure and flushing solutions through at a controlled rate. The type of solution is chosen based on the crystal of interest (calcium oxalate, calcium phosphate, etc.) during a particular study. Crystals are visible within 20 minutes and their materialization can be viewed in real-time with microscopy. While the quick results under stable conditions are desirable, there are limitations to widespread use of this model. For example, only one crystal at a time can be studied and the specialized equipment required is very expensive.

The Madine Darby Canine Kidney (MDCK) cell culture model, derived from canine renal distal tubular epithelium, has been used to study calcium phosphate stone formation.<sup>8</sup> In this case, cells are grown as monolayers in plastic culture flasks, three-dimensional soft agar culture or collagen gel culture. Light microscopy is used to count the colonies with microliths and compare that to the total number of colonies grown over time. For this technique, it takes weeks for crystal propagation and the maintenance of cell cultures is quite labour intensive.<sup>8</sup>

Beyond the three models mentioned above, artificial urine with the addition of urease has been used to successfully produce calcium phosphate and struvite crystals simultaneously in the same experiment.<sup>9</sup> Benefits of this model setup include consistent concentrations of the components, relatively low cost, long shelf life of components involved and the ease at which a large number of urinary modulators can be tested. A wide range of urease concentrations have been investigated in infectious crystal formation in prior studies with no evidence to support the most suitable urease concentration for studying urinary modulators. Monitoring and controlling for pH are also important considerations in the development of the experimental design as it has

consistently been shown that increasing pH will accelerate calcium phosphate and struvite crystal formation.<sup>1,10,11</sup>

### **2.1.2 Urine media**

In the past, urine from healthy and stone forming humans has been used to study infectious stone formation.<sup>12</sup> Hedelin et al. noted that the crystallization of calcium phosphate and struvite in urine from individual humans differed markedly.<sup>13</sup> In the study, two patients had the exact same urine pH, but the volume of struvite and calcium phosphate crystals varied by a factor of 1:5, supporting the premise that other factors are involved besides urinary alkalization.<sup>13</sup> Furthermore, the composition and components of human urine also can vary by gender, age, race, weight and diet.<sup>14-17</sup>

A variety of solutions and artificial urines have been utilized to study stone formation. In an effort to create a solution to help investigate struvite crystal formation, Asakura et al. used a “minimal urine solution” comprised of only a few compounds.<sup>18</sup> Additionally, modifying calcium concentration has commonly been studied for differences in the ratio of calcium phosphate and struvite crystal formation.<sup>11,18,19</sup>

Common types of artificial urine include Griffith’s as well as Brooks and Keevil (hereto referred to as Brooks). Griffith’s artificial urine was first described in 1976 and has been frequently used when investigating infectious stone formation.<sup>20</sup> Brooks developed a different artificial urine model to specifically study urinary pathogens, but they noted formation of rudimentary struvite and calcium phosphate crystals.<sup>21</sup> Unsurprisingly, Brooks artificial urine has been used in experimental models for infectious kidney stone formation.<sup>22</sup> Despite these prior studies, the ideal urine media and

experimental conditions have not been clearly elucidated for the study of infectious stone formation.

The purpose of this study was to identify the best urine media and urease concentration to study infectious stone formation. We hypothesize that Griffith's artificial urine would be the best media for the current study because both calcium phosphate and struvite crystal have consistently formed *in vitro*. We aim to identify a urease concentration that allows crystal formation to occur, but slowly enough that we can add urinary modulators that will have modifiable and detectable differences in the reaction.

## **2.2 Materials and Methods**

Review ethics board approval from Western University was attained for urine for testing biomaterials (116471).

### **2.2.1 Infectious stone experimental model**

#### **2.2.1.1 Optimization of crystal forming assay**

Griffith's artificial urine (Table 4)<sup>20</sup> and Brooks artificial urine (Table 5)<sup>21</sup> was made as previously described. Both artificial urines were filtered through a 0.22 µm pore vacuum filter and stored at 4°C. Jack bean urease (Cat# 94280-5G, Sigma-Aldrich, Oakville, Ontario, Canada) was partitioned into 50 U/mL aliquots and frozen at -20°C to avoid freeze-thaw degradation of the enzyme.

**Table 4: Composition of Griffith's artificial urine.**

Compound	Amount (g/L)
CaCl <sub>2</sub> •2H <sub>2</sub> O	0.65
MgCl <sub>2</sub> •6H <sub>2</sub> O	0.65
NaCl	4.6
Na <sub>2</sub> SO <sub>4</sub>	2.3
Na <sub>3</sub> citrate•2H <sub>2</sub> O	0.65
Na <sub>2</sub> oxalate	0.02
KH <sub>2</sub> PO <sub>4</sub>	2.8
KCl	1.6
NH <sub>4</sub> Cl	1.0
Creatinine	1.1
Urea	25.0
<i>Initial pH = 5.7</i>	

**Table 5: Composition of Brooks artificial urine.**

Compound	Amount (g/L)
Peptone L37	1
Yeast extract	0.005
Lactic acid	0.1
Citric acid	0.4
Sodium bicarbonate	2.1
Urea	10
Uric acid	0.07
Creatinine	0.8
CaCl <sub>2</sub> •2H <sub>2</sub> O	0.37
NaCl	5.2
FeSO <sub>4</sub> •7H <sub>2</sub> O	0.0012
MgSO <sub>4</sub> •7H <sub>2</sub> O	0.49
NaSO <sub>4</sub> •10H <sub>2</sub> O	3.2
KH <sub>2</sub> PO <sub>4</sub>	0.95
K <sub>2</sub> HPO <sub>4</sub>	1.2
NH <sub>4</sub> Cl	1.3
<i>Initial pH = 6.5</i>	

Griffith's artificial urine, Brooks artificial urine, and human pooled (HPU) from three non-stone forming female donors were tested. In brief, volumes of 10 mL urine and concentrations of 0.01 U/mL, 0.02 U/mL, 0.05 U/mL, 0.1 U/mL, 0.2 U/mL, and 0.25 U/mL of Jack bean urease were mixed in test tubes. These urease concentrations were

selected based on the experiments by Hedelin et al.<sup>11</sup> From each reaction, 200  $\mu$ L of urine was pipetted into a 96-well plate (Sarstedt, Nümbrecht, Germany) in technical duplicate. Plates were incubated at 37°C for 8 hours and absorbance was recorded every 10 minutes at 660 nm. The Biotek Eon Microplate Spectrophotometer (Winooski, Vermont, USA) and the Gen 5 v2.0 (Winooski, Vermont, USA) software were used for analyzing all 96-well plates.

The next experimental run was completed with Brooks artificial urine, Griffith's artificial urine, and human urine from a single male non-stone former. In this experimental run, a urease concentration over 0.2 U/mL was not tested based on the results of the previous experiment. Since the precipitation of the reactions were observed within 2 hours with little change beyond 4 hours, plates were incubated at 37°C for 4 hours and absorbance was recorded every 5 minutes at 660 nm.

While this will be elaborated on further, it was important to identify early the appropriate urease concentration and ideal medium which was determined to be Griffith's artificial urine owing to its consistent results and similar growth curves to human media. Given these findings, Griffith's artificial urine using concentrations of 0 U/mL, 0.05 U/mL, 0.075 U/mL, 0.1 U/mL, 0.125 U/mL, 0.15 U/mL, 0.175 U/mL, 0.2 U/mL Jack bean urease were tested. Griffith's artificial urine with a low calcium concentration (0.4 M) was tested with because Ebisuno et al. showed that a higher concentration of calcium led to more calcium phosphate crystals compared to a low calcium concentration, which favours struvite crystal formation.<sup>19</sup> Both Griffith's and low calcium Griffith's artificial urine were placed in a 96-well plate in technical triplicate. Plates were incubated at 37°C

for 4 hours and absorbance was recorded every 5 minutes at 660 nm. After 4 hours, pH levels were assessed using pH test strips (VWR Chemicals BDH, Germany).

The pH levels within the experiments were drastically different, so we added a Tris buffer to the model. A 1 M Tris HCl pH 8.3 solution was prepared by dissolving 12.114 g Tris in deionized water, pH adjusted by NaOH to a final volume of 100 mL. Since Tris buffer is temperature sensitive, a buffer with a pH of 8.3 at 20°C was made resulting in a final pH of 8.0 at the incubation temperature of 37°C. The solution was then vacuum filtered through a 0.22 µm filter for sterilization. In between experiments, the Tris buffer was stored at 4°C.

The experiment was repeated using Griffith's artificial urine, a low calcium concentration (0.4 M) Griffith's urine and human urine from a non-stone former used with concentrations of 0.075 U/mL and 0.15 U/mL Jack Bean urease with 40 µL 1 M Tris buffer providing a buffering capacity of 4 mM. Comparative experiments were done with the same concentration of urease without Tris buffer. Plates were incubated at 37°C for 4 hours and absorbance was recorded every 5 minutes at 660 nm. After 24 hours, the pH values were checked for each reaction.

### **2.2.1.2 Microscopic analysis of crystal formation**

Crystals were collected for microscopy to confirm the presence of struvite or calcium phosphate crystals after 24 hours of incubation in the test tubes filled with 10 mL urine media and other reactants. Briefly, crystal suspensions were centrifuged at  $1620 \times g$  (3000 rpm) (Eppendorf 5804 R, Mississauga, Ontario, Canada) for 5 minutes at 22°C.

The supernatant was decanted and, using a wide bore pipette, the crystal suspension was

placed on a microscope slide. Slides were examined under a Nikon Eclipse Ts2R (Melville, New York, USA) microscope at 400x magnification to look for struvite and calcium phosphate crystals. Multiple images of the crystals were taken with both the birefringent lens and white light and processed using NIS elements software (Melville, New York, USA).

### **2.2.1.3 Scanning electron microscopy and X-ray diffraction**

Each solution was filtered through a 0.22  $\mu\text{m}$  vacuum filtration system and the crystals were washed off the filter paper with deionized water. The crystals were left suspended in water to allow for preparation for scanning electron microscopy (SEM) and energy dispersive X-ray spectroscopy (EDX). A random sample of each solution was mounted on silica and examined with SEM (Zeiss/Leo 1540XB FESEM, Oberkochen, Germany). EDX (Oxford Instruments X Max 50, England, United Kingdom) was performed to assess the molecular composition of the crystals.

### **2.2.1.4 Adjusting Tris buffering capacity**

The pH values in the initial experiments were not remaining within a physiologic range that would be amenable to studying urinary modulators in the model. Consequently, a second Tris buffer was prepared at 7.52 at 37°C. After which, an experimental run using normal Griffith's and low calcium Griffith's artificial urine with 0.075 U/mL and 0.1 U/mL Jack bean urease with the newly modified Tris buffer was conducted.

### **2.2.2 Statistical analysis**

Statistical analysis was carried out with RStudio version 2022.02.1 (Boston, MA, USA) using the Growthcurver package version 0.3.1 to analyze crystal growth curves.<sup>23</sup> All graphs and figures were created were accomplished using Prism – GraphPad version 9.3.1(San Diego, CA, USA).

## **2.3 Results**

### **2.3.1 Experimental model**

#### **2.3.1.1 Comparing Brooks and Griffith's artificial urine to human pooled urine**

Concentrations of urease had a clear effect on the timing and rapidity of crystal formation in all urine media. The crystals formed very quickly with little time from the initiation of the experiment to crystal formation for the higher concentrations of urease. As seen in Figure 1, a steep curve on the graph correlates with a more rapid reaction while the area under the curve demonstrates overall crystal volume in the reaction. Quantitative values were calculated using “growth curver package” and results from the first experimental run can be found in Table 6.

Slope of the growth curves ( $r$ ) for crystal formation were different between the Griffith's and Brooks artificial urine as demonstrated in Table 3. When observing the slopes for all three media at 0.1 U/mL, Griffith's was 0.027, Brooks was 0.130 and HPU was 0.038. Overall, the slopes are more similar for a given concentration between Griffith's and HPU compared to Brooks. Another area of interest is the doubling time

( $t_{gen}$ ) of the analysis. A much quicker reaction is demonstrated given that Brooks had a faster doubling time compared to HPU and Griffith's (Figure 1). However, such robust reactions leading to early crystal formation would make it challenging to evaluate added urinary modulators as the urease might overwhelm the modulating effect. A lower concentration range was tested to see how it would affect the slopes of the graphs.

Timing of the reactions started within two hours and most of the reactions were completed by four hours. This shortening of the experimental length and interval time with the spectrophotometer limits extraneous data and improve efficiency of the model.

**Table 6: Growth curve output for Griffith's, Brooks, and human pooled urine at varying urease concentrations.**

Urine Sample	k	n <sup>0</sup>	r	t_mid	t_gen	auc_l	auc_e	sigma
0.25 U/mL Griffith's	0.30	0.00	0.04	136.21	19.32	103.15	101.98	0.02
0.20 U/mL Griffith's	0.35	0.01	0.03	104.94	22.30	131.68	130.30	0.03
0.1 U/mL Griffith's	0.24	0.01	0.03	138.65	26.15	82.45	81.35	0.02
0.05 U/mL Griffith's	0.15	0.00	0.04	174.64	16.44	45.63	45.39	0.01
0.02 U/mL Griffith's	0.00	0.03	0.12	-0.14	5.61	0.30	0.45	0.00
0.01 U/mL Griffith's	0.00	0.02	0.03	-1.08	24.03	0.36	0.42	0.00
0.25 U/mL Brooks	0.43	0.03	0.18	15.47	3.92	199.36	198.62	0.01
0.20 U/mL Brooks	0.42	0.01	0.19	20.92	3.67	191.17	189.80	0.02
0.1 U/mL Brooks	0.40	0.00	0.13	36.56	5.34	176.24	174.98	0.02
0.05 U/mL Brooks	0.31	0.00	0.07	61.53	9.78	128.22	127.50	0.02
0.02 U/mL Brooks	0.23	0.01	0.02	132.67	29.41	80.58	79.45	0.02
0.01 U/mL Brooks	0.23	0.01	0.02	143.27	28.89	77.10	75.95	0.02
0.25 U/mL HPU	0.08	0.00	0.06	56.28	11.37	32.64	32.50	0.00
0.20 U/mL HPU	0.08	0.00	0.06	64.99	12.30	30.90	30.74	0.01
0.1 U/mL HPU	0.08	0.00	0.04	106.25	18.29	28.14	27.88	0.01
0.05 U/mL HPU	0.05	0.00	0.03	183.11	21.63	15.45	15.23	0.00
0.02 U/mL HPU	0.05	0.00	0.03	235.28	21.55	11.12	11.01	0.00
0.01 U/mL HPU	0.05	0.00	0.03	236.47	20.74	10.94	10.88	0.00

$k$  = growth capacity,  $n^0$  = degrees of freedom,  $r$  = growth rate,  $t_{mid}$  = time to inflection point,  $t_{gen}$  = doubling time,  $auc_l$  = logistic area under the curve,  $auc_e$  = empiric area under the curve,  $\sigma$  = goodness of fit.

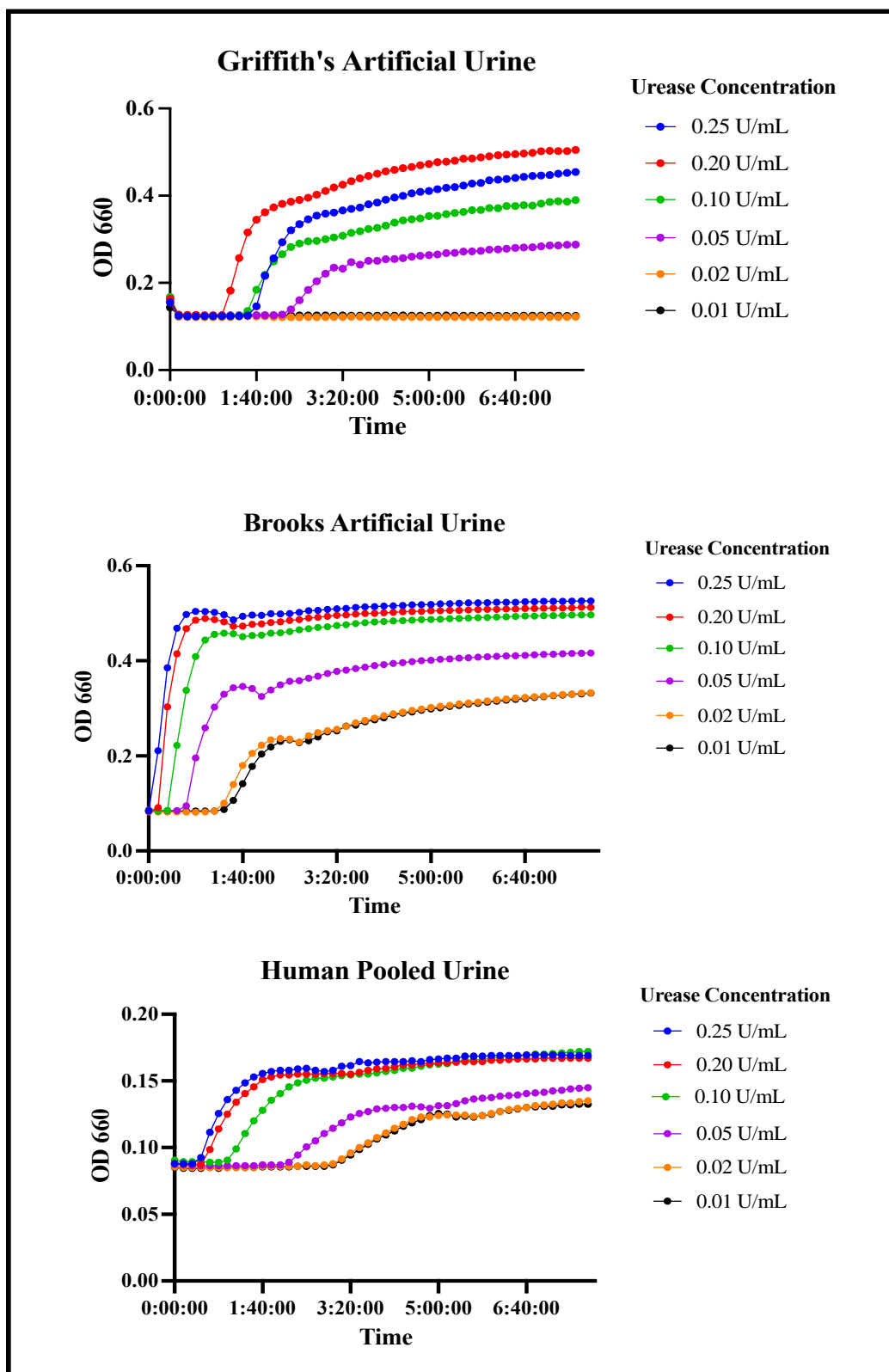


**Figure 1: Crystal growth curves with Griffith's, Brooks, and human pooled urine with varying urease concentrations measured by absorbance at a wavelength of 660 nm.**

### **2.3.1.2 Comparing Brooks and Griffith's artificial urine to human urine from a non-stone former**

Brooks artificial urine had extremely rapid crystal formation even at low urease concentrations which can be seen in Table 7 with high  $r$  values and faster doubling times ( $t_{gen}$ ). This is consistent with the curves seen in Figure 2A. Across the various concentrations of urease, Brooks developed crystals quicker than both human urine and Griffith's artificial urine. Griffith's artificial urine was noted only to develop crystals at concentrations of 0.1 and 0.085 U/mL, however, this was not consistent with later experiments (Figure 5). In contrast, human urine produced crystals at all tested concentrations of urease. Of the developed crystals, the visual quality was superior in Griffith's urine compared to Brooks artificial urine (Figures 2 and 3). The crystals in Brooks were more widely spaced with less cohesion, thus making accurate identification under light microscopy more uncertain while the crystals in Griffith's were easier to identify and categorize into calcium phosphate and struvite.

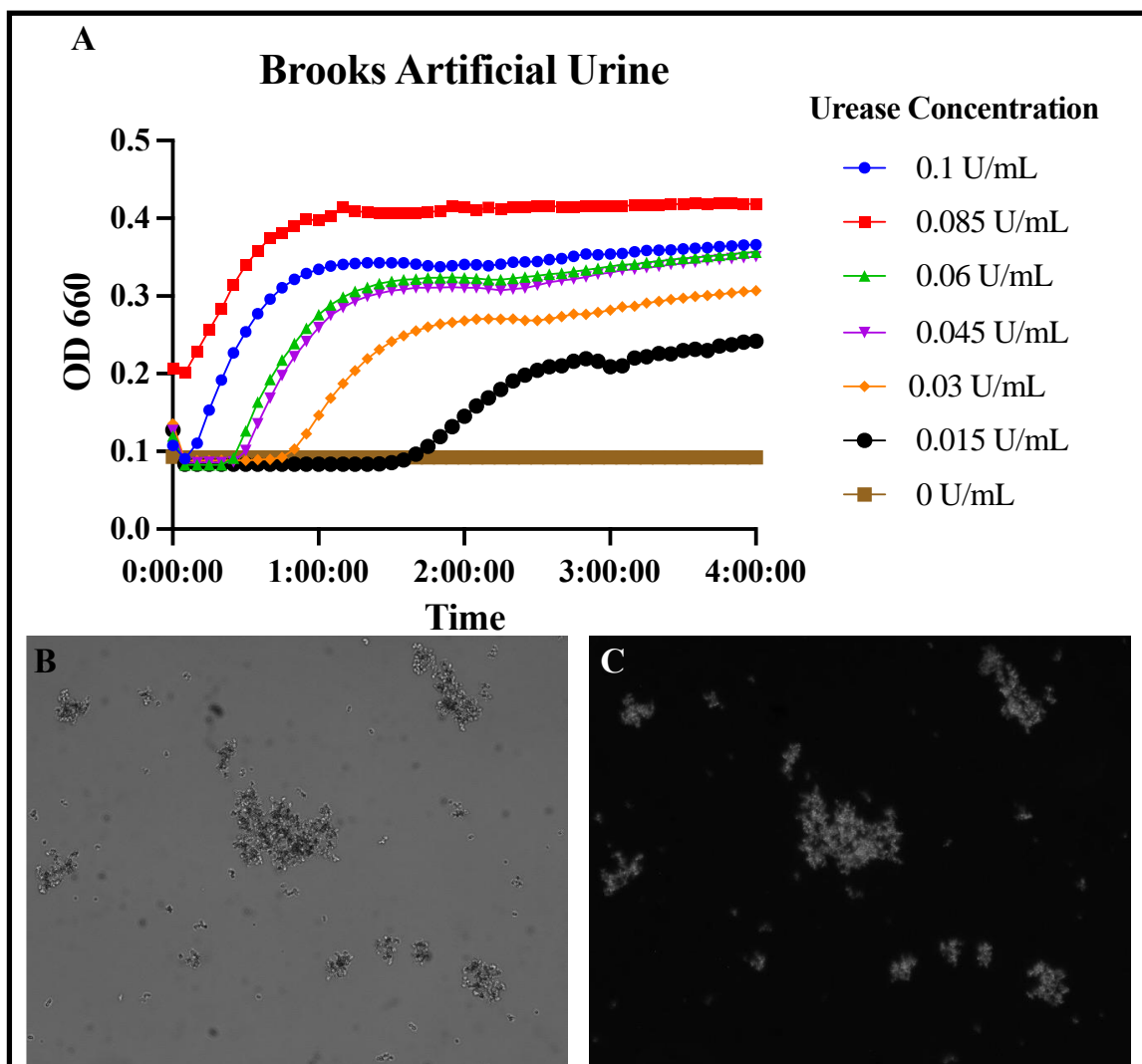


**Figure 2:** A) Crystal growth curves of Brooks artificial urine measured by absorbance at a wavelength of 660 nm. B) Brightfield microscopy of crystals in Brooks artificial urine at 400x. C) Polarized microscopy of crystals in Brooks artificial urine at 400x.

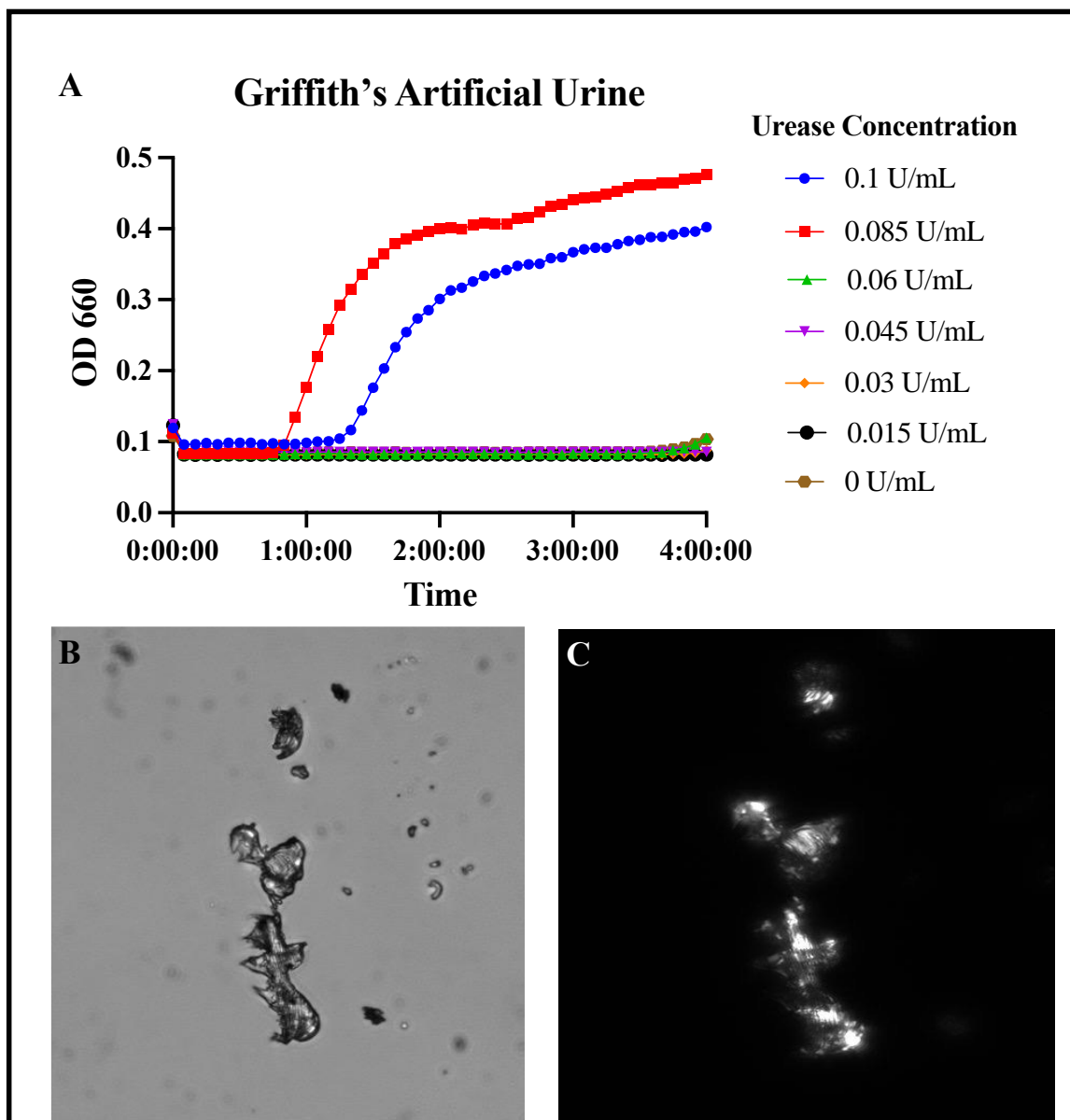


**Figure 3: A) Crystal growth curves of Griffith's artificial urine measured by absorbance at a wavelength of 660 nm. B) Brightfield microscopy of crystals in Griffith's artificial urine at 400x. C) Polarized microscopy of crystals in Griffith's artificial urine at 400x.**

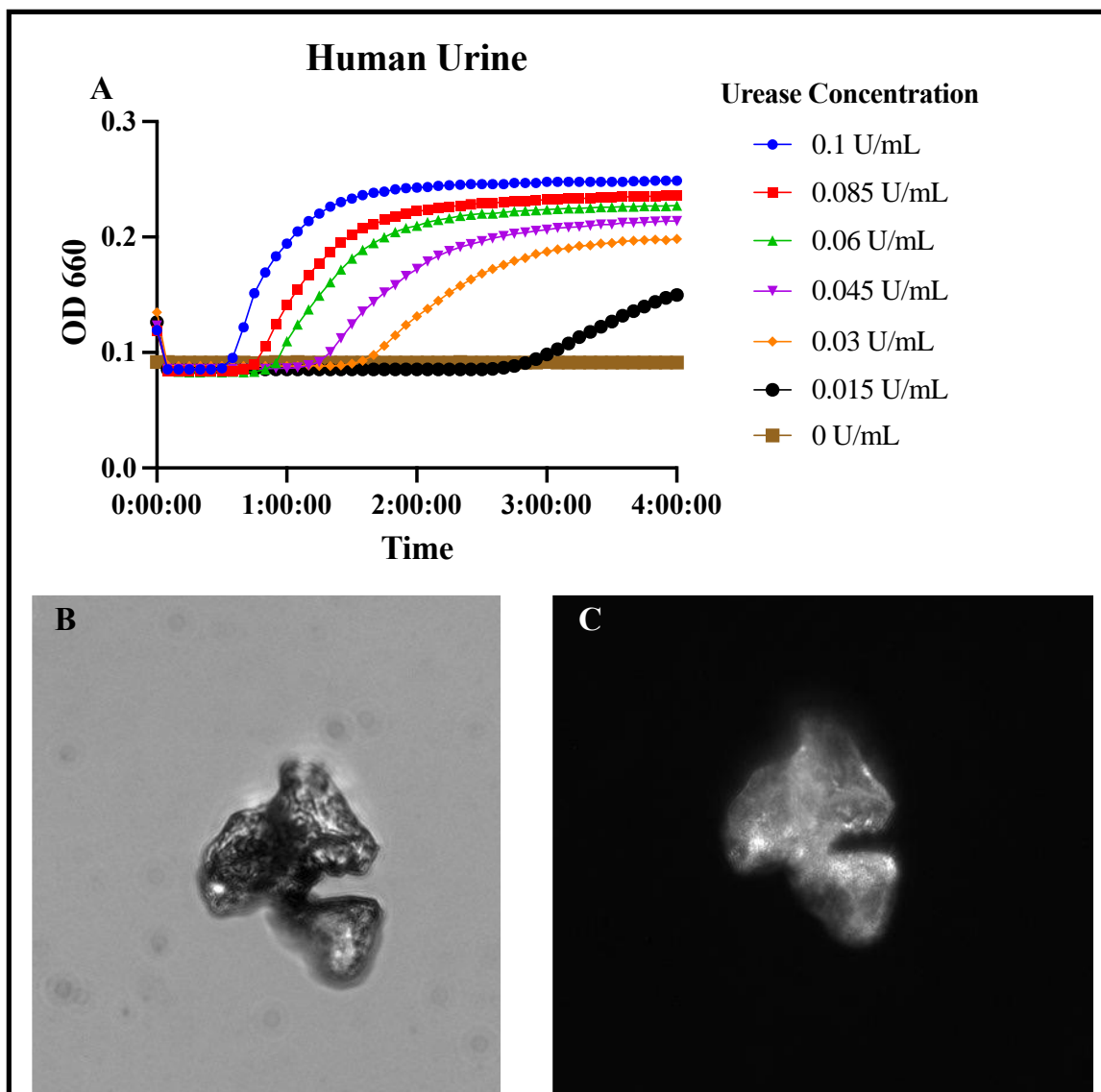


**Figure 4:** A) Crystal growth curves of human urine from a non-stone former measured by absorbance at a wavelength of 660 nm. B) Brightfield microscopy of crystals in human urine at 400x. C) Polarized microscopy of crystals in human urine at 400x.

**Table 7: Growth curve output for Griffith's, Brooks, and human urine from a non-stone former at varying urease concentrations.**

Urine Sample	k	n0	r	t_mid	t_gen	auc_l	auc_e	sigma
0.1 U/mL Griffith's	0.65	0.01	0.04	103.66	15.81	88.40	90.06	0.04
0.085 U/mL Griffith's	0.35	0.00	0.08	73.98	9.22	58.60	58.02	0.02
0.060 U/mL Griffith's	0.41	0.00	0.10	268.00	6.95	0.24	0.38	0.01
0.045 U/mL Griffith's	0.00	0.04	0.09	-0.30	8.10	0.28	0.35	0.00
0.03 U/mL Griffith's	0.00	0.04	2.97	-0.01	0.23	0.14	0.21	0.00
0.015 U/mL Griffith's	0.00	0.04	0.61	-0.02	1.14	0.12	0.21	0.00
0 U/mL Griffith's	1907.18	0.00	0.09	375.53	8.18	0.23	0.42	0.00
0.1 U/mL Brooks	0.26	0.02	0.11	25.94	6.51	55.18	55.01	0.01
0.085 U/mL Brooks	0.21	0.01	0.11	25.44	6.50	45.57	45.34	0.01
0.060 U/mL Brooks	0.25	0.00	0.09	45.74	7.87	48.81	48.55	0.01
0.045 U/mL Brooks	0.24	0.00	0.09	49.28	7.78	45.63	45.38	0.02
0.03 U/mL Brooks	0.20	0.00	0.08	72.68	9.13	32.83	32.62	0.01
0.015 U/mL Brooks	0.14	0.00	0.07	125.85	9.46	16.39	16.29	0.01
0 U/mL Brooks	0.00	0.00	0.00	0.00	0.00	0.00	0.00	0.00
0.1 U/mL Human Urine	0.16	0.00	0.10	52.31	7.30	29.95	29.82	0.01
0.085 U/mL Human Urine	0.15	0.00	0.08	69.15	9.00	25.07	24.94	0.01
0.060 U/mL Human Urine	0.14	0.00	0.07	78.98	9.32	22.52	22.41	0.01
0.045 U/mL Human Urine	0.12	0.00	0.06	105.68	11.11	16.53	16.42	0.01
0.03 U/mL Human Urine	0.11	0.00	0.06	130.11	11.50	11.71	11.66	0.01
0.015 U/mL Human Urine	0.07	0.00	0.07	201.78	10.10	2.63	2.68	0.01
0 U/mL Human Urine	0.00	0.00	0.11	-7.18	6.56	0.13	0.13	0.00

$k$  = growth capacity,  $n^0$  = degrees of freedom,  $r$  = growth rate,  $t_{mid}$  = time to inflection point,  $t_{gen}$  = doubling time,  $auc_l$  = logistic area under the curve,  $auc_e$  = empiric area under the curve,  $sigma$  = goodness of fit.

## 2.3.2 Determining the effect of urease and calcium concentration on crystal formation and pH

### 2.3.2.1 Identifying the optimal urease concentration

Considering the previous experiments, it appeared that any urease concentration above 0.2 U/mL drove the reaction very quickly, therefore, concentrations of 0.25 U/mL were removed from further experiments. The pH values from an experimental run without a pH buffer are demonstrated in Table 8. As can be seen in the table, the pH values rose with increasing urease concentration as one might expect. A pH over 9 was likely driving the reaction and would be difficult for urinary modulators at normal concentrations in human urine to cause an effect. Ideally, a pH of 7.5 would allow for struvite and calcium phosphate crystals to form without overpowering the potential effects of a urinary modulator. At this point, no clear and consistent urease concentration best suited for the model was determined, so further testing was required.

**Table 8: pH levels in Griffith's artificial urine and urease without a buffer after 4 hours.**

Urease Concentration	pH
0 U/mL	5.7
0.075 U/mL	7.25
0.1 U/mL	7.50
0.125 U/mL	8.50
0.15 U/mL	8.60
0.175 U/mL	8.80
0.2 U/mL	9.10

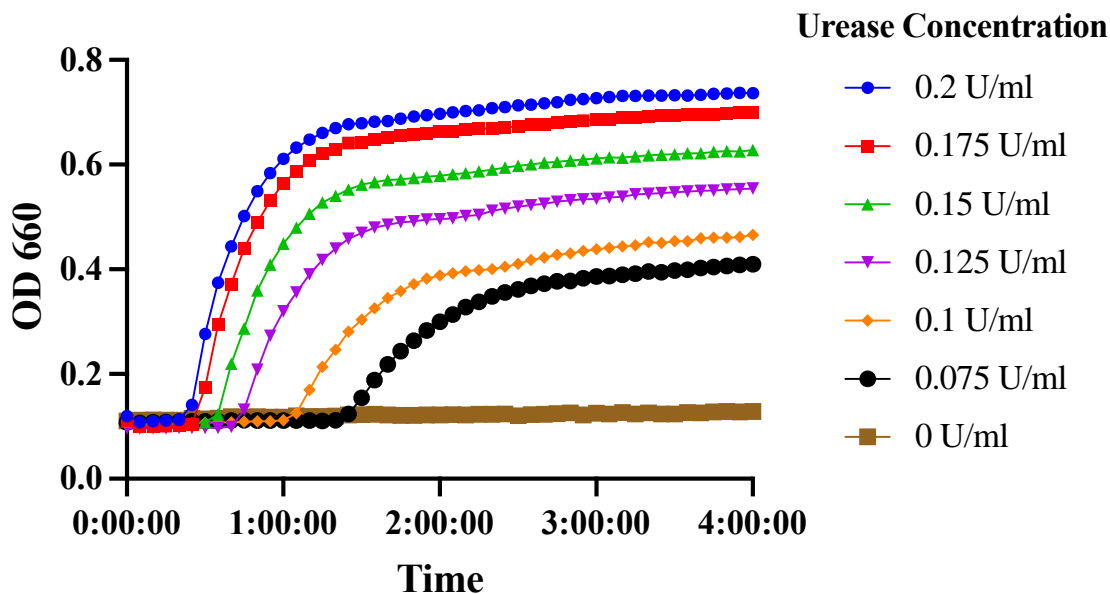


**Figure 5: Crystal growth curves of Griffith's artificial urine measured by absorbance at a wavelength of 660 nm.**

### 2.3.2.2 A trial of normal Griffith's artificial urine compared to low calcium Griffith's artificial urine

Normal Griffith's artificial urine compared to low calcium Griffith's artificial urine was trialed to see if it would affect the predominant crystal formed in the experiment (which has been previously demonstrated<sup>19</sup>). As the presence of calcium phosphate and struvite crystals in the experiment were being confirmed, a Tris buffer was added to help modulate pH. Table 9 shows the pH results after including the Tris buffer with a set point pH of 8.0. However, despite the buffer, the pH levels still rose close to 9.0. Although the pH was a bit higher than desired, the attempt was to confirm that the presence of a buffer would still allow for calcium phosphate and struvite crystal growth. Figures 6 and 7 demonstrate the curves for the 0.15 U/mL urease reactions with and without a Tris buffer.

Interpreting EDX starts with observations of the elements with the largest and highest peaks, representing what the proportion of the structure being analyzed is comprised of. Silica (Si) is used as a mounting substance so it should be ignored when analyzing the composition of the molecules. In Figure 6B and 6C, a glass shard crystal shape is visible which is typical for calcium phosphate. This was also confirmed on SEM/EDX (Figure 6D and 6E). EDX shows that the structure is predominantly made out oxygen (O), calcium (Ca) and phosphate (P) elements. Figure 7B and 7C shows the classic “coffin lid” crystal shape for struvite, which was confirmed on SEM/EDX (Figure 7D and 7E). The struvite crystals show x-ray diffraction largely made up of oxygen (O), magnesium (Mg) and phosphate (P).

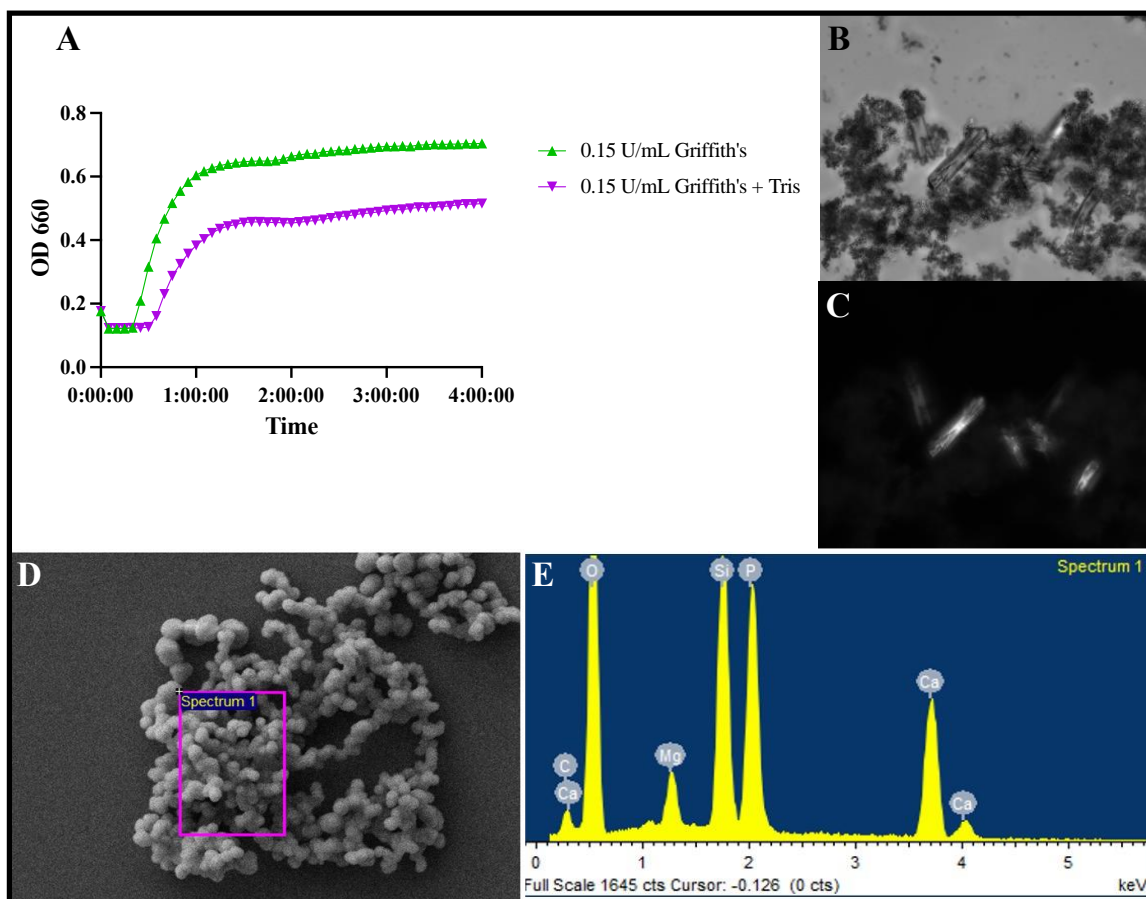


**Figure 6:** A) Crystal growth curves of Griffith's artificial urine with 0.15U/ml urease with or without Tris buffer measured by absorbance at a wavelength of 660 nm. B) Brightfield microscopy of calcium phosphate crystals at 400x. C) Polarized microscopy of calcium phosphate crystals at 400x. D) Scanning electron micrograph of calcium phosphate crystals with corresponding x-ray diffraction in E.

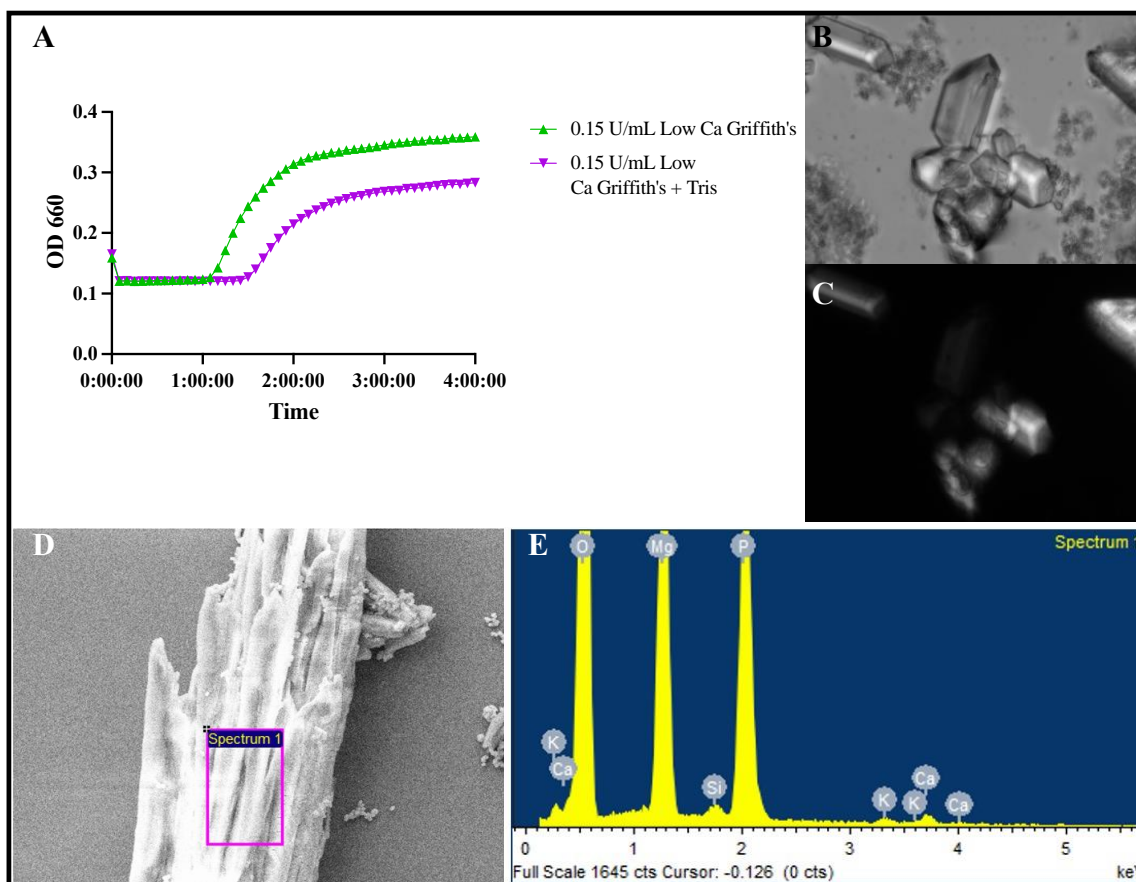


**Figure 7:** A) Crystal growth curves of low calcium Griffith's artificial urine with 0.15U/ml urease with or without Tris buffer measured by absorbance at a wavelength of 660 nm. B) Brightfield microscopy of struvite crystals at 400x. C) Polarized microscopy of struvite crystals at 400x. D) Scanning electron micrograph of struvite crystals with corresponding x-ray diffraction in E.

**Table 9: Urine media and urease with Tris buffer (pH =8.0 at 37°C).**

Urine Media	Urease Concentration	pH
Griffith's	0 U/mL	6.0
	0.075 U/mL	8.8
	0.15 U/mL	8.8
Low Ca Griffith's	0 U/mL	6.0
	0.075 U/mL	8.6
	0.15 U/mL	8.8
Human Urine	0 U/mL	6.0
	0.075 U/mL	8.8
	0.15 U/mL	8.8

Despite the buffer added to the reaction, pH levels were still reaching 8-9 after 24 hours, which does not reflect most clinical scenarios. Lowering the pH buffering point led to a more clinically relevant pH levels (Table 10) with gradual crystal time with an adequate lag time to the start of the reaction (Figure 8). Allowing the full reaction to occur over a 24-hour period yielded more crystals that were organized with the typical crystal shapes indicative of calcium phosphate and struvite crystal compositions.

**Table 10: Griffith's artificial urine with a Tris buffer (pH = 7.5 at 37°C).**

Urease concentration	pH after 24 hours
0 U/mL	6.25
0.075 U/mL	7.25
0.1 U/mL	7.50

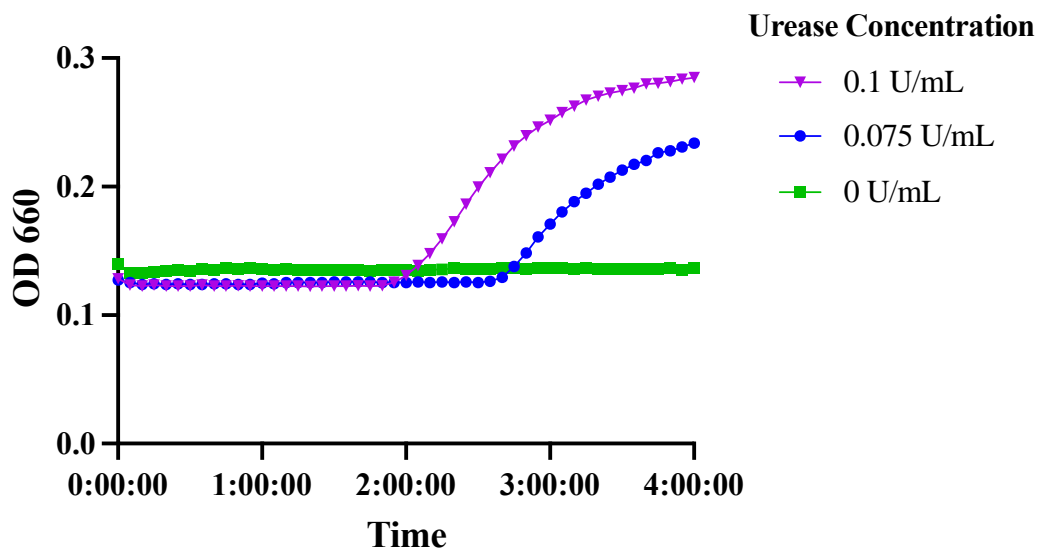


**Figure 8: Crystal growth curves of Griffith's artificial urine with a Tris buffer (pH = 7.5 at 37°C) measured by absorbance at a wavelength of 660 nm.**

## 2.4 Discussion

The results of this study demonstrate that calcium phosphate and struvite crystal formation can be cultivated in an experimental model with artificial urine. Griffith's artificial urine was determined to be the best media to use in the model. The presence of both calcium phosphate and struvite crystal formation was confirmed using SEM/EDX. The optimal concentration was 0.1 U/mL of urease to test urinary modulators and the pH could be controlled using a Tris buffer to limit its effects on crystal formation without impacting the underlying reaction. Consistent results were yielded within four hours under the experimental conditions suitable for testing urinary modulators. This model has broad applicability because it consists of easily accessible compounds found in most labs, is inexpensive (\$0.08 per reaction with urease) and is easily reproducible, as the individual components can be maintained for a long time under adequate storage conditions.

While Brooks and Griffith's artificial urine have both been used in the study of infectious kidney stone formation, it is clear they produce different results. With Brooks urine, crystal formation occurred extremely quickly and at very low concentrations of urease. Brooks was originally developed for assessment of bacterial growth so it is understandable that it would also promote infectious kidney stone formation.<sup>21</sup> The most obvious difference is the starting pH of Brooks is 6.5, which is higher compared to Griffith's artificial urine at 5.7.<sup>20,21</sup> This is likely a significant difference because the urease increases the pH and has a much shorter path to reaching a pH of 7.0 when struvite stones crystals would start to form.<sup>11</sup> Furthermore, it is also possible that calcium phosphate crystals would start forming prior to this pH level, but higher pH favours

calcium phosphate crystal formation.<sup>24</sup> Although the pH of Brooks was not measured, it would be interesting to see if the pHs were typically higher in Brooks for the same urease concentration compared to Griffith's. Brooks pH could have been lowered to match Griffith's, but it was important to follow the recipes as described with no modifications. The overall goal of this work was not to create a new artificial urine, but to identify of the ones already established which would serve as the best media.

Not only was the starting pH different, but the compounds and concentrations differed as well between the artificial urine media. Brooks artificial urine does not have any oxalate, which may promote calcium phosphate stones rather than calcium oxalate crystals compared to Griffith's artificial urine. Calcium oxalate formation is not dependent on pH so this reaction could occur prior to calcium phosphate or struvite formation, but this is impossible in Brooks artificial urine.<sup>25</sup> There is also less citrate in Brooks artificial urine, which is a risk factor for calcium phosphate crystallization.<sup>26</sup> Clinically this would correlate with a patient with hypocitraturia or distal renal tubular acidosis which is not an appropriate baseline *in vitro* scenario and limits its broad applicability.

When comparing Griffith's artificial urine to human urine crystal formation, notable differences were observed. The slopes of the curves were not as steep in human urine and the peak of the curves were typically lower than Griffith's. This is an important distinction as it is direct evidence that there are natural modulating factors within human urine that are not possible to replicate in this scenario. Likely this is due to additional proteins or compounds not found in Griffith's that can be found in human urine.

Identifying these modulators may allow their targeted manipulation to effect clinical stone formation, which is something we hope to later achieve with our model.

A benefit of the model is that results can be seen within 2-3 hours and numerous inhibitors can be tested at once. Analyzing the reaction with spectrophotometry for 4 hours elicited adequate growth curve analysis, but more definitive results occurred when carrying out microscopic evaluation after 24 hours. Allowing the reaction to occur over 24 hours improved crystal morphology viewed under the microscope and with more crystal yield.

As mentioned earlier, concentrations of urease in prior experiments have varied widely in the literature.<sup>11,19</sup> A urease concentration of 0.1 U/mL provides the appropriate experimental conditions to study urinary modulators, but it is currently unknown how this might compare to urease concentrations typically found in the presence of urease producing bacteria. It is possible that the concentration varies based on bacterial strain, an active urinary tract infection or the amount of colony forming units.<sup>27-29</sup> In an effort to make the reaction more clinically applicable, this would be a logical area to investigate further.

Throughout this experiment, only urease concentrations of 0.1 U/mL formed crystals in Griffith's artificial urine (Figure 3), however, this was not seen in later experiments (Figure 5) and could be due to degradation of the urease enzyme. More than one vial of urease is required for each experiment; therefore, it is possible that some of the reactions could occur normally while select individual experiments did not have effective urease. Repeating experiments with lower urease concentrations below 0.085 U/mL showed that Griffith's artificial urine would produce crystals (Appendix B).

As seen throughout this chapter, decreasing the concentration of calcium in the artificial urine drove the reaction toward the formation of struvite crystals. In their study on urease-induced crystallization in human and synthetic urine, Ebisuno et al. not only reduced, but eliminated calcium completely from the reaction and were therefore able to yield solely struvite crystals.<sup>19</sup> While not clinically applicable in human urine, it can be a consideration if looking to isolate struvite over calcium phosphate and to investigate modulators or other properties specific to their formation.

For regular Griffith's artificial urine, there is an earlier take off for the reaction, steeper slope, and higher peak than low calcium Griffith's artificial urine. This was seen in both reactions with and without a Tris buffer when comparing it to the low calcium Griffith's. It is possible that this could be due to the earlier calcium phosphate crystallization as it can form in more acidic conditions, thus beginning before the struvite crystal formation. This premise of early and late phase crystallization has been previously demonstrated in a study by Ebisuno et al. (1997) when separating calcium phosphate (early phase) and struvite (late phase) crystallization.<sup>19</sup>

Our results show that there is a difference when using a pH buffer with urease in urine. While the speed of the reaction may not differ significantly, the peak of the curve is much lower. We demonstrated that a Tris buffer in the reaction does not prevent the formation of calcium phosphate and struvite crystal formation. In fact, we determined that it is critical to minimize the effect of pH as a confounding variable when testing urinary modulators in infectious stone formation because of the rapid and increased crystal growth seen with higher pHs.

Infectious kidney stones are highly recurrent with the risk of recurrence as high as 75% within 5 years.<sup>29</sup> Struvite stones can commonly lead to staghorn calculi that can form within 4-6 weeks.<sup>30</sup> Patients at risk include those with spinal cord injuries, chronic indwelling catheters, neurogenic bladders, ileal conduits or ureteral reflux.<sup>31-33</sup> There is limited success with medical therapies to decrease the risk of recurrent infection-based stones. Antibiotics have limited ability to infiltrate the stone matrices and there are obviously concerns with long term antibiotic use that can lead to secondary infections and bacterial resistance.<sup>34</sup>

Infection-related stones typically require more invasive surgical management with more technical challenges given the stone characteristics. Calcium phosphate stones are typically hard stones that are resistant to SWL, also impacting their surgical management.<sup>35</sup> Treating these endoscopically or percutaneously takes more time because they can be more dense (calcium phosphate) and much larger (struvite and/or calcium phosphate). If larger staghorn calculi are not managed in a timely fashion it can lead to renal loss, sepsis or death.<sup>36</sup>

Taking the model through this rigorous process of trialling multiple variables to yield the best results has created a validated model that is well-suited for testing urinary modulators. Using a consistent urease concentration of 0.1 U/mL with a Tris buffer with a set point of 7.5 allows for rapid, high throughput testing of many urinary modulators to assess their effect on infectious crystal formation. The benefits of this model provide us with the opportunity to identify new or add more supportive evidence for urinary modulators in infectious stone formation. The clinical importance of such a significant

discovery cannot be understated and the following chapter will outline our breakthroughs and how they might shape clinical practice.

## 2.5

## References

1. Chauhan CK, Joshi MJ. *In vitro* crystallization, characterization and growth-inhibition study of urinary type struvite crystals. *J Cryst Growth*. 2013;362(1):330-337. doi:10.1016/j.jcrysgro.2011.11.008
2. Kaleeswaran B, Ramadevi S, Murugesan R, Srigopalram S, Suman T, Balasubramanian T. Evaluation of anti-urolithiatic potential of ethyl acetate extract of *Pedalium murex* L. on struvite crystal (kidney stone). *J Tradit Complement Med*. 2019;9(1):24-37. doi:10.1016/j.jtcme.2017.08.003
3. Meyer JL, Bergert JH, Smith LH. Epitaxial relationships in urolithiasis: The calcium oxalate monohydrate hydroxyapatite system. *Clin Sci Mol Med*. 1975;49(5):369-374. doi:10.1042/cs0490369
4. Pak CY, Eanes ED, Ruskin B. Spontaneous precipitation of brushite in urine: Evidence that brushite is the nidus of renal stones originating as calcium phosphate. *Proc Natl Acad Sci U S A*. 1971;68(7):1456-1460. doi:10.1073/pnas.68.7.1456
5. Njegić-Džakula B, Brečević L, Falini G, Kralj D. Calcite crystal growth kinetics in the presence of charged synthetic polypeptides. *Cryst Growth Des*. 2009;9(5):2425-2434. doi:10.1021/cg801338b
6. Kim D, Olympiou C, McCoy CP, Irwin NJ, Rimer JD. Time-resolved dynamics of struvite crystallization: Insights from the macroscopic to molecular scale. *Chem Eur J*. 2020;26(16):3555-3563. doi:10.1002/chem.201904347
7. Wei Z, Amponsah PK, Al-Shatti M, Nie Z, Bandyopadhyay BC. Engineering of polarized tubular structures in a microfluidic device to study calcium phosphate stone formation. *Lab Chip*. 2012;12(20):4037-4040. doi:10.1039/c2lc40801e
8. Naito Y, Ohtawara Y, Kageyama S, et al. Morphological analysis of renal cell culture models of calcium phosphate stone formation. *Urol Res*. 1997;25(1):59-65. doi:10.1007/BF00941907
9. Wang Y, Grenabo L, Hedelin H, McLean RJC, Nickel JC, Pettersson S. Citrate and urease-induced crystallization in synthetic and human urine. *Urol Res*. 1993;21(2):109-115. doi:10.1007/BF01788828
10. Hansen NM, Felix R, Bisaz S, Fleisch H. Aggregation of hydroxyapatite crystals. *Biochim Biophys Acta*. 1976;451:549-559. doi:10.1016/0304-4165(76)90150-1
11. Hedelin H, Grenabo L, Pettersson S. Urease-induced crystallization in synthetic urine. *J Urol*. 1985;133(3):529-532. doi:10.1016/S0022-5347(17)49047-1
12. Tiselius HG. Measurement of the risk of calcium phosphate crystallization in urine.

- Urol Res.* 1987;15(2):79-81. doi:10.1007/BF00260937
13. Hedelin H, Grenabo L, Pettersson S. The effects of urease in undiluted human urine. *J Urol.* 1986;136(3):743-745. doi:10.1016/S0022-5347(17)45040-3
  14. Sarigul N, Korkmaz F, Kurultak İ. A new artificial urine protocol to better imitate human urine. *Sci Rep.* 2019;9(1):1-11. doi:10.1038/s41598-019-56693-4
  15. Taylor EN, Curhan GC. Differences in 24-hour urine composition between black and white women. *J Am Soc Nephrol.* 2007;18(2):654-659. doi:10.1681/ASN.2006080854
  16. Robinson-Cohen C, Ix JH, Smits G, et al. Estimation of 24-hour urine phosphate excretion from spot urine collection: Development of a predictive equation. *J Ren Nutr.* 2014;24(3):194-199. doi:10.1053/j.jrn.2014.02.001
  17. Abu-Ghanem Y, Kleinmann N, Erlich T, Winkler HZ, Zilberman DE. The impact of dietary modifications and medical management on 24-hour urinary metabolic profiles and the status of renal stone disease in recurrent stone formers. *Isr Med Assoc J.* 2021;23(1):12-16.
  18. Asakura H, Selengut JD, Orme-Johnson WH, Dretler SP. The effect of calprotectin on the nucleation and growth of struvite crystals as assayed by light microscopy in real-time. *J Urol.* 1998;159(4):1384-1389. doi:10.1016/S0022-5347(01)63621-8
  19. Ebisuno S, Komura T, Yamagiwa K, Ohkawa T. Urease-induced crystallizations of calcium phosphate and magnesium ammonium phosphate in synthetic urine and human urine. *Urol Res.* 1997;25(4):263-267. doi:10.1007/BF00942096
  20. Griffith DP, Musher DM, Itin C. Urease. The primary cause of infection induced urinary stones. *Invest Urol.* 1976;13(5):346-350.
  21. Brooks T, Keevil CW. A simple artificial urine for the growth of urinary pathogens. *Lett Appl Microbiol.* 1997;24(3):203-206. doi:10.1046/j.1472-765X.1997.00378.x
  22. Hobbs T, Schultz LN, Lauchnor EG, Gerlach R, Lange D. Evaluation of biofilm induced urinary infection stone formation in a novel laboratory model system. *J Urol.* 2018;199(1):178-185. doi:10.1016/j.juro.2017.08.083
  23. Sprouffske K. growthcurver: Simple Metrics to 0.3.1., Growth Curves. R package version. 2020. <https://cran.r-project.org/package=growthcurver>.
  24. Carpentier X, Daudon M, Traxer O, et al. Relationships between carbonation rate of carbapatite and morphologic characteristics of calcium phosphate stones and etiology. *Urology.* 2009;73(5):968-975. doi:10.1016/j.urology.2008.12.049

25. Gault HH, Chafe LL, Morgan JM, et al. Comparison of patients with idiopathic calcium phosphate and calcium oxalate stones. *Medicine*. 1991;70(6):345-359. doi:10.1097/00005792-199111000-00001
26. Fleisch H. Inhibitors and promoters of stone formation. *Kidney Int*. 1978;13(5):361-371. doi:10.1038/ki.1978.54
27. Cohen MS, Davis CP, Czerwinski EW, Warren MM. Calcium phosphate crystal formation in *Escherichia coli* from human urine: An *in vitro* study. *J Urol*. 1982;127(1):184-185. doi:10.1016/S0022-5347(17)53658-7
28. Chutipongtanate S, Sutthimethakorn S, Chiangjong W, Thongboonkerd V. Bacteria can promote calcium oxalate crystal growth and aggregation. *J Biol Inorg Chem*. 2013;18(3):299-308. doi:10.1007/s00775-012-0974-0
29. Maurice-Estépa L, Levillain P, Lacour B, Daudon M. Crystalline phase differentiation in urinary calcium phosphate and magnesium phosphate calculi. *Scand J Urol Nephrol*. 1999;33(5):299-305. doi:10.1080/003655999750017365
30. Bichler K, Eipper E, Naber K, Braun V, Zimmerman R, Lahme S. Urinary infection. *Int J Antimicrob Agents*. 2002;19:488-498. doi:10.1159/000281177
31. Kracht H, Büscher HK. Formation of staghorn calculi and their surgical implications in paraplegics and tetraplegics. *Paraplegia*. 1974;12(2):98-110. doi:10.1038/sc.1974.17
32. Dretler SP. The pathogenesis of urinary tract calculi occurring after ileal conduit diversion. I. Clinical study. II. Conduit study. III. Prevention. *J Urol*. 1973;109(2):204-209. doi:10.1016/S0022-5347(17)60389-6
33. Burr RG. Urinary calcium, magnesium, crystals and stones in paraplegia. *Paraplegia*. 1972;10(1):56-63. doi:10.1038/sc.1972.10
34. Schwartz BF, Stoller ML. Nonsurgical management of infection-related renal calculi. *Urol Clin North Am*. 1999;26(4):765-778. doi:10.1016/S0094-0143(05)70217-2
35. Elmansy HE, Lingeman JE. Recent advances in lithotripsy technology and treatment strategies: A systematic review update. *Int J Surg*. 2016;36:676-680. doi:10.1016/j.ijsu.2016.11.097
36. Rous SN, Turner WR. Retrospective study of 95 patients with staghorn calculus disease. *J Urol*. 1977;118(6):902-904. doi:10.1016/S0022-5347(17)58242-7

## Chapter 3

### **3 Testing urinary modulators in infectious stone formation using a high-throughput experimental model**

Scientific interest into the pathogenesis of kidney stones has been ongoing for centuries, however, most of this research has focused on one stone type, calcium oxalate. There is a paucity of knowledge on the pathogenesis of infectious kidney stones including urinary modulators that may promote or inhibit their formation. In the previous chapter, it was shown that human pooled urine had a less robust reaction with urease compared to artificial urine media. This suggests that there may be natural modulators within human urine that we have not fully elucidated. Now that we have developed and validated a high-throughput experimental model, we have a unique opportunity to explore the profound knowledge gap in the pathogenesis of infectious stones from a basic science and clinical perspective.

An experimental model using Griffith's artificial urine, Jack bean urease and a Tris buffer can provide a rapid experimental model with strict conditions to test infectious stone modulators. The urinary modulators selected for this study were prioritized based on the quality of evidence in the literature. Additional compounds were included based on anecdotal evidence in our lab for demonstrating calcium oxalate stone modulation. Growth curve analysis, pH changes and crystal structure with light microscopy were used to evaluate the results from the experiments. The comparison of these data points will allow us to better understand the pathogenesis of infectious stones and propose therapeutic approaches to minimize risk of infectious stone formation in patients.

## 3.1 Introduction

### 3.1.1 Infectious stone pathogenesis

Currently, the general consensus is to associate infectious stones with UTIs and the bacteria that cause them, rather than an underlying metabolic abnormality in these cases. The basis of infectious stones forming in association with UTIs is the result of urease-producing bacteria converting urea into ammonium and carbon dioxide. The ammonium leads to a rise in pH and provides more favourable crystal formation for calcium phosphate and struvite stones.<sup>1,2</sup> However, calcium phosphate stones are known to form in the absence of UTIs with hypercalciuria (i.e., primary hyperparathyroidism) and hypocitraturia (i.e., dRTA). There are two hypotheses for calcium phosphate stone formation without any clinical signs of a UTI. Firstly, a clinically asymptomatic UTI was responsible for the stone formation and secondly, an infectious process was involved in the initial steps of the stone formation and disappeared secondarily.<sup>3</sup>

On the other hand, struvite stone formation is almost always associated with UTIs and is not known to form without the presence of urease-producing bacteria. Although struvite stones require an alkaline pH, they have been shown to be more resilient to pH changes compared with calcium phosphate crystallization.<sup>4</sup> Maximal crystallization for both calcium phosphate and struvite occurs between pH of 7.5-8.0.<sup>2</sup> The importance of pH for both calcium phosphate and struvite crystal formation is well documented and it will be a significant variable in our model. A high pH in the reaction could mitigate or alter the effect of the modulator and the goal is to minimize potential confounders to optimize the conditions for the potential modulators being investigated.

### 3.1.2 Urinary modulators

There is a long list of compounds associated with non-infectious kidney stone modulation,<sup>5</sup> but an active infection radically alters the urinary environment and can alter the function of these urinary modulators. For example, inhibitors for calcium oxalate stone disease could act as promoters of infectious stone formation because of the elevated pH, presence of bacteria, or other biochemical factors that are present in the infectious urinary environment. The following paragraphs will provide a brief summary of the existing literature on the modulators selected for this project.

*In vivo* data suggests that pyrophosphate acts as an inhibitor of crystal nucleation.<sup>6</sup> Sodium pyrophosphate, specifically, has no influence on pH changes, urease activity and bacterial growth.<sup>7</sup> Ethane-1-hydroxy-1,1-diphosphonate (EHDP or etidronic acid) displaces previously bound pyrophosphate on calcium phosphate crystals and has been shown to be a more effective inhibitor of calcium phosphate crystals compared to pyrophosphate.<sup>7</sup> Citrate demonstrates urease-induced crystal inhibition and it delayed onset of nucleation and growth of struvite crystals.<sup>8</sup> Chondroitin sulfate (CS) appears to have no effect on calcium phosphate crystal formation,<sup>9</sup> but *in vitro* studies with *Proteus mirabilis* in Griffith's artificial urine actually led to increased struvite and calcium phosphate crystallization.<sup>7</sup> There may be some inhibitory effect by heparin with calcium oxalate crystallization, but heparin has no impact on urease-induced stone crystallization.<sup>10,11</sup>

OPN tested *in vivo* and *in vitro* demonstrates decreased aggregation of calcium phosphate crystal formation.<sup>5,9</sup> Structural changes to calcium phosphate crystals in the presence of PASP has been documented with scanning electron microscopy,<sup>12</sup> as well as

decreased calcium phosphate crystal aggregation.<sup>9,13</sup> Evidence suggests that magnesium ions inhibit calcium phosphate crystallization, but these findings have not been consistently shown.<sup>10,14</sup> Methionine has been shown to acidify urine in normal men<sup>15</sup> and oral supplementation leads to significant decreases in supersaturation of calcium phosphate and struvite crystals with no effect on calcium oxalate crystallization.<sup>16</sup> High quality clinical data on the effects of methionine is lacking.

Vanillic acid can inhibit urease enzymes at very low concentrations and at higher concentrations it can be bactericidal for *P. mirabilis*.<sup>7</sup> Sulfate is a titratable acid in the kidney with a modest effect in decreasing urinary calcium supersaturation and raising the upper limit of metastability for calcium oxalate and calcium phosphate crystal formation.<sup>17</sup> Zinc ions have been shown to stimulate calcium aggregation and aid stone formation.<sup>14</sup>

Given the lack of evidence for these modulators in infectious stone formation, we set out to test these substances in our model to determine their ability to modulate infectious crystal formation. The culmination of this research will further assist in developing a rudimentary understanding of the pathogenesis of infectious stone formation and determine substances that could be used to significantly reduce the clinical burden.

### **3.2 Materials and Methods**

As this was an in vitro study, IRB approval from Western University was not required.

### 3.2.1 Experimental conditions for model

The base components for the model included Griffith's artificial urine, 0.1 U/mL Jack Bean urease and 1M Tris buffer (pH = 7.52 at 37°C). Once we had selected our urinary modulators, we next determined the appropriate concentration for each (Table 11). For those compounds found in human urine, the normal human urinary concentrations were used in the assay. If there is a range of concentrations for a particular compound, then a value was selected from the upper half of the range. These concentrations were then multiplied by a factor of 10 to amplify any modulatory effect. For those compounds that are not normally found in human urine, concentrations were selected if they were previously used in the literature, or a concentration of 1 mM was used if there was no prior relevant data.

### 3.2.2 Making stock solutions for each urinary inhibitor

Stock solutions of each inhibitor were made with 100 mL of Griffith's artificial urine and 1 mL 1 M Tris buffer (pH buffering = 7.52 at 37°C) at the corresponding concentrations in Table 11. The concentration of Tris buffer results in a buffering capacity of 10 mM for each experiment. After creating the stock solutions, the initial pH was taken using a Mettler-Toledo FiveEasy Plus pH meter F20 (Gerifensee, Switzerland). The solutions were then filter sterilized through a 0.22 µm filter and stored at 4°C.

**Table 11: Concentrations of urinary modulators.**<sup>5,18-23</sup>

Modulator	Concentration
-----------	---------------

Heparin	5 $\mu$ M
Osteopontin (OPN)	600 nM
Sodium pyrophosphate	250 $\mu$ M
Vanillic acid	375 $\mu$ M
Zinc sulfate	3.1 $\mu$ M
Etidronic acid	25 $\mu$ M
Polyaspartic acid (PASP)	10 $\mu$ M
Chondroitin sulfate	47 $\mu$ M
Methionine	300 $\mu$ M
Citric acid	1.6 mM
Sodium citrate	1 mM
Magdolate (magnesium pidolate)	1 mM
Aspartic acid	1 mM
Indole	1 mM
Metformin	1 mM
Sodium bicarbonate	1 mM
Salicylic acid	1 mM
P-cresol	1 mM
Ibuprofen	1 mM

### 3.2.3 Running experimental model with urinary modulators

Ten mL of the stock solution was placed into a test tube and mixed with 0.1 U/mL urease. Control reactions included Griffith's artificial urine with 0.1 U/mL urease and 10 mM Tris buffer or Griffith's artificial urine with 10 mM Tris buffer only. A volume of 200  $\mu$ L was pipetted into the 96-well plate in technical triplicate for each reaction. The Biotek Eon Microplate Spectrophotometer (Winooski, Vermont, USA) and the Gen 5 v2.0 (Winooski, Vermont, USA) software were used for analyzing all 96-well plates. The reader was set at an optical density of 660 nm at 37°C with readings every 5 minutes for 24 hours. The remaining solutions were placed in an incubator at 37°C for 24 hours. After 24 hours, the test tubes were measured for pH levels using the Mettler-Toledo FiveEasy Plus pH meter F20 (Gerifensee, Switzerland). A 3-point calibration of the pH meter was performed prior to taking the pH measurements. The test tubes were then

visually interrogated for crystal growth, and this was compared with the crystal growth curves. If there was no evidence of crystal growth, then no further testing was performed for those particular modulators.

### **3.2.4 Microscopic analysis of crystal formation**

To evaluate the presence of struvite or calcium phosphate crystals, we collected the crystals from the test tubes for microscopic analysis after 24 hours. During our model validation (see Chapter 2), it was determined that centrifuging the crystals made microscopic analysis more challenging because of the significant volume of crystals transferred to the slide. Therefore, this aspect was omitted from this part of the project. The supernatant was decanted and 10  $\mu\text{L}$  of the crystal suspension was placed on a microscope slide using a wide bore pipette. Slides were examined under a Nikon Eclipse Ts2R (Melville, New York, USA) microscope and multiple images of the crystals were taken in both the birefringent lens and white light and processed using NIS elements software (Melville, New York, USA).

### **3.2.5 Statistical analysis**

Statistical analysis was carried out with RStudio version 2022.02.1 (Boston, MA, USA) using the Growthcurver package version 0.3.1 to analyze crystal growth curves.<sup>24</sup> All graphs and figures were created were accomplished using Prism – GraphPad version 9.3.1(San Diego, CA, USA).

## **3.3 Results**

### 3.3.1 Urinary modulators that prevented crystal formation

The list of urinary modulators that were not associated with crystals formation in the reaction include: etidronic acid, ibuprofen, metformin, salicylic acid, citric acid, zinc sulfate (Zn sulfate), aspartic acid, magdolate and sodium citrate (Na citrate). Table 12 demonstrates the pH levels before and after the experiment regarding these modulators. The initial pH values for all these modulators were lower than Griffith's with Tris buffer (pH = 5.70). After completing the experiments most of the pHs values increased, but the highest pH was with Na citrate in biologic replicate number 3 at 6.42. In biologic replicates number 1 and number 2, none of the urinary modulators had a pH above 6.0.

**Table 12: pH values of urinary modulators with no crystal growth before and after experiment.**

<b>Modulator</b>	<b>Initial pH</b>	<b>Biologic rep #1</b>	<b>Biologic rep #2</b>	<b>Biologic rep #3</b>
Etidronic acid	1.39	1.09	1.11	1.11
Ibuprofen	4.76	4.81	5.74	6.23
Metformin	5.01	4.92	5.82	6.20
Salicylic acid	4.89	4.84	5.76	6.05
Citric acid	2.93	2.81	3.82	3.90
Zinc sulfate	4.99	5.01	5.91	6.13
Aspartic acid	5.01	4.92	5.86	6.37
Na citrate	4.85	5.07	5.86	6.42
Magdolate	4.96	4.99	5.80	6.21
Griffith's with urease and Tris	5.02	7.69	8.17	8.72
Griffith's with Tris	5.01	5.00	5.87	6.23

Growth curves for all these reactions were essentially horizontal and at least one biologic replicate showed all zeroes with growth curve analysis, however, some did

produce values. Further inspection of these values showed a very low  $r$  (growth rate) and very little AUC demonstrating very minimal growth over time. No crystals were seen visually in the test tubes with these modulators over the course of any of the experiments.

**Table 13: Growth curve output for urinary modulators with no crystal formation.**

Modulator	k	$n^0$	r	t_mid	t_gen	auc_l	auc_e	sigma
Etidronic acid	0	0	0	0	0	0	0	0
Ibuprofen	0	0	0	0	0	0	0	0
Metformin	0	0	0	0	0	0	0	0
Salicylic acid	0	0	0	0	0	0	0	0
Citric acid	0	0	0	0	0	0	0	0
Zinc sulfate	0	0	0	0	0	0	0	0
Aspartic acid	0	0	0	0	0	0	0	0
Na citrate	0	0	0	0	0	0	0	0
Magdolate	0	0	0	0	0	0	0	0

$k$  = growth capacity,  $n^0$  = degrees of freedom,  $r$  = growth rate,  $t_{mid}$  = time to inflection point,  $t_{gen}$  = doubling time,  $auc_l$  = logistic area under the curve,  $auc_e$  = empiric area under the curve,  $\sigma$  = goodness of fit.

### 3.3.2 Urinary modulators that inhibited crystal formation

The only inhibitor that demonstrated strong inhibition while allowing crystal formation is OPN. The pH values show that the initial pH was higher compared to our control and resulting pH values after the experiment for all 3 biologic replicates were higher compared to Griffith's with urease and Tris (pH ~ 8.17). Figure 1A shows a spectrophotometry growth curve for OPN and this was plotted out to 24 hours to fully appreciate the difference in curves compared to the controls. OPN has an  $r = 0.008$  and

$t_{mid} = 447.93$ , which is approximately double compared to Griffith's with urease and Tris with a much lower area under the curve (AUC). Interestingly, the crystals were consistent with struvite on light microscopy (Figure 9B and 9C) with no obvious calcium phosphate crystals found.

**Table 14: pH values of osteopontin before and after experiment.**

Modulator	Initial pH	Biologic rep #1	Biologic rep #2	Biologic rep #3
OPN	6.15	9.19	9.28	9.23
Griffith's with urease and Tris	5.02	7.69	8.17	8.72
Griffith's with Tris	5.01	5.00	5.87	6.23

**Table 15: Growth curve output for osteopontin.**

Modulator	k	$n^0$	r	$t_{mid}$	$t_{gen}$	auc_l	auc_e	sigma
OPN	0.119	0.003	0.008	447.93	85.29	117.64	118.15	0.008
Griffith's with urease and Tris	0.270	0.030	0.010	224.58	69.64	320.56	318.52	0.020
Griffith's with Tris	0.000	0.000	0.000	0	0	0	0	0.000

$k$  = growth capacity,  $n^0$  = degrees of freedom,  $r$  = growth rate,  $t_{mid}$  = time to inflection point,  $t_{gen}$  = doubling time,  $auc_l$  = logistic area under the curve,  $auc_e$  = empiric area under the curve,  $\sigma$  = goodness of fit.

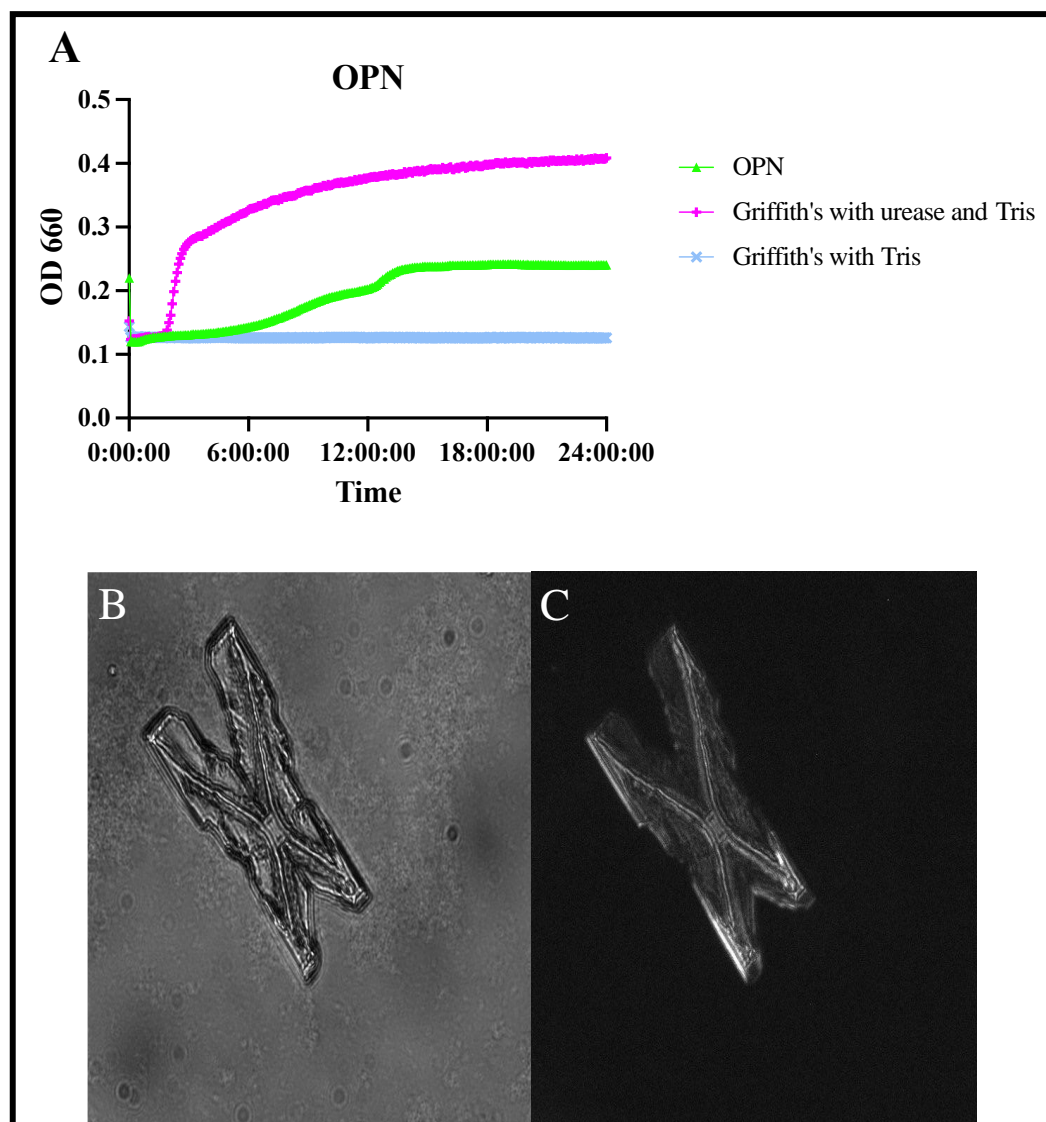


**Figure 9: A) Crystal growth curve of OPN measured by absorbance at a wavelength of 660 nm. Bright field microscopy (B) and polarized light microscopy (C) of struvite crystal from OPN reaction at 200x.**

### 3.3.3 Urinary modulators that promoted crystal formation

In contrast to the modulators that prevented crystal formation, the following modulators were found to promote infectious crystal formation: indole, chondroitin sulfate (CS), sodium bicarbonate (Na bicarbonate) and vanillic acid promoted infectious crystal formation. The initial pH values were greater for CS, indole, and vanillic acid but

not Na bicarbonate when compared to the controls. However, after the experiments all pH values were equivalent or increased compared to controls. In Figure 10, the growth curves start earlier in time and have a greater AUC, which is consistent with the  $r$  and  $t_{mid}$  (Table 17) values for the modulators except for Na bicarbonate. The only modulator that had an equivalent  $r$  with the control was Na bicarbonate while, the rest had a greater  $r$  and shorter  $t_{mid}$ . AUC values for these modulators were also all greater compared to the controls with CS having the largest empiric AUC 652.15.

**Table 16: pH values of urinary modulators that promote crystal growth before and after experiment.**

Modulator	Initial pH	Biologic rep #1	Biologic rep #2	Biologic rep #3
Na bicarbonate	5.11	7.35	8.49	8.69
Indole	6.34	8.66	8.77	8.83
CS	6.18	8.97	8.97	9.06
Vanillic acid	6.17	8.83	8.90	8.90
Griffith's with urease and Tris	5.02	7.69	8.17	8.72
Griffith's with Tris	5.01	5.00	5.87	6.23

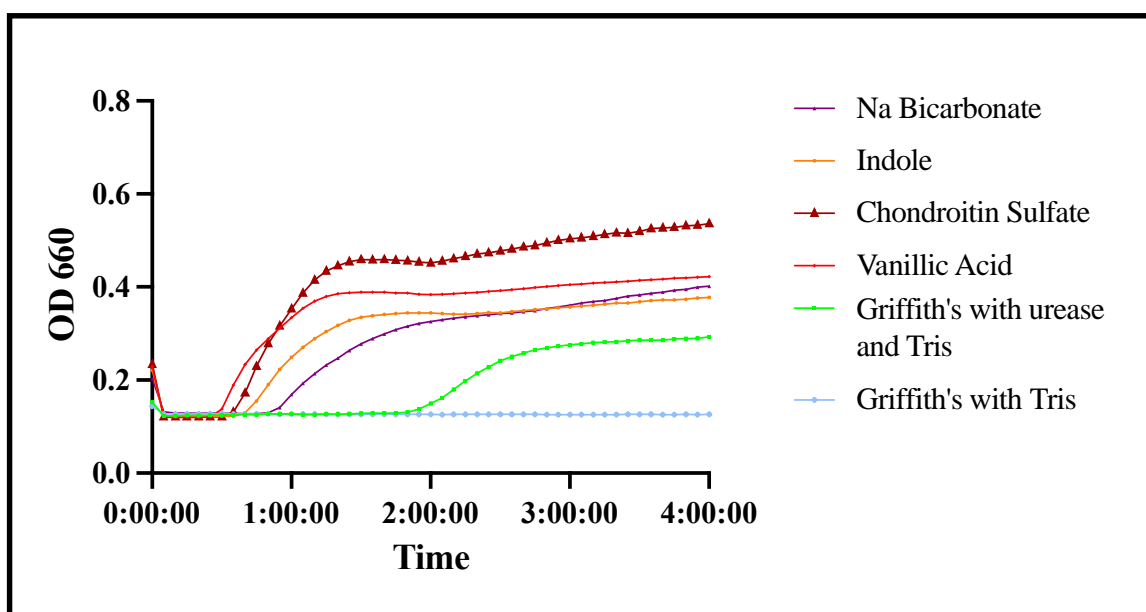


**Figure 10: Crystal growth curves for modulators that promote crystal formation measured by absorbance at a wavelength of 660 nm.**

**Table 17: Growth curve output for urinary modulators promoting crystal formation.**

Modulator	k	$n^0$	r	t_mid	t_gen	auc_l	auc_e	sigma
Na Bicarbonate	0.410	0.060	0.010	215.31	89.28	493.39	491.26	0.030
Vanillic acid	0.302	0.086	0.011	81.22	60.95	401.88	401.16	0.022
Indole	0.317	0.073	0.012	102.91	58.65	417.24	416.18	0.025
CS	0.489	0.093	0.016	90.81	43.39	653.59	652.15	0.032
Griffith's with urease +Tris	0.270	0.030	0.010	224.58	69.64	320.56	318.52	0.020
Griffith's with Tris	0.000	0.000	0.000	0	0	0	0	0.000

$k$  = growth capacity,  $n^0$  = degrees of freedom,  $r$  = growth rate,  $t_{mid}$  = time to inflection point,  $t_{gen}$  = doubling time,  $auc_l$  = logistic area under the curve,  $auc_e$  = empiric area under the curve,  $\sigma$  = goodness of fit.

Crystals from CS (Figure 11) and Na bicarbonate (Figure 12) are shown below.

Both modulators appear to predominantly have calcium phosphate crystals from the reaction. On close inspection of Figure 11, one can see that the crystals from CS appear larger and better defined than the Na bicarbonate crystals. There was no clear evidence of struvite crystals on microscopic assessment with these modulators.

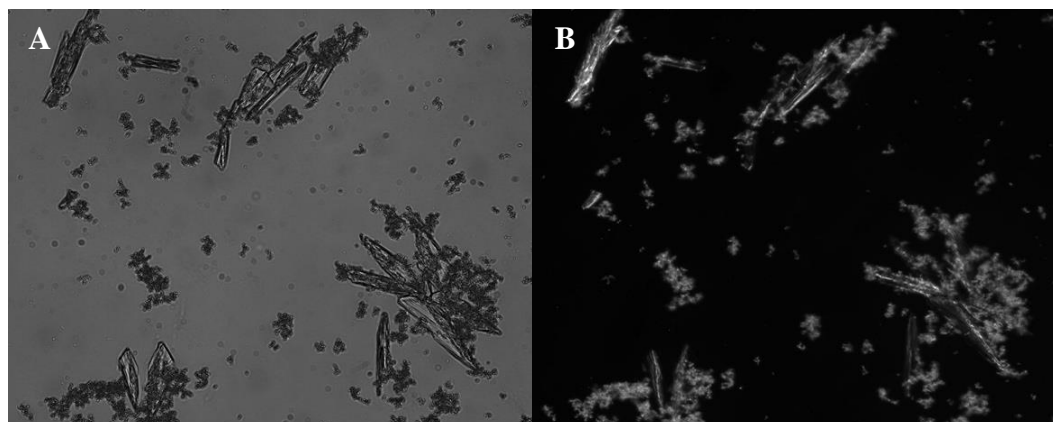


**Figure 11: Brightfield (A) and polarized (B) microscopy of crystals from chondroitin sulfate reaction at 100x.**

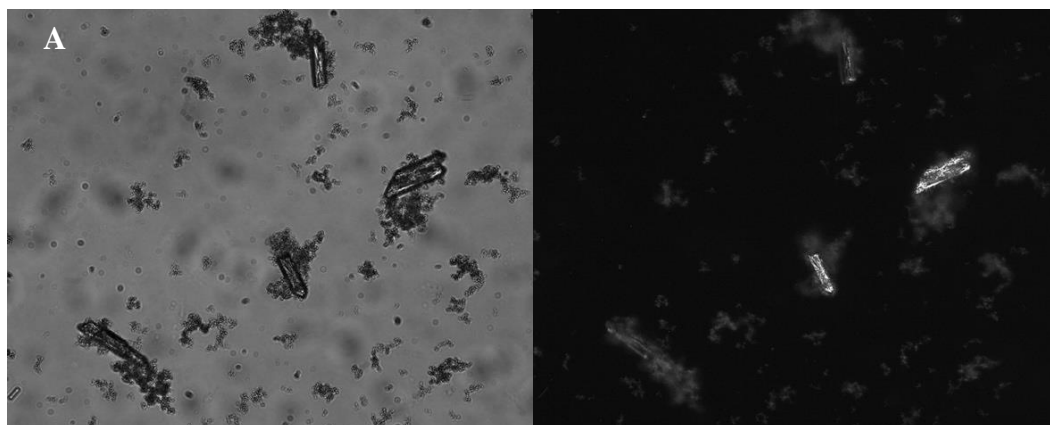


**Figure 12: Brightfield (A) and polarized (B) microscopy of crystals from Na bicarbonate reaction at 100x.**

### 3.3.4 Urinary modulators with no effect on crystal formation

The modulators that had a largely neutral effect despite their pH values starting relatively low were found to be methionine and heparin. After conducting the experiment, the pH levels, slope of the curves and  $t_{mid}$  were similar to Griffith's with urease and Tris. The visual overlap of the curves in Figure 13 demonstrates the comparable reaction dynamics between methionine, heparin and Griffith's with urease and Tris.

**Table 18: pH values of urinary modulators with no effect on crystal growth before and after experiment.**

Modulator	Initial pH	Biologic rep #1	Biologic rep #2	Biologic rep #3
Methionine	5.00	7.19	8.04	8.48
Heparin	5.01	7.64	8.16	8.53
Griffith's with urease and Tris	5.02	7.69	8.17	8.72
Griffith's with Tris	5.01	5.00	5.87	6.23

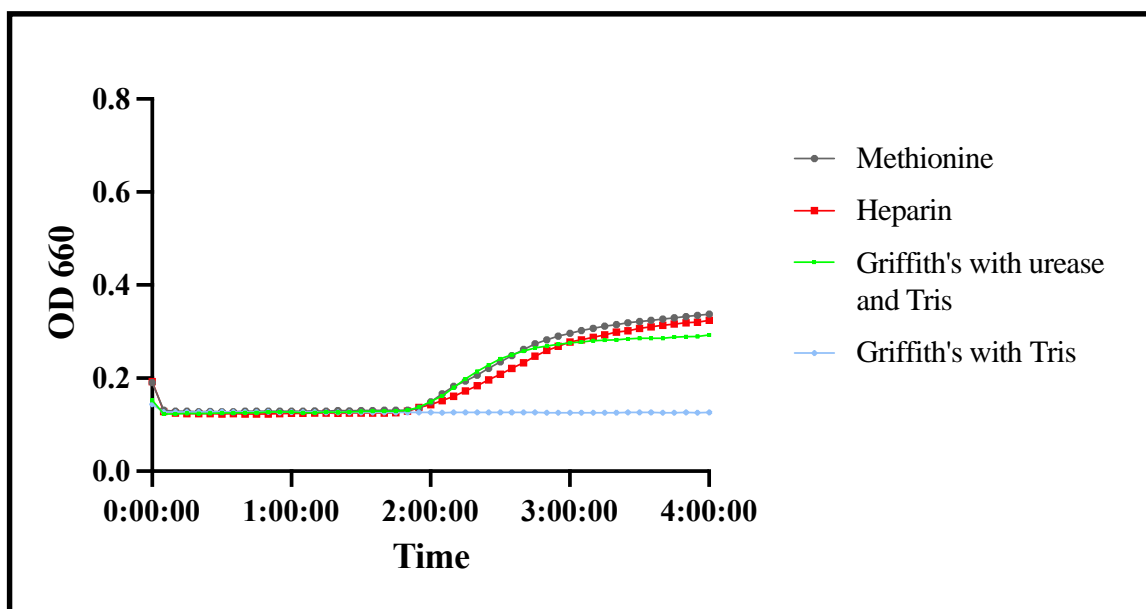


**Figure 13: Crystal growth curves for modulators with a no effect on crystal formation measured by absorbance at a wavelength of 660 nm.**

**Table 19: Growth curve output for urinary modulators with no effect on crystal formation.**

Modulator	k	$n^0$	r	$t_{mid}$	$t_{gen}$	auc_l	auc_e	sigma
Methionine	0.430	0.040	0.010	288.04	87.04	487.62	484.21	0.030
Heparin	0.420	0.040	0.010	295.75	87.1	472.85	469.46	0.030
Griffith's with urease and Tris	0.270	0.030	0.010	224.58	69.64	320.56	318.52	0.020
Griffith's with Tris	0.000	0.000	0.000	0	0	0	0	0.000

$k$  = growth capacity,  $n^0$  = degrees of freedom,  $r$  = growth rate,  $t_{mid}$  = time to inflection point,  $t_{gen}$  = doubling time,  $auc_l$  = logistic area under the curve,  $auc_e$  = empiric area under the curve,  $\sigma$  = goodness of fit.

### 3.3.5 Urinary modulators with mixed effect on crystal formation

The modulation and pH changes of sodium pyrophosphate (Na pyrophosphate), PASP and P-Cresol were mixed. The pH of PASP was consistently higher than the control, but the other reactions had pHs similar to controls, except for biologic replicate number 1 for Na pyrophosphate.

**Table 20: pH values of urinary modulators with mixed effect on crystal growth before and after experiment.**

Modulator	Initial pH	Biologic rep #1	Biologic rep #2	Biologic rep #3
Na pyrophosphate	5.06	5.07	8.21	8.39
PASP	6.17	8.71	8.75	8.72
P-Cresol	6.18	8.04	8.15	8.09
Griffith's with urease and Tris	5.02	7.69	8.17	8.72
Griffith's with Tris	5.01	5.00	5.87	6.23

As can be seen in Figure 14, the growth curves all started earlier than Griffith's with urease and Tris while the slopes appear more gradual. The  $r$  values for PASP and P-Cresol were lower, but Na pyrophosphate had the same  $r$  as the control with urease.  $T_{mid}$  (303.38) and  $t_{gen}$  (113.92) were both lower for Na pyrophosphate over PASP, P-Cresol and controls. While the  $t_{mid}$  values for PASP and P-Cresol are comparable to Griffith's with urease and Tris, but  $t_{gen}$  is slightly higher. Overall, the only modulator that decreased overall crystal growth is P-Cresol.

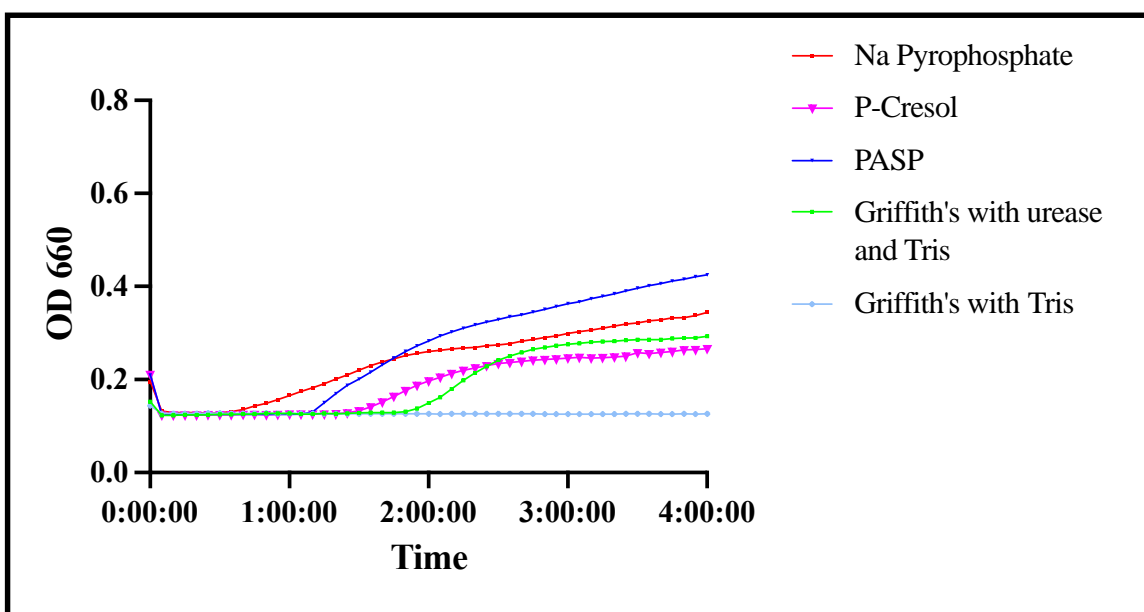


**Figure 14: Crystal growth curves for modulators with mixed effect on crystal formation measured by absorbance at a wavelength of 660 nm.**

**Table 21: Growth curve output for urinary modulators with mixed effect on crystal formation.**

Modulator	k	$n^0$	r	t_mid	t_gen	auc_l	auc_e	sigma
Na Pyrophosphate	0.430	0.060	0.010	303.38	113.92	477.46	474.88	0.020
PASP	0.510	0.061	0.009	231.06	80.22	608.66	605.69	0.029
P-Cresol	0.228	0.032	0.008	225.82	86.64	272.01	270.46	0.017
Griffith's with urease +Tris	0.270	0.030	0.010	224.58	69.64	320.56	318.52	0.020
Griffith's with Tris	0.000	0.000	0.000	0	0	0	0	0.000

$k$  = growth capacity,  $n^0$  = degrees of freedom,  $r$  = growth rate,  $t_{mid}$  = time to inflection point,  $t_{gen}$  = doubling time,  $auc_l$  = logistic area under the curve,  $auc_e$  = empiric area under the curve,  $\sigma$  = goodness of fit.

Crystals formed with Na pyrophosphate, P-Cresol and PASP are shown in the figures below. Overall, these crystals are smaller compared to CS and Na bicarbonate. Na pyrophosphate and PASP appear to have calcium phosphate crystals, but P-Cresol appears to have struvite crystals with the “coffin lid” shape.

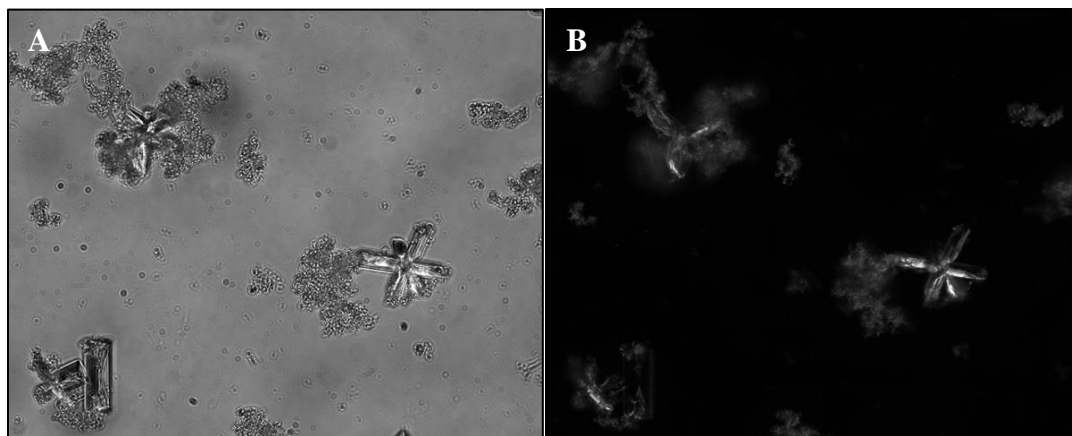


**Figure 15: Brightfield (A) and polarized (B) microscopy of crystals from Na pyrophosphate reaction at 200x.**

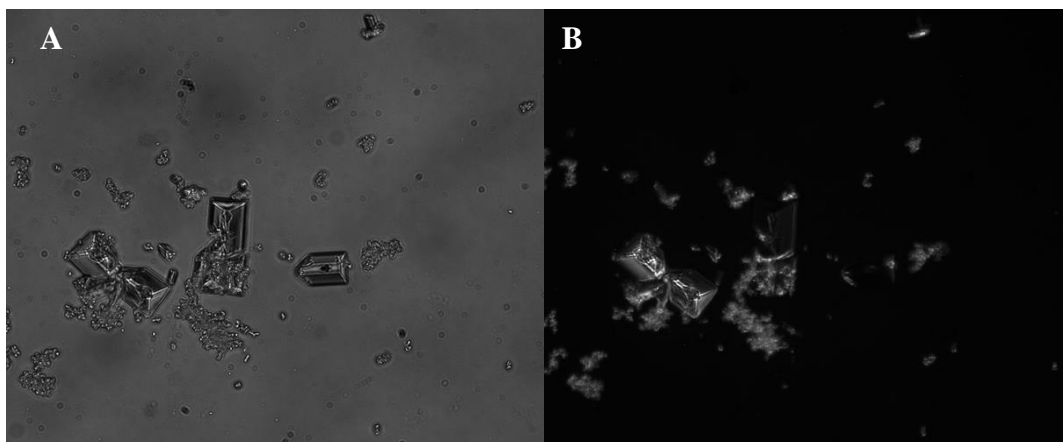


**Figure 16: Brightfield (A) and polarized (B) microscopy of crystals from P-Cresol reaction at 200x.**

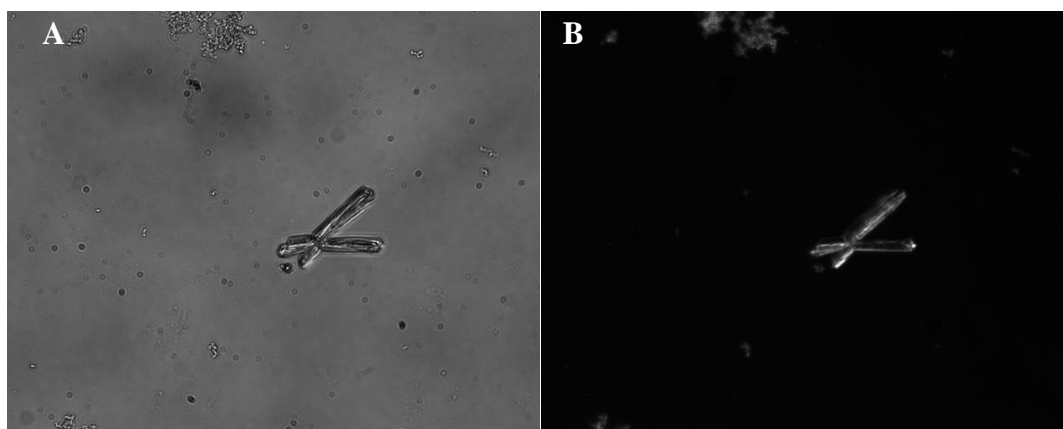


**Figure 17: Brightfield (E) and polarized (F) microscopy of crystals from PASP reaction at 200x.**

### 3.4 Discussion

The urinary modulators tested in this study demonstrated enhancing, inhibitory, neutral, and mixed effects on infectious crystal formation. While the pH level appears to have an important role, an alkaline pH does not automatically equate to improved crystal formation. Acids appear to have the most consistent ability to prevent infectious crystal formation, except for sodium citrate, OPN and magdolate, which also had inhibitory/preventative properties. Urinary acidification has been a proposed treatment

approach for infectious stones,<sup>25</sup> and these results further support that strategy. These findings could be used to alter the treatment paradigm for patients with infectious kidney stones.

The benefit of acids in preventing crystal formation could have been due to preventing a rise in pH, active-site directed inhibition or mechanism directed inhibition of urease, which has been documented previously.<sup>26</sup> There are many compounds that have been investigated in the past for urease inhibition including hydroxamic acids, phosphoramidates, urea derivatives, quinone, polyphenols, quinolones, flavinoids and heterocyclic compounds.<sup>27,28</sup> For example, Svane et al. tested 71 compounds for urease inhibiting activity with a variety of different mechanisms and identified 30 with significant urease inhibition but etidronic acid was not one of them.<sup>29</sup> This is very surprising given that etidronic acid in our study yielded a pH less than 2 and demonstrated complete crystal inhibition. There were several other acids tested that were effective at inhibiting urease and some of the ones in our study may have overlapping properties, but we cannot identify the mechanisms of inhibition in our study.

Some of the other compounds that were successful in inhibiting stone formation potentially behave similar to acid in their mechanism. As previously mentioned, sulfate is a titratable acid found in the kidney and is suspected to be the more dominant modulator in zinc sulfate to prevent infectious crystal formation. Ibuprofen should also be considered an acid because it's chemical name of (R,S)-2-(4-isobutylphenyl)propionic acid, however there can be a variety of chemical metabolites within the urine due to methylation.<sup>30</sup> Although it may act as an acid with promising results in our experiment,

these cannot be automatically applied clinically given the variability of urine metabolite levels.

Magdolate is magnesium pidolate and magnesium is likely the predominant modulating factor in this supplement. Evidence suggests that magnesium inhibits calcium phosphate crystallization, but findings have not been consistent.<sup>10,14</sup> Future work could include investigating the correlation between 24-hour urinary magnesium levels and stone formation/composition.

Citrate has been shown to inhibit urease-induced crystallization and delay the onset of nucleation and growth of struvite crystals<sup>8</sup> and in our study we observed no crystal formation whatsoever. While there may be hesitancy in implementing a clinical therapy that might raise the urinary pH, the crystal inhibitory effects are compelling. While the exact mechanism is not clear, there may be an indirect effect of increased crystal inhibition with the use of citrate at higher pH levels.<sup>5</sup> Therefore, citrate may be an underutilized clinical treatment strategy in infectious stones.

Metformin in our experiment showed complete inhibition of crystal formation which has been demonstrated with *in vitro* and *in vivo* models through antioxidant effects.<sup>31</sup> An important consideration, is that metformin does not undergo any metabolic changes after being excreted into the urine,<sup>32</sup> making our results of particular interest clinically. Urinary citric acid has been shown to significantly increase in patients with early type 2 diabetes treated with metformin out to 6 months of follow up.<sup>33</sup> Although this is unlikely to be the mechanism of action in our study, this coupled with the aforementioned benefits of urinary citrate could be critical for those with diabetes and infectious stones; and possibly even those without diabetes.

OPN did not completely inhibit crystal formation, but delayed the onset of the formation of crystals, slowed the reaction, and decreased the overall crystal volume quite dramatically. This is consistent with other studies showing its inhibitory effect on calcium oxalate and calcium phosphate crystal formation.<sup>9</sup> The exact inhibitory mechanism of calcium phosphate crystallization can vary depending on the phosphorylation of OPN.<sup>34</sup> There is limited evidence on struvite inhibition with OPN, and given our findings, there may be no effect at all. There was a slow and gradual formation of crystals that could represent the normal growth of struvite crystals only. Presumably, we did not see the early phase growth of calcium phosphate crystallization which has been shown to occur earlier in the urease-induced crystallization pathway.<sup>35</sup> That being said it, it may still be effective if it can be used while avoiding a pH rise above 7.0 and subsequent struvite crystallization. The other added challenge with OPN is causing upregulation in the kidney because it is mediated by inflammation and healing.

*In vitro* studies by Torzewska and Rozalski<sup>7</sup>, demonstrated that chondroitin sulfate in Griffith's artificial urine infected with *Proteus mirabilis* actually led to increased struvite and calcium phosphate crystallization. A similar effect was seen in our experiment with a greater AUC, but also a more robust reaction with urease leading to rapid crystal formation. Vanillic acid at higher concentrations can be bactericidal for *P. mirabilis* and can also inhibit urease at very low concentrations.<sup>7</sup> The concentration in our experiment was 10x lower, which may explain the difference in results. Sodium bicarbonate enhanced crystal formation which is not surprising given its propensity to dissociate in water and alkalinize the solution, thus providing better conditions for urease. This is an important clinical comparison because some physicians will use sodium

bicarbonate (baking soda) for urinary alkalization and as we can see in our study the effect in infectious stone formation is not the same with a citrate supplement.

Indole dramatically enhanced the effect on stone formation, but we are unsure of the mechanism. Our lab has also demonstrated that indole can enhance calcium oxalate crystal formation (unpublished data). Similarly, there is preliminary evidence associated with P-Cresol causing increased calcium oxalate crystal formation in our lab. This compound appears to have a mixed effect on crystal formation with early onset of crystal development, but possible disruption via crystal aggregation and nucleation leading to a slower doubling time and rate of crystal growth.

There were mixed effects with sodium pyrophosphate in our study which is consistent with prior literature showing no influence on pH changes, urease activity, bacterial growth and subsequent crystallization.<sup>7</sup> Although it may have altered the initial behaviour of the reaction, the end result overtime is a crystal yield similar to the controls in our study. PASP was another modulator that had early onset of crystallization, but slower growth over time. This supports prior studies showing that the mechanism of action is by reducing aggregation.<sup>9,13</sup> However, there does appear to be a dose-dependent response with increasing concentrations leading to more inhibition<sup>36,37</sup> so increasing the dose in our experiment may lead to different results and could be explored further in the future.

Compared to controls, heparin did not alter the reaction to any dramatic effect. Prior studies have not shown any effect of heparin on urease-induced crystallization.<sup>11</sup> We did not see a clear change in infectious stone formation with methionine in our study, but this could be dose dependent on the amount of methionine used. One study noted that

methionine gets converted into sulfate within the urine<sup>16</sup> which may result in its actual clinical benefit and not the methionine metabolite itself. In addition, many of these studies use large amounts of methionine which may significantly raise the methionine or sulfate levels in the urine and lead to a clinical benefit.

Overall, the strengths of our study are that the experimental conditions were standardized and testing in artificial urine ensured that the effects demonstrated were solely related to the modulator. We tested a large number of inhibitors, and the concentrations of test substances were based on normal human urine concentrations whenever possible. Limitations of this study include the effect of some of the urinary modulators that may be concentration dependent, whereas we examined a single concentration for each modulator. Additionally, we were unaware as to how the urinary modulators would behave in the presence of bacteria, which could also be clinically important.

Many urinary modulators were tested with our validated model and there were results that were anticipated, but also exciting novel discoveries. This study provides more evidence of the importance of urinary acidification to prevent infectious kidney stone formation. The findings of significant infectious stone crystal inhibition with citrate and OPN is noteworthy. Citrate is already clinically available as a well-known treatment for calcium oxalate and uric acid stone prevention but has not been used in infectious stone patients. Clinical evaluation of citrate in patients with infectious urinary stones seems worthy of further investigation. Attempts to upregulate OPN for clinical effect has yet to be successfully realized and would require further study. Another key finding in this work was the somewhat counterintuitive role of urine pH and its impact on infectious

stone formation. It has always been assumed that the higher the pH, the greater the amount of infectious stone formation that occurs, however this is not always the case. For example, both citrate and OPN were associated with similar or higher pH values yet demonstrated effective inhibitory properties. This data calls into question some of our long-held beliefs about how infectious stones form and in the next chapter, the relationship between urinary pH, stone formation, urease, and bacteria will be further explored.

### 3.5 References

1. Chauhan CK, Joshi MJ. *In vitro* crystallization, characterization and growth-inhibition study of urinary type struvite crystals. *J Cryst Growth*. 2013;362(1):330-337. doi:10.1016/j.jcrysgro.2011.11.008
2. Hedelin H, Grenabo L, Pettersson S. Urease-induced crystallization in synthetic urine. *J Urol*. 1985;133(3):529-532. doi:10.1016/S0022-5347(17)49047-1
3. Maurice-Estépa L, Levillain P, Lacour B, Daudon M. Crystalline phase differentiation in urinary calcium phosphate and magnesium phosphate calculi. *Scand J Urol Nephrol*. 1999;33(5):299-305. doi:10.1080/003655999750017365
4. Carpentier X, Daudon M, Traxer O, et al. Relationships between carbonation rate of carbapatite and morphologic characteristics of calcium phosphate stones and etiology. *Urology*. 2009;73(5):968-975. doi:10.1016/j.urology.2008.12.049
5. Khan SR, Kok DJ. Modulators of urinary stone formation. *Front Biosci*. 2004;9:1450-1482. doi:10.2741/1347
6. Caballero D, Li Y, Fetene J, et al. Intraperitoneal pyrophosphate treatment reduces renal calcifications in *Npt2a* null mice. *PLoS One*. 2017;12(7):1-14. doi:10.1371/journal.pone.0180098
7. Torzewska A, Rozalski A. Inhibition of crystallization caused by *Proteus mirabilis* during the development of infectious urolithiasis by various phenolic substances. *Microbiol Res*. 2014;169(7-8):579-584. doi:10.1016/j.micres.2013.09.020
8. Wang Y, Grenabo L, Hedelin H, McLean RJC, Nickel JC, Pettersson S. Citrate and urease-induced crystallization in synthetic and human urine. *Urol Res*. 1993;21(2):109-115. doi:10.1007/BF01788828
9. Beshensky AM, Wesson JA, Worcester EM, Sorokina EJ, Snyder CJ, Kleinman JG. Effects of urinary macromolecules on hydroxyapatite crystal formation. *J Am Soc Nephrol*. 2001;12(10):2108-2116. doi:10.1681/asn.v12i102108
10. Ryall RL. Urinary inhibitors of calcium oxalate crystallization and their potential role in stone formation. *World J Urol*. 1997;15(3):155-164. doi:10.1007/BF02201852
11. Hedelin H, Grenabo L, Pettersson S. The effects of glycosaminoglycans, pyrophosphate and allopurinol treatment on urease-induced crystallization *in vitro*. *Urol Res*. 1986;14(6):305-307. doi:10.1007/BF00262380

12. Bigi A, Bracci B, Panzavolta S, et al. Morphological and structural modifications of octacalcium phosphate induced by poly-L-aspartate. *Cryst Growth Des.* 2004;4(1):141-146. doi:10.1021/cg034078d
13. Schaad P, Gramain P, Gorce F, Voegel JC. Dissolution of synthetic hydroxyapatite in the presence of lanthanum ions. *J Chem Soc Faraday Trans.* 1994;90(22):3405-3408. doi:10.1039/FT9949003405
14. Hansen NM, Felix R, Bisaz S, Fleisch H. Aggregation of hydroxyapatite crystals. *Biochim Biophys Acta.* 1976;451:549-559. doi:10.1016/0304-4165(76)90150-1
15. Lemann J, Relman AS. The relation of sulfur metabolism to acid-base balance and electrolyte excretion: The effects of DL-methionine in normal man. *J Clin Invest.* 1959;38:2215-2223. doi:10.1172/JCI104001
16. Siener R, Struwe F, Hesse A. Effect of L-methionine on the risk of phosphate stone formation. *Urology.* 2016;98:39-43. doi:10.1016/j.urology.2016.08.007
17. Rodgers A, Gauvin D, Edeh S, Allie-Hamdulay S, Jackson G, Lieske JC. Sulfate but not thiosulfate reduces calculated and measured urinary ionized calcium and supersaturation: Implications for the treatment of calcium renal stones. *PLoS One.* 2014;9(7). doi:10.1371/journal.pone.0103602
18. Aggarwal KP, Narula S, Kakkar M, Tandon C. Nephrolithiasis: Molecular mechanism of renal stone formation and the critical role played by modulators. *Biomed Res Int.* 2013;2013:1-22. doi:10.1155/2013/292953
19. Basavaraj DR, Biyani CS, Browning AJ, Cartledge JJ. The role of urinary kidney stone inhibitors and promoters in the pathogenesis of calcium containing renal stones. *EAU-EBU Updat Ser.* 2007;5:126-136. doi:10.1016/j.eeus.2007.03.002
20. Siener R, Ebert D, Nicolay C, Hesse A. Dietary risk factors for hyperoxaluria in calcium oxalate stone formers. *Kidney Int.* 2003;63(3):1037-1043. doi:10.1046/j.1523-1755.2003.00807.x
21. Ditscheid B, Fünfstück R, Busch M, Schubert R, Gerth J, Jahreis G. Effect of L-methionine supplementation on plasma homocysteine and other free amino acids: A placebo-controlled double-blind cross-over study. *Eur J Clin Nutr.* 2005;59(6):768-775. doi:10.1038/sj.ejcn.1602138
22. Jung A, Bisaz S, Fleisch H. The binding of pyrophosphate and two diphosphonates by hydroxyapatite crystals. *Calcif Tissue Res.* 1973;11(4):269-280. doi:10.1007/BF02547227

23. Zamora-Ros R, Achaintre D, Rothwell JA, et al. Urinary excretions of 34 dietary polyphenols and their associations with lifestyle factors in the EPIC cohort study. *Sci Rep*. 2016;6(26905):1-9. doi:10.1038/srep26905
24. Sprouffske K. growthcurver: Simple Metrics to 0.3.1., Growth Curves. R package version. 2020. <https://cran.r-project.org/package=growthcurver>.
25. Abou Chakra M, Dellis AE, Papatsoris AG, Moussa M. Established and recent developments in the pharmacological management of urolithiasis: An overview of the current treatment armamentarium. *Expert Opin Pharmacother*. 2020;21(1):85-96. doi:10.1080/14656566.2019.1685979
26. Amtul Z, Rahman A, Siddiqui R, Choudhary M. Chemistry and mechanism of urease inhibition. *Curr Med Chem*. 2012;9(14):1323-1348. doi:10.2174/0929867023369853
27. Kosikowska P, Berlicki Ł. Urease inhibitors as potential drugs for gastric and urinary tract infections: A patent review. *Expert Opin Ther Pat*. 2011;21(6):945-957. doi:10.1517/13543776.2011.574615
28. Kafarski P, Talma M. Recent advances in design of new urease inhibitors: A review. *J Adv Res*. 2018;13:101-112. doi:10.1016/j.jare.2018.01.007
29. Svane S, Sigurdarson JJ, Finkenwirth F, Eitinger T, Karring H. Inhibition of urease activity by different compounds provides insight into the modulation and association of bacterial nickel import and ureolysis. *Sci Rep*. 2020;10(1):1-14. doi:10.1038/s41598-020-65107-9
30. Maurer HH, Tauvel FX, Kraemer T. Anti-inflammatory drugs and their metabolites in urine. *J Anal Toxicol*. 2001;25:237-244.
31. Yang X, Ding H, Qin Z, et al. Metformin prevents renal stone formation through an antioxidant mechanism *in vitro* and *in vivo*. *Oxid Med Cell Longev*. 2016;2016:1-10. doi:10.1155/2016/4156075
32. Azar JA, Bassil M, Irani J, et al. Factors determining blood and urine concentrations of metformin among patients with type 2 diabetes: A cross sectional study. *J Biomed Sci*. 2018;7(4):1-6. doi:10.4172/2254-609x.100093
33. Park JE, Jeong GH, Lee IK, et al. A pharmacometabolomic approach to predict response to metformin in early-phase type 2 diabetes mellitus patients. *Molecules*. 2018;23(7):1-13. doi:10.3390/molecules23071579
34. de Bruyn JR, Goiko M, Mozaffari M, et al. Dynamic light scattering study of inhibition of nucleation and growth of hydroxyapatite crystals by osteopontin. *PLoS One*. 2013;8(2):1-9. doi:10.1371/journal.pone.0056764

35. Ebisuno S, Komura T, Yamagiwa K, Ohkawa T. Urease-induced crystallizations of calcium phosphate and magnesium ammonium phosphate in synthetic urine and human urine. *Urol Res*. 1997;25(4):263-267. doi:10.1007/BF00942096
36. Sikirić M, Babić-Ivančić V, Milat O, Sarig S, Füredi-Milhofer H. Factors influencing additive interactions with calcium hydrogenphosphate dihydrate crystals. *Langmuir*. 2000;16(24):9261-9266. doi:10.1021/la000704m
37. Burke EM, Guo Y, Colon L, Rahima M, Veis A, Nancollas GH. Influence of polyaspartic acid and phosphophoryn on octacalcium phosphate growth kinetics. *Colloids Surfaces B Biointerfaces*. 2000;17(1):49-57. doi:10.1016/S0927-7765(99)00084-3

## Chapter 4

### 4 Testing bacterial species for infectious stone formation in an experimental model using artificial urine

Classically, urease producing bacteria have been associated with struvite and calcium phosphate stone formation. Urease produced by certain bacterial species result in the conversion of urea and water into ammonia and carbon dioxide which leads to a rise in pH. The previous chapter demonstrated that an elevated pH does not always equate to infectious stone development and an appropriate urinary milieu is required. In an effort to expand our understanding of the relationship with bacteria and stone formation, we used our experimental model to examine if crystals will originate from bacteria in the absence of other urinary modulators.

A selection of the top 10 bacterial species associated with struvite stone formation were used in our experimental model to permit their natural intracellular metabolic pathways to develop crystals. Crystal growth curves, pH values, SEM/EDX and a qualitative urease test were collected and analyzed. The results suggest that urease may not be the only metabolic pathway involved in stone formation and calcium oxalate crystal formation may be associated with bacterial activity.

#### 4.1 Introduction

##### 4.1.1 Urease producing bacteria and stone formation

The relationship between bacteria and urolithiasis is centred around urease-splitting bacteria that were first discovered in 1901.<sup>1</sup> It is estimated that over 200

microorganisms have the ability to produce urease, but the activity varies between species.<sup>2</sup> Kalwasser et al. first demonstrated that nitrogen starvation can increase urease activity, but certain strains like *Proteus* have urease activity regardless of the nitrogen level.<sup>3</sup> The ability of ureolytic bacteria to flourish in the human urinary tract is aided by the large quantity of nitrogenous sources which allow for rapid development of ammonia.<sup>2</sup> One previous study isolated bacterial strains within kidney stones from patients after SWL and none of the strains isolated were urease negative, regardless of the stone type (non-infectious or infectious).<sup>4</sup> The association between urease-producing bacteria was taken a step further by McLean et al. by identifying that infectious stones are only produced once the pH reaches 7-8.<sup>2</sup> Despite the clear evidence showing the connection between urease and infectious stones, there is still scientific skepticism on whether or not this provides the complete story.

#### **4.1.2 Alternative bacterial pathways leading to stone formation**

In 1938, Hellström not only recognized the association of urease-splitting bacteria and rapid stone formation, but hypothesized that UTIs likely played a role in all stone types to varying degrees.<sup>5</sup> This theory was not robustly investigated for many years, however, more contemporary data shines a light on the importance of urinary microbiomes. Urine has a natural microbiome that is distinctly different in stone formers compared to healthy subjects.<sup>6</sup> Additionally, urinary stones have demonstrated their own microbiome<sup>7,8</sup> and the connection between these microbiomes and stone composition may hold the key to comprehending the stone-bacterial relationship. This recent area of

research has continued to expand and supplementary concepts will be presented in the following paragraphs to better portray the stone-bacterial relationship.

Reviewing the historical data on stone cultures shows anywhere from 15-70% of stones are positive for bacteria further subdivision of this group into calcium oxalate stones only, indicates positive stone cultures in 13-44% of case.<sup>9</sup> A large multi-centre clinical database of struvite stones documented the rates of bacterial strains within the stones and the most prevalent were *E. coli*, *Proteus* and *Enterococcus*.<sup>10</sup> It is interesting to note, that two bacteria (*E. coli* and *Enterococcus*) out of the top three are non-urease producing bacteria in that study. Moreover, there were many other non-urease producing bacteria identified in the stones, albeit with lesser frequency.

Nanobacteria is a term used to define the most diminutive bacteria identified in bovine and human serum, which have been proposed to play a role in urinary stone formation. Research has proposed that nanobacteria can lead to further crystal propagation through either on cell induced injury<sup>11</sup> or creation of a mineralized shell with hydroxyapatite (calcium phosphate) crystals.<sup>12-15</sup> Nanobacteria have also been identified in Randall's plaques, which have long been viewed as a nidus for crystal formation.<sup>16</sup> Ultimately, it is hard to directly connect nanobacteria to crystal formation or whether they are an incidental finding within the urine and kidney.

Bacterial mechanisms being involved in more than calcium phosphate and struvite crystal formation would have substantial clinical implications for an appreciably larger stone patient population. In a study by Dornbrier et al., 51 stones were analyzed with 16S rRNA gene sequencing and 12 stones were found to have a predominant bacterial strain present, which was compared to the expanded quantitative urine culture (EQUC) taken

from the patients urine.<sup>17</sup> Their results established that stone and urine bacteria were not always congruent and that both calcium phosphate and calcium oxalate came from patients with a negative urine culture.<sup>17</sup>

Barr-Beare et al. demonstrated increased calcium oxalate formation with uropathogenic injury proceeding to increased cell injury, which has been shown to increase crystal adherence and stone development.<sup>7,14</sup> Individual bacterial components provide crystals another surface to develop and bacterial flagellum appear to have the greatest positive affect on calcium oxalate crystal aggregation and growth.<sup>18</sup> It is possible that just having additional physical structures to allow for improved crystal precipitation is part of the explanation, but there are suspected bacterial metabolic pathways besides urease involved.

Alternative bacterial metabolic pathways affecting kidney stone formation have been identified from the gut microbiome and this knowledge has expanded our outlook on the stone-bacterial relationship. *Lactiplantibacillus plantarum* N-1 appears to decrease calcium oxalate crystal formation in the urine by regulating arginine levels and, also in the same study, *in vitro* experiments proved that arginine exposure to renal epithelial HK-2 cells prevents calcium oxalate adhesion.<sup>19</sup> A case study looking at pathogenic *Kalamiella piersonii* isolated from the urine of a struvite stone former showed without any subunits for urease, bacteria can use amino acids for nitrogenous sources and elevate the pH.<sup>20</sup>

Due to the growing uncertainty of the mechanism and total effect of stone formation linked to bacteria, it is imperative to enhance our knowledge on the stone-bacterial connection. We believe our high-throughput experimental model can shed some

light on this complex relationship. This chapter analyzes the relationship between urease, bacteria, and stone formation in an effort to validate our hypothesis that urease and non-urease producing bacteria will promote crystallization.

## 4.2 Materials and Methods

As this was an *in vitro* study, IRB approval from Western University was not required.

### 4.2.1 Preparation of intracellular bacterial proteins

Bacterial strains tested for infectious stone formation were chosen based on a list curated by the EDGE consortium on the rates of bacterial strains in struvite stones (Table 22).<sup>10</sup>

**Table 22: List of bacterial strains tested for infectious stone formation with experimental model.**

Bacterial Strains		
<i>Proteus mirabilis</i> 175A	<i>Enterobacter cloacae</i> A4-RS-21	<i>Klebsiella pneumoniae</i> RCA+18
<i>Proteus mirabilis</i> 177A	<i>Klebsiella oxytoca</i> RCA+2	<i>Staphylococcus agalactiae</i> A3-MS-19
<i>Escherichia coli</i> UTI89	<i>Pseudomonas aeruginosa</i> PAO1	<i>Enterococcus faecalis</i> A2-FV-11
<i>Staphylococcus aureus</i> USA300	<i>Citrobacter freundii</i> RCA+1	<i>Staphylococcus epidermidis</i> A2-FV-12

After the bacteria were streaked and incubated at 37°C for 24 hours, one colony was placed in 1.5 mL of Griffith's artificial urine in a microcentrifuge tube.

Approximately 100 µL of 100 µm glass beads were added to the microcentrifuge tubes.

The bacteria were bead beat for 2 cycles of 1-minute intervals at 3,450

oscillations/minute while being placed on ice for 1 minute in between. After bead beating, the tubes were centrifuged at 20,817 x g for 5 minutes and the supernatant was collected for the stone model.<sup>21</sup>

#### **4.2.2 Running experimental model with bacteria**

One mL supernatant was added to 9 mL Griffith's artificial urine. Aliquots of 200  $\mu$ L were placed into a 96-well plate in technical triplicate. Plates were incubated at 37°C for 24 hours and absorbance was recorded every 5 minutes at 660 nm. Controls included Griffith's artificial urine with 0.1 U/mL urease and without urease were utilized. No Tris buffer was added to this experiment. The Biotek Eon Microplate Spectrophotometer (Winooski, Vermont, USA) and the Gen 5 v2.0 (Winooski, Vermont, USA) software were used for analyzing the 96-well plate. Test tubes of the original mixture were placed in an incubator at 37°C at the same time for microscopy analysis. Upon completion of the experiments at 24 hours, pH measurements were taken using a Mettler-Toledo FiveEasy Plus pH meter F20 (Gerifensee, Switzerland). The bacteria that produced crystals had a pH measured again after 48 hours of incubation at 37°C.

#### **4.2.3 Microscopic crystal evaluation and identification**

Each of the original test tube solutions were filtered through 0.22  $\mu$ m vacuum filtration system and the crystals were washed off the filter paper with deionized water. The crystals were left suspended in water to allow for preparation for SEM/EDX. A random sample of each solution was mounted on silica and examined with SEM (Zeiss/Leo 1540XB FESEM, Oberkochen, Germany). Molecular composition of the

crystals was determined with EDX (Oxford Instruments X Max 50, England, United Kingdom).

#### 4.2.4 Qualitative urease test with Christensen's agar

Christensen's agar is formulated to detect and differentiate ureolytic and urea degrading microorganisms. The ingredients required to make Christensen's agar can be found below in Table 23 and 24.<sup>22</sup>

**Table 23: Initial ingredients for Christensen's agar.**<sup>22</sup>

Ingredient	Amount
Peptone	1 g/L
NaCl	5 g/L
Dextrose	1 g/L
KH <sub>2</sub> PO <sub>4</sub>	2 g/L
Phenol red	0.012 g/L
Agar	15 g/L
Distilled water	900 mL

The mixture in Table 23 was autoclaved for 15 minutes at 121°C. The solution was cooled down to 50-55°C and the following ingredients were added under sterile conditions:

**Table 24: Final ingredients for Christensen's agar after autoclaving.**<sup>22</sup>

Ingredient	Amount
Urea	20 g/L
Distilled water	100 mL

After the components were adequately mixed, the solution was poured out into individual agar plates to solidify and was stored at 4°C.

To determine if the bacteria produced urease, a single colony was suspended in 1 mL of PBS. A 10  $\mu$ L aliquot was pipetted onto the agar plate and the plates were incubated at 37°C for 48 hours.

#### 4.2.5 Statistical analysis

Statistical analysis was carried out with RStudio version 2022.02.1 (Boston, MA, USA) using the Growthcurver package version 0.3.1 to analyze crystal growth curves.<sup>23</sup> All graphs and figures were created were accomplished using Prism – GraphPad version 9.3.1(San Diego, CA, USA).

### 4.3 Results

#### 4.3.1 Urease results from Christensen's agar

After 48 hours of incubation the bacterial strains on Christensen's agar exhibited strongly positive, weakly positive or negative for urease activity (Table 25). *E. coli* UTI89, *E. cloacae* A4-RS-21, *C. freundii* RCA+1, *S. agalactiae* A3-MS-19, *E. faecalis* A2-FV-11, and *P. aeruginosa* PAO1 were negative for urease activity. *S. epidermidis* A2-FV-12, *K. oxytoca* RCA+2 and *K. pneumoniae* RCA+18 were weakly positive for urease with only a ring around the bacterial colony turning pink (see Figure 18). *S. aureus* USA300, *P. mirabilis* 175A and *P. mirabilis* 177A were strongly positive for urease activity with the whole plate turning pink.

**Table 25: Bacterial strains incubated on Christensen's agar for 48 hours.**

<b>Bacterial Species</b>	<b>Urease</b>
<i>E. coli</i> UTI89	Negative
<i>S. aureus</i> USA300	Strongly positive
<i>E. cloacae</i> A4-RS-21	Negative
<i>C. freundii</i> RCA+1	Negative
<i>S. agalactiae</i> A3-MS-19	Negative
<i>E. faecalis</i> A2-FV-11	Negative
<i>S. epidermidis</i> A2-FV-12	Weakly positive
<i>P. mirabilis</i> 175A	Strongly positive
<i>P. mirabilis</i> 177A	Strongly positive
<i>K. oxytoca</i> RCA+2	Weakly positive
<i>K. pneumoniae</i> RCA+18	Weakly positive
<i>P. aeruginosa</i> PAO1	Negative

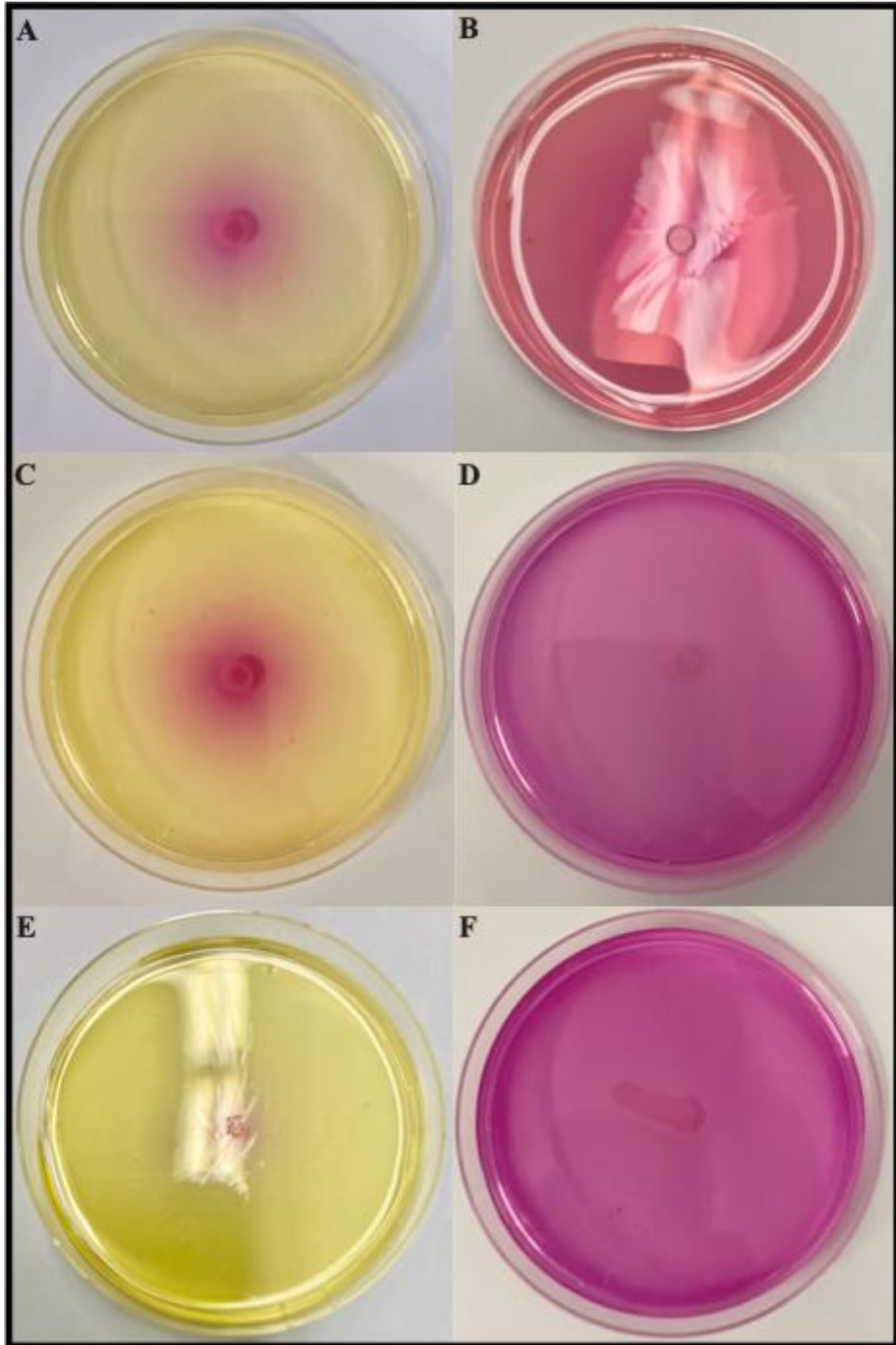


**Figure 18:** Christensen's agar after 48 hours for *K. oxytoca* RCA+2 (A), *S. aureus* USA300 (B), *K. pneumoniae* RCA+18 (C), *P. mirabilis* 175A (D), *S. epidermidis* A2-FV-12 (E), and *P. mirabilis* 177A (F).

### 4.3.2 Bacterial species that did not produce crystals

The following bacterial strains did not produce any crystals: *E. coli* UTI89, *S. aureus* USA300, *E. cloacae* A4-RS-21, *C. freundii* RCA+1, *S. agalactiae* A3-MS-19, *E. faecalis* A2-FV-11, *S. epidermidis* A2-FV-12. When evaluating their pHs after 24 hours (Table 26), the majority ranged from 5.80-6.00 except for *S. epidermidis* A2-FV-12, which rose above 6.20 on all three biologic replicates.

**Table 26: pH values after 24 hours for bacterial species that did not produce crystals.**

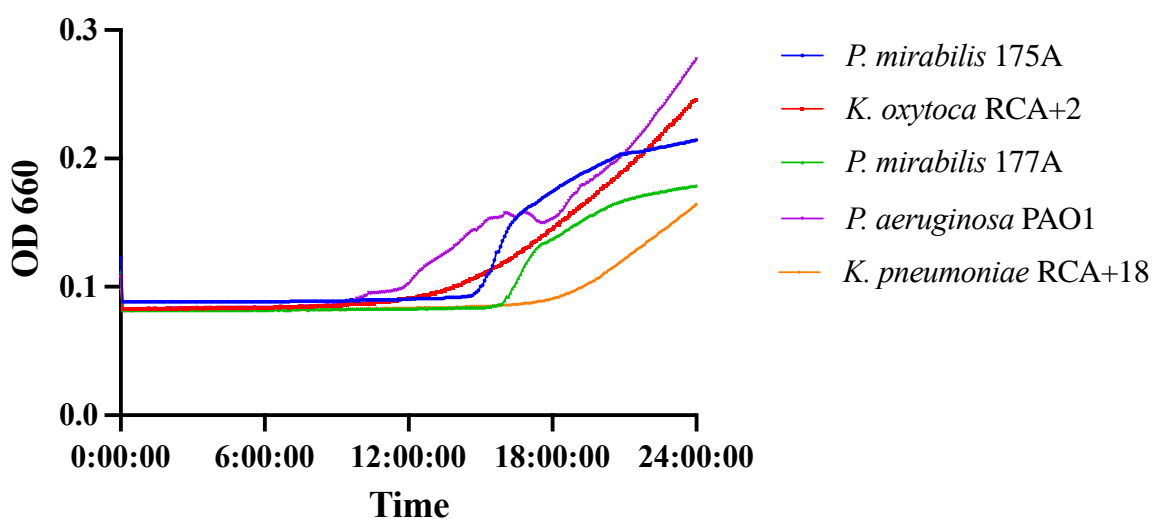
Bacterial Species	Biologic rep #1	Biologic rep #2	Biologic rep #3
<i>E. coli</i> UTI89	5.74	5.74	5.79
<i>S. aureus</i> USA300	5.81	5.82	5.81
<i>E. cloacae</i> A4-RS-21	6.02	5.99	5.99
<i>C. freundii</i> RCA+1	5.93	5.85	5.95
<i>S. agalactiae</i> A3-MS-19	5.83	5.88	5.84
<i>E. faecalis</i> A2-FV-11	5.77	5.77	5.83
<i>S. epidermidis</i> A2-FV-12	6.27	6.22	6.21

### 4.3.3 Bacteria species that produced crystals

The bacteria that did produce crystals included: *P. mirabilis* 175A, *P. mirabilis* 177A, *K. oxytoca* RCA+2, *K. pneumoniae* RCA+18, *P. aeruginosa* PAO1 (Figure 19). These bacterial strains showed a rise in pH, but not to the same degree as the Griffith's with urease (Table 27). The bacterial strains associated with the greatest rise in pH were both *P. mirabilis* strains, which also were close to reaching Griffith's with urease (pH=9.15). The only other bacteria that was able to reach a pH of 7.0 was *K. pneumoniae* RCA+18 after 48 hours. Both *P. mirabilis* strains were adherent to the test tubes and created a film with crystals that was not seen with any other strain.

**Table 27: pH values for bacterial species that produced crystals.**

Bacteria	pH after 24 hours	pH after 48 hours
<i>P. mirabilis</i> 175A	7.92	8.99
<i>P. mirabilis</i> 177A	7.61	8.64
<i>K. oxytoca</i> RCA+2	6.20	6.82
<i>K. pneumoniae</i> RCA+18	6.27	7.02
<i>P. aeruginosa</i> PAO1	6.40	6.77
Griffith's with urease	8.91	9.15
Griffith's only	5.80	5.96

**Figure 19: Crystal growth curves from crystal producing bacterial strains measured by absorbance at a wavelength of 660 nm.**

Both *P. mirabilis* strains were found to have the steepest curve and initiated the reaction early, which is supported by their greater  $r$  values and lower  $t_{mid}$  values in table 28. The *Klebsiella* species have a similar shaped curve, but *K. oxytoca* RCA+2 has an  $r = 0.006$  compared to *K. pneumoniae* RCA+18 at  $r = 0.009$ . *K. pneumoniae* appears to have the latest initiation of crystal growth of all bacteria and this coincides with it having the lowest pH at 6.20 after 24 hours before it surpasses the pH of *P. aeruginosa*

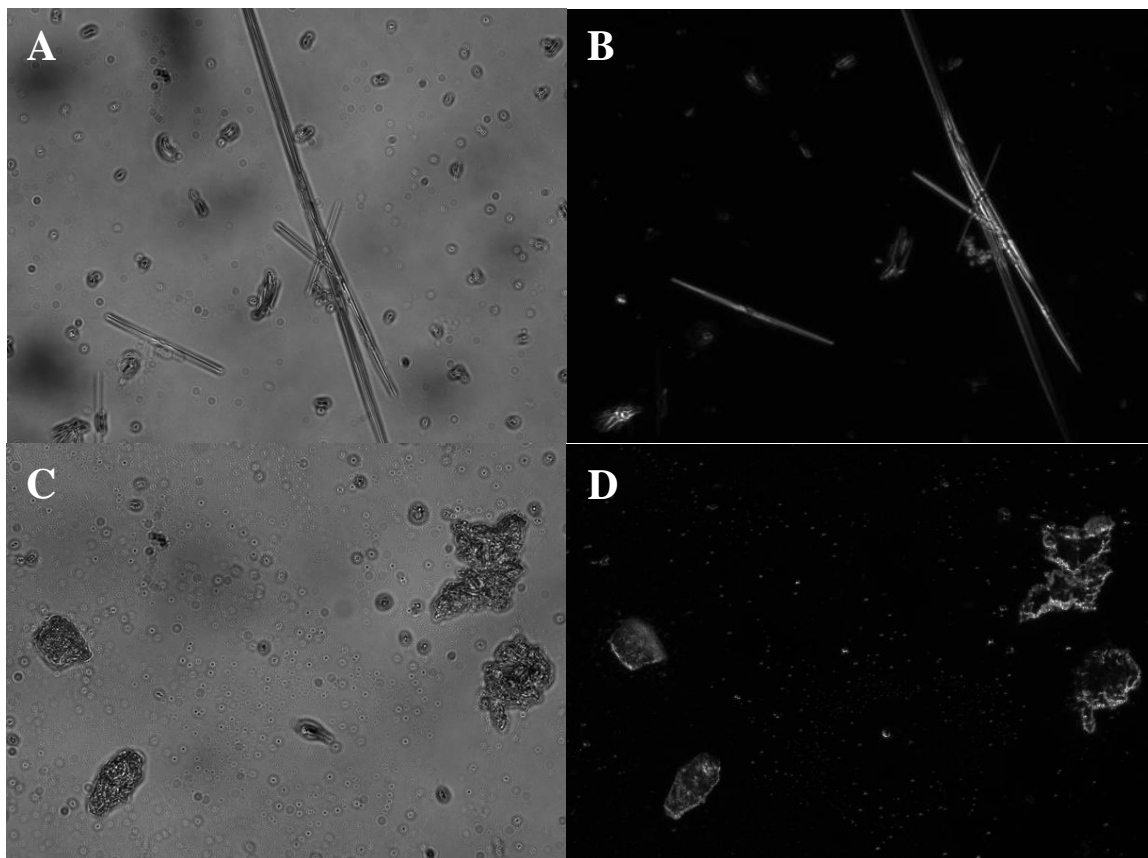
PAO1 at 48 hours. The empiric AUC for *K. oxytoca* RCA+2 is 52.27 which is second highest. *Pseudomonas aeruginosa* PAO1 has a distinctive growth curve with early crystal formation then reaching a plateau before increasing crystal formation again. Despite the earlier crystal formation, *P. aeruginosa* PAO1 has the highest  $t_{mid}$ , (1382.57) and has the greatest empiric AUC and growth capacity of all bacterial strains.

**Table 28: Growth curve analysis for crystal producing bacterial strains.**

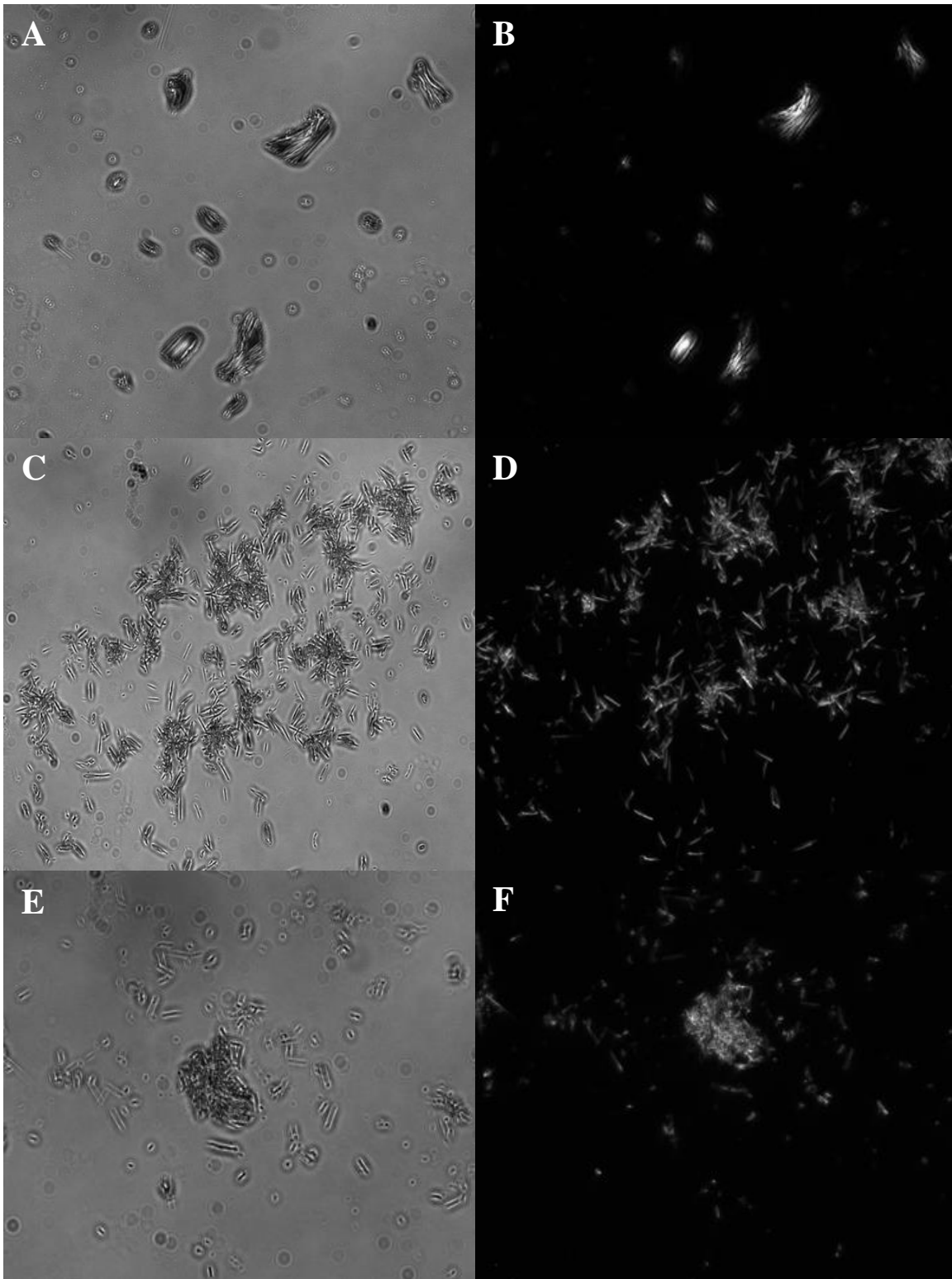
Bacteria	l	n <sup>0</sup>	r	t <sub>mid</sub>	t <sub>gen</sub>	auc <sub>l</sub>	auc <sub>e</sub>	sigma
<i>P. mirabilis</i> 175A	0.146	0.000	0.008	1149.46	86.16	44.03	50.77	0.009
<i>K. oxytoca</i> RCA+2	0.210	0.000	0.006	1239.54	122.62	52.47	52.27	0.002
<i>P. mirabilis</i> 177A	0.092	0.000	0.016	1061.18	44.57	34.75	34.69	0.004
<i>P. aeruginosa</i> PAO1	0.333	0.002	0.004	1382.57	185.44	71.36	69.44	0.008
<i>K. pneumoniae</i> RCA+18	0.112	0.000	0.009	1328.38	76.00	16.41	17.42	0.001

$k$  = growth capacity,  $n^0$  = degrees of freedom,  $r$  = growth rate,  $t_{mid}$  = time to inflection point,  $t_{gen}$  = doubling time,  $auc_l$  = logistic area under the curve,  $auc_e$  = empiric area under the curve,  $sigma$  = goodness of fit.

The figures below depict crystals under light microscopy for bacteria that produced crystals. Both *Proteus* strains are found in Figure 20 with *P. mirabilis* 175A showing a large calcium phosphate crystal (“glass shard”) and less developed grouping of possible calcium phosphate crystals with *P. mirabilis* 177A. The crystals shown in Figure 21 from *K. oxytoca* RCA+2, *K. pneumoniae* RCA+18 and *P. aeruginosa* PAO1 appear to be more consistent with calcium phosphate crystals but do not have a well-defined structure, therefore it is difficult to be certain based on these photographs what the true composition is.

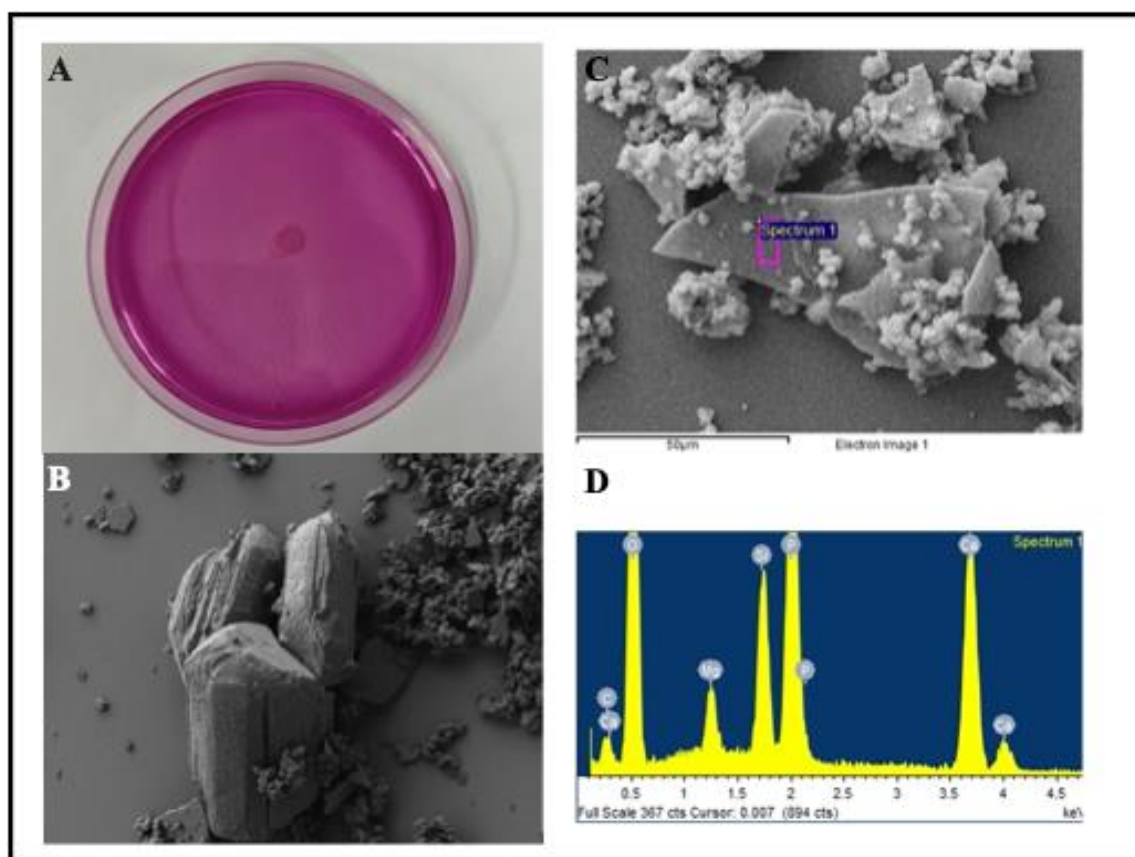


**Figure 20: *P. mirabilis* 175A crystals under brightfield light (A) and polarized light (B) at 200x magnification. *P. mirabilis* 177A crystals under brightfield light (C) and polarized light (D) at 200x magnification.**



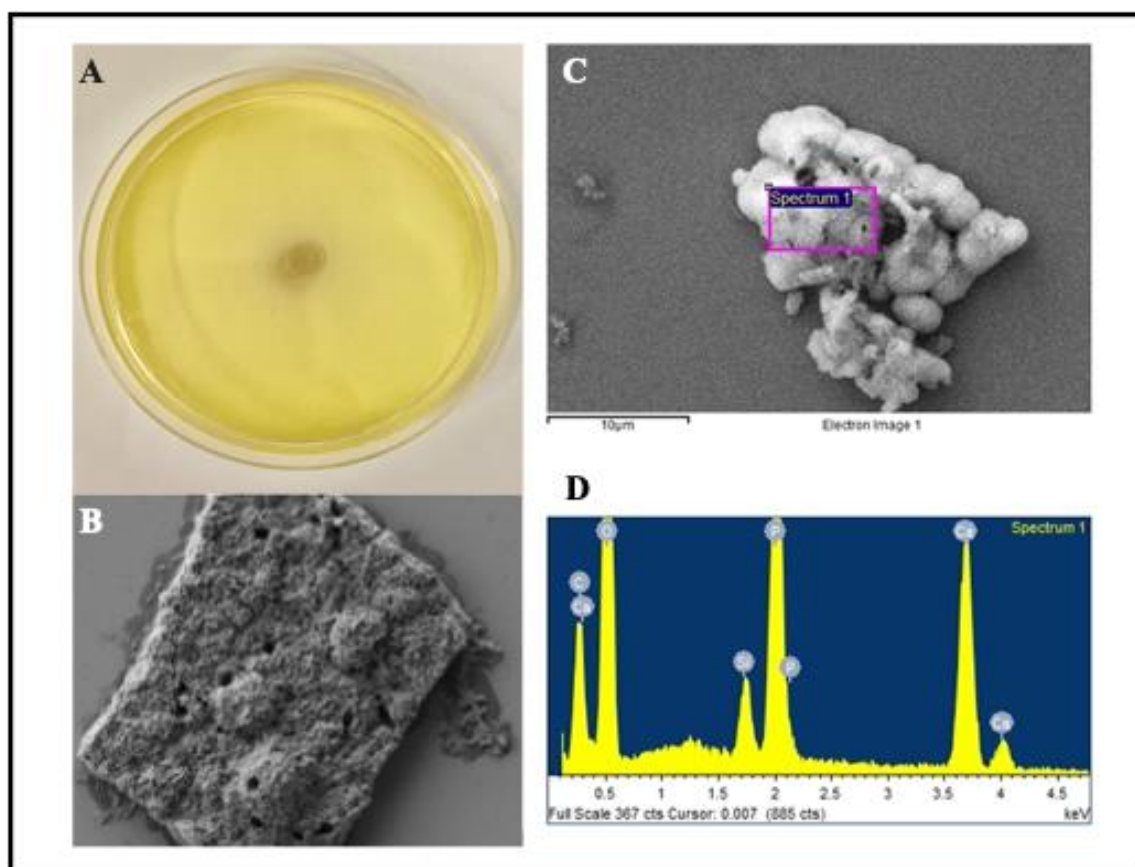
**Figure 21:** *K. oxytoca* RCA+2 crystals under brightfield light (A) and polarized light (B) at 200x magnification. *K. pneumoniae* RCA+18 crystals under brightfield light (C) and polarized light (D) at 200x magnification. *P. aeruginosa* PAO1 under brightfield light (E) and polarized light (F) at 200x magnification.

Figure 22A shows high urease productivity represented by a completely pink Christensen's agar with *P. mirabilis* 175A. The archetypal “coffin lid” appearance of struvite crystals is found in Figure 22B with groupings of spherical crystals that is seen with immature calcium phosphate crystallization. Figure 22C also depicts mixed composition calcium phosphate and struvite crystals and this was confirmed with EDX (Figure 22D) having large peaks for both phosphate and magnesium consistent with both stone types.



**Figure 22: A) Christensen's agar with colony of *P. mirabilis* 175A. *P. mirabilis* 175A crystals under SEM at 500x (B) and SEM (C) with EDX analysis (D).**

Results from Christensen's agar show no urease activity with *P. aeruginosa* PAO1 in Figure 23A, but it still produced calcium phosphate crystals (Figure 23C and 23D). The structure in Figure 23B is unique and there appears to be a filmy substance, which may be representative of bacterial biofilm. There is no magnesium present in the EDX analysis (Figure 23D), and the composition is consistent with calcium phosphate only. The calcium phosphate crystals from *P. aeruginosa* PAO1 appear more cohesive and mature regarding the structure compared to *P. mirabilis* 175A.



**Figure 23:** A) Christensen's agar with colony of *P. aeruginosa* PAO1. *P. aeruginosa* PAO1 crystals under SEM at 5000x (B) and SEM (C) with EDX analysis (D).

*K. oxytoca* RCA+2 was weakly positive for urease activity (Figure 24A) and rectangular crystals can be seen in the encircled area in Figure 24B. The crystal structure in Figure 24C is distinctly different in the shape and architecture compared to the other crystals shown. Analysis of crystal composition shows predominantly calcium (Ca), carbon (C), and oxygen (O) with no magnesium and very little phosphate (Figure 24D). This is most consistent with a calcium oxalate stone composition and this was not attained in any other experimental run during this entire project.

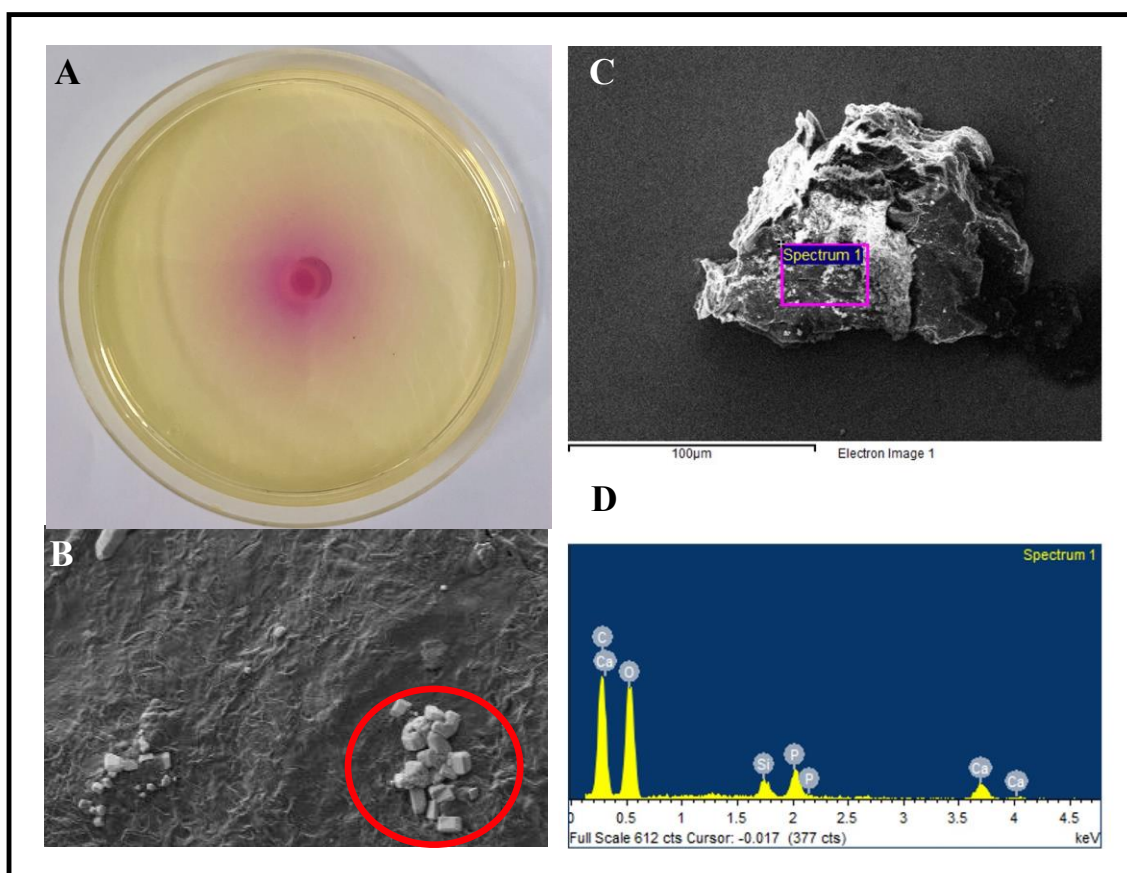


**Figure 24: A) Christensen's agar with colony of *K. oxytoca* RCA+2. *K. oxytoca* RCA+2 crystals under SEM at 2000x (B) and SEM (C) with EDX analysis (D).**

#### 4.4 Discussion

In this chapter, we evaluated the ability of uropathogenic bacteria to promote infectious stone crystal formation and we were able to identify bacterial strains that could spontaneously create crystals in artificial urine. As anticipated, we observed that urease producing bacterial strains such as *P. mirabilis* created an alkaline pH with calcium phosphate and struvite crystal formation. Surprisingly, *Klebsiella oxytoca* RCA+2, which was weakly urease positive, produced calcium oxalate crystals and did not increase the pH comparably to *Proteus* strains. Furthermore, we were able to show calcium phosphate crystal formation without urease activity with *P. aeruginosa* PAO1.

Only the *P. mirabilis* 175A and 177A strains had the urease activity to raise the pH high enough to yield calcium phosphate and struvite crystal formation. Notably, *S. aureus* USA300 was strongly positive for urease, but did not raise pH or produce crystals. None of the other bacterial strains appeared to produce any struvite crystals, which is not surprising given that struvite crystals will not form with a pH less than 7.0.<sup>24</sup> The only other bacterial strain to rise above a pH of 7 was *Klebsiella pneumoniae* RCA+18 after 48 hours, but reviewing the results of SEM/EDX and light microscopy only showed calcium phosphate crystal composition. This could be related to the delayed growth and the lack of rapid pH rise driven by a high urease activity favours calcium phosphate rather than struvite crystal formation.

Identifying mixed stone compositions clinically with struvite and calcium phosphate is quite common and this could be due to the slow rise of pH even demonstrated with *Proteus* strains. The time required to raise the pH above 7.0 appears to provide ample time for calcium phosphate to crystallize out of solution and could be the

initial nidus that allows further stone growth. However, there are patients with a urine pH above 7.0 that only produce calcium phosphate stones, and in these instances, there could be two different physiochemical explanations. The first is that the magnesium to calcium ratio is very low so limited available magnesium allows for predominantly calcium phosphate crystallization. The opposite would be true for struvite stone formers having low calcium and ample magnesium available. The second is that there is evidence to show that UTIs can cause hypocitraturia which increases the risk of calcium stone disease.<sup>25</sup> This clinical scenario would be analogous to patients with dRTA who are characteristically calcium phosphate stone formers.

Muted pH elevations and calcium phosphate crystal formation is supported by our results from *P. aeruginosa* PAO1. Despite not producing a very high pH or any urease, *P. aeruginosa* PAO1 was able to produce calcium phosphate crystals. Clinically we see calcium phosphate stones at many different pH levels although its growth is improved with higher pH levels as with struvite stones. Another notable finding in the SEM photos is the unusual appearance of the crystals and the appearance of fluid around the structures which could be a biofilm. Both *P. mirabilis* strains were adherent to the test tube possibly from biofilm formation, and the ability to create a biofilm could play a role in improved crystal formation, which will be discussed further below.

Although *Klebsiella oxytoca* RCA+2 was weakly positive for urease, it was able to produce a crystal formation not previously seen with this model. With no magnesium and minimal phosphate, the composition on EDX appears to be consistent with calcium oxalate. A positive link with calcium oxalate crystallization and all bacteria including non-urease producing bacteria has been established previously.<sup>26</sup> Our results suggest that

there may be bacterial intracellular proteins that are able to drive these crystal forming reactions besides urease and the role of urease could may be less involved in the pathogenesis of kidney stones than previously thought.

Initial pH measurements were not taken for the experiments, however the experiments with non-crystal producing bacteria the pH ranged from 5.80-6.00, which is akin to our control of Griffith's artificial urine (pH ~ 5.80). The only bacterial strain that behaved differently was *S. epidermidis* A2-FV-12 which had a pH of greater than 6.20, but given it produced urease, we would expect a pH rise. Despite *S. epidermidis* A2-FV-12 having a similar pH to both *Klebsiella* species after 24 hours, *S. epidermidis* A2-FV-12 was unable to produce crystals. As we have seen with OPN and citrate modulation, a high urinary does not guarantee crystal formation and other factors are likely at play.

The findings from this study suggest that there are other factors involved in stone development in association with bacteria besides urease. The *Proteus* strains most likely used urease to elevate the pH in the experiment high enough to see both calcium phosphate and struvite crystal formation. There are possibly non-urease proteins that use urea (or other nitrogen sources) to raise pH and lead to crystal formation, which could explain our findings from *P. aeruginosa* PAO1. Both *Klebsiella* species had weakly positive urease activity, but it is not clear how this led to crystal formation especially since *K. oxytoca* RCA+2 formed calcium oxalate crystals.

The presence of bacterial biofilm could be important for two reasons, the biofilm allows concentration and localized activity of urease or the matrix acting as its own nidus for crystal growth.<sup>27</sup> A study by Whitchurch et al. discovered that extracellular DNA is required for *P. aeruginosa* biofilm and this could be similar with other bacteria.<sup>28</sup>

Therefore, just having the intracellular components in our experiments may have allowed for a biofilm/matrix to form to further enhance the crystal production, specifically with the *Proteus* strains and *P. aeruginosa* PAO1.

The lack of a pathophysiologic understanding in infectious urinary stones has led to a paucity of preventative strategies with a proven track record of clinical benefit.

Antimicrobial agents cannot fully penetrate the crystal lattices of the stone to treat all bacteria, so its benefit is limited once a stone has formed.<sup>29</sup> Antimicrobial stewardship is vitally important because there are long term-risks with prolonged antibiotic use including bacterial resistance and secondary infections.<sup>29</sup> Acetohydroxamic acid is a urease inhibitor that has shown success in small studies but has a significant side effect profile that has prevented its widespread use. Its clinical relevancy is nullified by non-urease producing bacteria forming stones and only exposes patients to harm. With a better understanding of the mechanisms behind infectious stone formation, more reliable prevention of their occurrence may lead to improvement in patient care and quality of life.

The strengths of this study are that the bacteria used their own intracellular proteins to react with the artificial urine. We tested the most common bacteria associated with struvite stone which make the findings clinically relevant. Limitations of this study are the bead beating protocol may not have been adequate to disrupt the cellular wall. *S. aureus* is an example of this where it had high urease activity but did not create any crystals owing to the notoriously hard cellular wall to break in this bacterium. Furthermore, protein levels were not standardized across the experiment that could skew our growth curves. Christensen's agar is a qualitative test and may not be sensitive

enough to pick up low or optional urease producing bacteria. Two strategies to improve the sensitivity of Christensen's agar would be eliminating all non-urea nitrogenous sources and lengthening the incubation period up to 96 hours.<sup>4</sup>

The results of this experiment suggest that infectious stone formation is a more intricate clinical entity than previously understood. We were able to show that urease activity is not directly related to calcium phosphate formation, but high urease activity does appear necessary to raise the pH above 7.0 to allow for struvite formation. The most surprising finding is calcium oxalate crystals forming with *K. oxytoca*, which supports the theory that bacteria may be involved in more stone types than calcium phosphate and struvite. Further investigation into these bacterial species to identify the exact intracellular proteins involved in the development of urinary crystals is required. Enhancing our working knowledge of the bacterial-stone relationship could lead to improved clinical approaches to minimize infectious and calcium oxalate stone recurrence.

## 4.5

## References

1. Griffith DP. Struvite stones. *Kidney International*. 1978;13(5):372-382. doi:10.1038/ki.1978.55
2. Mclean RJC, Nickel JC, Cheng KJ, Costerton JW, Banwell JG. The ecology and pathogenicity of urease-producing bacteria in the urinary tract. *Critical Reviews in Microbiology*. 1988;16(1):37-79. doi:10.3109/10408418809104467
3. Kaltwasser H, Krämer J, Conger WR. Control of urease formation in certain aerobic bacteria. *Archiv für Mikrobiologie*. 1972;81(2):178-196. doi:10.1007/BF00412327
4. Leusmann DB, Sabinski F. Potential contribution of optional urease-positive bacteria to idiopathic urinary calcium stone formation I. Expression of urease activity in bacteria from the urinary tract that are commonly classified as urease-negative. *Urological Research*. 1996;24(2):51-54. doi:10.1007/bf00431082
5. Hellström J. The significance of *Staphylococci* in the development and treatment of renal and ureteral stones. *British Journal of Urology*. 1938;10(4):348-372. doi:10.1111/j.1464-410X.1938.tb10342.x
6. Xie J, Huang JS, Huang XJ, et al. Profiling the urinary microbiome in men with calcium-based kidney stones. *BMC Microbiology*. 2020;20(1):1-10. doi:10.1186/s12866-020-01734-6
7. Barr-Beare E, Saxena V, Hilt EE, et al. The interaction between *Enterobacteriaceae* and calcium oxalate deposits. *PLoS ONE*. 2015;10(10):1-17. doi:10.1371/journal.pone.0139575
8. Al KF. Characterizing the role of the microbiome in kidney stone disease. Published online 2020. <https://ir.lib.uwo.ca/etdhttps://ir.lib.uwo.ca/etd/7122>
9. Schwaderer AL, Wolfe AJ. The association between bacteria and urinary stones. *Annals of Translational Medicine*. 2017;5(2):3-8. doi:10.21037/atm.2016.11.73
10. Flannigan RK, Battison A, De S, et al. Evaluating factors that dictate struvite stone composition: A multi-institutional clinical experience from the EDGE research consortium. *Canadian Urological Association Journal*. 2018;12(4):131-136. doi:10.1016/j.juro.2018.05.098
11. Hong X, Wang X, Wang T, Yu C, Li H. Role of nanobacteria in the pathogenesis of kidney stone formation. *American Journal of Translational Research*. 2016;8(7):3227-3234.
12. Ansari H, Sepahi AA, Sepahi MA, Branch TN. Different approaches to detect

- “nanobacteria” in patients with kidney stones: An infectious cause or a subset of life? 2017;14(05):5001-5007.
13. Çiftçioglu N, Björklund M, Kuorikoski K, Bergström K, Kajander EO. Nanobacteria: An infectious cause for kidney stone formation. *Kidney International*. 1999;56:1893-1898. doi:10.1046/j.1523-1755.1999.00755.x
  14. Coe FL, Evan A, Worcester E. Science in medicine kidney stone disease. *The Journal of Clinical Investigations*. 2005;115(10):2598-2608. doi:10.1172/JCI26662.2598
  15. Basavaraj DR, Biyani CS, Browning AJ, Cartledge JJ. The role of urinary kidney stone inhibitors and promoters in the pathogenesis of calcium containing renal stones. *EAU-EBU Update Series*. 2007;5:126-136. doi:10.1016/j.eeus.2007.03.002
  16. Abrol N, Panda A, Kekre NS, Devasia A. Nanobacteria in the pathogenesis of urolithiasis: Myth or reality? *Indian Journal of Urology*. 2015;31(1):3-7. doi:10.4103/0970-1591.134235
  17. Dornbier RA, Bajic P, Van Kuiken M, et al. The microbiome of calcium-based urinary stones. *Urolithiasis*. 2020;48(3):191-199. doi:10.1007/s00240-019-01146-w
  18. Kanlaya R, Naruepantawart O, Thongboonkerd V. Flagellum is responsible for promoting effects of viable *Escherichia coli* on calcium oxalate crystallization, crystal growth, and crystal aggregation. *Frontiers in Microbiology*. 2019;10(2507):1-14. doi:10.3389/fmicb.2019.02507
  19. Liu Y, Jin X, Tian L, et al. *Lactiplantibacillus plantarum* reduced renal calcium oxalate stones by regulating arginine metabolism in gut microbiota. *Frontiers in Microbiology*. 2021;12:1-11. doi:10.3389/fmicb.2021.743097
  20. Rekha PD, Hameed A, Manzoor MAP, et al. First report of pathogenic bacterium *Kalamiella piersonii* isolated from urine of a kidney stone patient: Draft genome and evidence for role in struvite crystallization. *Pathogens*. 2020;9(9):1-20. doi:10.3390/pathogens9090711
  21. De Bruin OM, Birnboim HC. A method for assessing efficiency of bacterial cell disruption and DNA release. *BMC Microbiology*. 2016;16(1):1-10. doi:10.1186/s12866-016-0815-3
  22. United States Food and Drug Agency. Christensen’s Agar Recipe. Published 2001. Accessed April 9, 2022. <https://www.fda.gov/food/laboratory-methods-food/bam-media-m40-christensens-urea-agar>
  23. Sprouffske K. growthcurver: Simple Metrics to 0.3.1., Growth Curves. R package

version. Published online 2020.

24. Hedelin H, Grenabo L, Pettersson S. Urease-induced crystallization in synthetic urine. *Journal of Urology*. 1985;133(3):529-532. doi:10.1016/S0022-5347(17)49047-1
25. De Ferrari ME, Macaluso M, Brunati C, Pozzoli R, Colussi G. Hypocitraturia and *Ureaplasma urealyticum* urinary tract infection in patients with idiopathic nephrolithiasis. *Nephrology - Dialysis - Transplantation*. 1996;11(6):1185.
26. Chutipongtanate S, Sutthimethakorn S, Chiangjong W, Thongboonkerd V. Bacteria can promote calcium oxalate crystal growth and aggregation. *Journal of Biological Inorganic Chemistry*. 2013;18(3):299-308. doi:10.1007/s00775-012-0974-0
27. Parsek MR, Singh PK. Bacterial biofilms: An emerging link to disease pathogenesis. *Annual Review of Microbiology*. 2003;57:677-701. doi:10.1146/annurev.micro.57.030502.090720
28. Whitchurch CB, Tolker-Nielsen T, Ragas PC, Mattick JS. Extracellular DNA required for bacterial biofilm formation. *Science*. 2002;295:1487. doi:10.1126/science.295.5559.1487
29. Schwartz BF, Stoller ML. Nonsurgical management of infection-related renal calculi. *Urologic Clinics of North America*. 1999;26(4):765-778. doi:10.1016/S0094-0143(05)70217-2

## Appendices

### Appendix A: R code for “Growth Curver Package”

```
# Script to run GrowthCurver on Infectious Crystal Formation

# Load library
library(growthcurver)

# Load data
data1 <- read.csv("input_filename.csv", header = TRUE, sep = ",", quote = "\"", fill =
TRUE, comment.char = "")

data1$Time <- seq(from = 0, to = 1440, by = 5)

# Run GrowthCurver this will normalize each well to the lowest value
gc_out <- SummarizeGrowthByPlate(plate = data1, bg_correct = "min", plot_fit = TRUE,
plot_file = "trial_1_gc_plots.pdf")

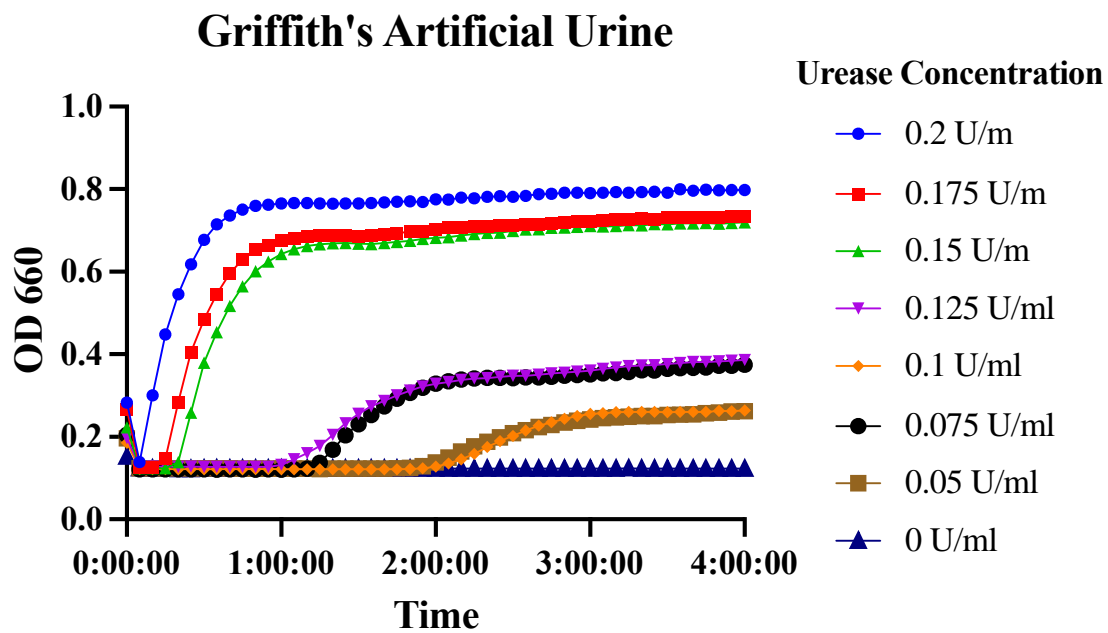
# Look for notes about bad fit (dont want any of these)
gc_out$note != ""

# Print the CSV file with the data
write.csv(gc_out, file = "output_filename.csv", row.names=FALSE)

##### Legend

# k --> carrying capacity
# n0 --> initial population size
# r --> growth rate r
# t_mid --> time at which the population density reaches 1/2K (which occurs at the
inflection point)
# t_gen --> fastest possible generation time (also called the doubling time)
# auc_l --> area under the logistic curve obtained by taking the integral of the logistic
equation
# auc_e --> empirical area under the curve which is obtained by summing up the area
under the experimental curve from the measurements in the input data
# sigma --> smaller sigma values indicate a better fit
# note --> to find poor fitting values
```

**Appendix B:** Crystal growth curves of Griffith's artificial urine with varying urease concentrations measured by absorbance at a wavelength of 660 nm.



## Curriculum Vitae

<b>Name:</b>	Brendan Wallace
<b>Post-secondary Education and Degrees:</b>	<p>St. Francis Xavier University Antigonish, Nova Scotia, Canada 2007-2011 BSc in Human Kinetics, First Class Honours.</p> <p>Memorial University St. John's, Newfoundland and Labrador, Canada 2011-2015 Doctor of Medicine.</p> <p>University of Ottawa Ottawa, Ontario, Canada 2015-2020 Urology Residency.</p> <p>The University of Western Ontario London, Ontario, Canada 2020-2022 Endourology Fellowship.</p> <p>The University of Western Ontario London, Ontario, Canada 2021-2022 MSc in Surgery.</p>
<b>Honours and Awards:</b>	<p>Member of President's Circle St. Francis Xavier University, Antigonish, Nova Scotia, Canada 2015</p> <p>Larkin Memorial Trophy St. Francis Xavier University senior male student for outstanding contributions to academic, athletic, student and community life. 2015</p> <p>Guardian Angel Award The Ottawa Hospital, Ottawa, Ontario, Canada 2019</p> <p>Dr. John Denstedt Masters' of Surgery Research Excellence Award 2021-2022</p>
<b>Related Work Experience</b>	<p>Anatomy and Physiology Lab Demonstrator St. Francis Xavier University 2010</p>

**Publications:**

1. Bhojani N, Bjazevic J, Wallace B, Lee L, Kaler KS, Dion M, Cowan A, Sultan N, Chew BH, Razvi H. Canadian Urological Association Guideline: Evaluation and medical management of the kidney stone patient – 2021 update. *Published online and ahead of print.*
2. Wallace B, Van Uum S, Khan T, Cave A, Rjoob H, Golomb D, Pautler S. Robotic assisted laparoscopic partial cystectomy for bladder paraganglioma. *Videourology*. Ahead of print, November 12, 2021. <http://doi.org/10.1089/vid.2021.0040>.
3. Wallace B, Nham E, Watterson J, Mahoney J, Skinner T. “Between a rock and a hard place’’: A case report of stone fragment impaction causing a retained ureteroscope requiring open surgical intervention, *J Endourol Case Rep*, 2020.
4. Wallace B, Breau RH, Cnossen S, Knee C, McIsaac D, Mallick R, Cagiannos I, Morash C, Lavallee LT. Age-stratified perioperative mortality after urological surgeries. *Can Urol Assoc J*, 2018.
5. Wallace B, Organ M, Bagnell S, Rendon R, Merrimen J. Renal cell carcinoma after neuroblastoma: A case study and review of the literature. *Can Urol Assoc J*, 2015.
6. MacKenzie SJ, Lavers RJ, Wallace BB. A biomechanical comparison of the vertical jump, power clean, and jump squat. *J Sports Sci*, 2014.